Co-tutelle /Dual degree

Université de Lille

Ecole Doctorale Biologie-Santé (ED446)

et

Taipei Medical University College of Biomedical Engineering

THÈSE

Présentée par

Liling Delila

Pour l'obtention du grade de

DOCTEUR DE L'UNIVERSITÉ DE LILLE

Spécialité : Neurosciences et Ingénierie tissulaire

Characterization of human platelet lysates (HPLs) for dedicated clinical uses, and assessment of the neuroprotective and neuro-regenerative therapeutic functions of nanofiltered virus-safe heated-HPL and isolated platelet-extracellular vesicles

---

Date de soutenance : 21 Juin 2023

Membres du jury :

Monsieur le Dr. Cedric Raoul	Rapporteur
Monsieur le Pr. Jean-Jacques Lataillade	Rapporteur
Monsieur le Dr. David Blum	Examinateur
Madame Tseng Ching-Li (Professeur TMU)	Invite examinatrice
Madame Szu-Yi Chou (Professeur TMU)	Invite examinatrice

Directeurs de thèse

Messieurs le Pr. David Devos / Pr. Thierry Burnouf

Publications integrated in this thesis

Liling Delila, Yu-Wen Wu, Ouada Nebie, Rifa Widyaningrum, Ming-Li Chou, David Devos, and Thierry Burnouf. "Characterization and functional activity of five preparations of human platelet lysates for dedicated clinical uses". Platelets 32, no. 2 (2021): 259-272. (IF = 4.236)

Liling Delila, Ouada Nebie, Nhi Thao Ngoc Le, Lassina Barro, Yu-Wen Wu, Naoto Watanabe, Masayasu Takahara, David Blum, David Devos, Thierry Burnouf" Neuroprotective activity of a virus-safe nanofiltered human platelet lysate depleted of extracellular vesicles in Parkinson's disease and traumatic brain injury models". Bioengineering & Translational Medicine 8, no. 1 (2023): e10360. (IF: 10.684)

ACKNOWLEDGEMENTS

This work was achieved under a dual PhD diploma program between Taipei Medical University (Graduate Institute of Biomedical Materials & Tissue Engineering, GIBMTE), Taiwan, and Universitity of Lille (Laboratoire de Pharmacologie Médicale, Unité INSERM U1172), France, under the supervision of Professors Thierry Burnouf, and David Devos.

I would like to thank Dr Cedric Raoul and Dr Jean-Jacques Lataillade for being the rapporteur for my PhD thesis defense and for reviewing my work. I would like to thank all the jury of my thesis Dr David Blum, Prof Tseng Ching-Li and Prof Szu-Yi Chou for examining my study. I appreciate their time, effort, and valuable feedback.

I would like to express my gratitude to my PhD committee members: Prof. Fabrice Cognasse, Dr. David Blum, Prof. Szu-Yi Chou for following the progress of my research throughout the years. I appreciate their comments, advices, and valuable feedback. I appreciate their time, support and encouragement.

I would like to express my sincere gratitude to Professor David Devos, my advisor from University of Lille, France. I sincerely thank him for receiving me in his lab to perform my research (Inserm, CHU-Lille, U1172) and gave me the opportunity to gain the knowledge that surely will be valuable for my future career. I am grateful for his guidance and encouraging supports. I appreciate his comments and suggestions he gave to me each time, build my interest more and more in the neuroscience field. His contribution and time are highly appreciated. I am grateful for his enthusiastic, immediate support, constructive advices during my study.

I would like to express my deepest gratitude to my advisor, Professor Thierry Burnouf, for his guidance, support, and expertise that have been instrumental in shaping my research and helping me achieve my academic goals I grateful for his continuously supports and encouragements since day one during my master study and now during my PhD. I appreciate his constant encouragement and his compassion as my mentor to direct me and give me solid advice that led me develop a better knowledge and scientific thinking in research. I am honor to be his student and for having this precious opportunity. I would like also to thank him for giving me the chance to pursue this dual diploma and broaden my research expertise.

I would like to give my huge thanks to the team in Lille. My sincere thanks to Kelly Timmerman for guiding me to perform all the scientific work during my stay in Lille. I appreciate her time and kindness. I would like to also send my gratitude to Flore Gouel, Anne-Sophie Rolland, Charlotte Laloux, Dr. Jean-Christophe Devedjian, and overall ACDC team for their involvement, suggestions, and technical support in my research project. I would like to thank to other PhD fellow in the lab, Laura Mahoney, Hind Bouchaoui, Chirine El-katrib, for they have shared their knowledge and be my friend when I was in Lille. I would like to thank Maud Petrault and Patrick Gelé who often gave me some lab tips and share their experience of doing animal research.

I would like to express my gratitude to all of lab members in Taiwan, especially my seniors, Yu-Wen Wu (Ivy), Ouada Nebie, Ming-Li Chou (Natalie), Lassina Barro, Candy Renn, and Rifa Widyaningrum. I am grateful for what I have learned from them. I highly appreciate their time and sincere effort to teach me many of laboratory skills and techniques, show me a good habit and good attitude to do lab work. I am very much grateful for their help, encouragement and guidance throughout my research and study. They are my "niche' in this field and without them I will not be able to grow.

I would like to thank my classmate all of my friends in GIBMTE. I am very much thankful for their kindness and help during my study and stay in Taiwan. I am grateful for the time we spent together in the class and student room. It always a pleasure to talk and share with all of you create an unforgettable memory.

Last but not least, I would like to express my gratitude for my family, for their continuous support, love, and prayers during my studies.

Liling

TABLE OF CONTENTS

LIST OF FIGURES AND TABLES

List of Figures

List of Tables

ABBREVIATIONS

AD	Alzheimer's disease
ALS	Amyotrophic lateral sclerosis
BBB	Blood-brain barrier
BCA	Bicinchoninic acid
BFGF	Basic fibroblast growth factor
BDNF	Brain-derived neurotropic factor
DENV	Dengue virus (DENV), Zika virus (ZIKV), and West Nile virus (WNV) and
BMP	Bone morphogenetic protein
BSA	Bovine serum albumin
$CaCl_2$	Calcium chloride
CCI	Controlled cortical impact
CCK-8	Cell counting-8
CCL5	Chemokine ligand 5
CNS	Central nervous system
CTGF	Connective tissue growth factor
DAVID	The Database for annotation, visualization and integrated discovery
(db)-cAMP	dibutyryl-adenosine-cyclic monophosphate
DLS	Dynamic light scattering
DMEM	Dulbecco's modified Eagle's medium Brain-derived neurotrophic factor
EGF	Epidermal growth factor
ELISA	Enzyme-linked immunosorbent assay fetal bovine serum
EVs	Extracellular vesicles
FBS	Fetal bovine serum
FDR	False discovery rate
FTPL	Freeze and thaw platelet lysate
GO	Gene ontology
HDL	High-density lipoprotein
HGF	Hepatocyte growth factor
HIV	Human immune deficiency virus
HBV	Hepatitis B virus
HCV	Hepatitis C virus
HPL	Human platelet lysate

HPPL	Heat-treated platelet pellet lysate
HSCPL	Serum converted platelet lysate heated
IGF	Insulin-like growth factor
KEGG	Kyoto Encyclopedia of Genes and Genomes
LC-MS/MS	Liquid chromatography-tandem mass spectrometry
LDL	Low-density lipoprotein
LPS	Lipopolysaccharide
LRV	Long reduction value
LUHMES	Lund human mesencephalic
MPP	1-methyl-4-phenylpyridinium
MPTP	1-methyl-4-phenyl-1,2,3,6-tetrahydropyridine
MSC	Mesenchymal stromal cells
MVs	Microvesicles
MVM-MVP	Minute virus of mice-mock virus particle
NHPPL	Nanofiltered human platelet pellet lysate
NTA	Nanoparticle tracking analysis
PAS	Platelet additive solution
PBS	Phosphate buffer saline
PC	Platelet concentrates
PCS	Platelet concentrate supernatant
PD	Parkinson’s disease
PDGF	Platelet-derived growth factor
PEVs	Platelet extracellular vesicles
PF4	Platelet factor 4
PPL	Platelet pellet lysate
PRT	Pathogen reduction technology
PS	Phosphatidylserine
PLT	Platelet
RA	Retinoic acid
SCPL	Serum converted platelet lysate
SEC	Size exclusion chromatography
SN	Substantia nigra
SOD	Superoxide dismutase

TBI	Traumatic brain injury
TF	Tissue factor
TH	Tyrosine hydroxylase
TGF-β	Transforming growth factor-β
TNF-α	Tumor necrosis factor-α
TRPS	Tunable resistive pulse sensing
VEGF	Vascular endothelial growth factor
VT11A	Vesicle transport through interaction with t-SNAREs 1A

RÉSUMÉ SUBSTANTIEL EN FRANÇAIS

Il y a un intérêt croissant pour les applications cliniques de divers lysats plaquettaires humains (LPH) en médecine régénérative. Des preuves expérimentales et cliniques de plus en plus nombreuses soutiennent les produits dérivés des plaquettes sanguines, y compris le plasma riche en plaquettes (PRP) et le lysat plaquettaire d'origine autologue ou allogénique, comme étant à même de fournir des avantages thérapeutiques dans divers domaines de la médecine régénérative. Les domaines concernés sont entre autres la chirurgie orthopédique, la chirurgie maxillo-faciale et la cicatrisation des plaies des tissus mous, la thérapie cellulaire et l'ingénierie tissulaire. L'administration dans les yeux sous forme de gouttes des lysats semble également améliorer l'inconfort associé au syndrome de l'œil sec, favoriser la réparation des lésions cornéennes et améliorer les troubles épithéliaux. De nouvelles applications de préparations de lysats plaquettaires riches en neurotrophines sont en cours d'évaluation pour le traitement des troubles neurologiques, tels que l'accident vasculaire cérébral, la maladie de Parkinson, la maladie d'Alzheimer, la sclérose latérale amyotrophique et, éventuellement, d'autres, y compris les lésions cérébrales traumatiques.

Au fur et à mesure que la gamme d'applications cliniques validées scientifiquement s'élargit, il devient de plus en plus évident que des préparations de produits dérivés des plaquettes dédiées, ou « sur mesure », sont préférables sur le plan clinique pour s'adapter de manière optimale à chaque mécanisme de réparation tissulaire, avec une toxicité minimale due aux composants sanguins indésirables, le cas échéant. Par exemple, la présence de fibrinogène et de protéines plasmatiques adhésives dans les lysats plaquettaires standard suspendus dans le plasma peut être bénéfique pour la cicatrisation des tissus osseux et mous grâce à leur conversion en un puissant maillage à base de fibrine capable de favoriser la colonisation cellulaire et la régénération tissulaire. En revanche, le fibrinogène, en raison de sa neurotoxicité et de son implication dans la neuroinflammation et la pathogenèse des démences [1,2], peut-être indésirable pour une administration intracérébrale [3] ou pour les applications ophtalmologiques en raison des risques de gélification de la fibrine lors de l'application dans les yeux [4]. La méthode de préparation du LPH peut également affecter la teneur en vésicules extracellulaires [5], qui sont des messagers fonctionnels pour la réparation tissulaire et qui sont supposés influencer la capacité régénérative et stimulatrice de la croissance cellulaire des lysats dérivés des plaquettes sanguines [6-9]. Ces preuves indiquent que le mode de préparation des lysats plaquettaires peut

avoir des impacts importants sur leurs fonctions physiologiques et cliniques [10]. Il est donc crucial de mieux comprendre comment les méthodes de production des lysats affectent leurs diverses compositions et propriétés biochimiques afin que des produits dédiés de qualité, non toxiques et de fonctionnalité optimale soient disponibles pour une utilisation clinique sûre et efficace. Dans cette étude, nous avons préparé cinq types de LPH représentatifs de diverses préparations actuellement utilisées ou évaluées dans le domaine de la médecine régénérative et de la thérapie cellulaire. Ces produits ont été caractérisés en termes de contenu et de fonctionnalité.

De plus, les lysats plaquettaires, riches en facteurs trophiques neuroprotecteurs, anti-inflammatoires et anti-oxydants, ainsi qu'en vésicules extracellulaires (EVs), constituent désormais une biothérapie multifonctionnelle émergente pour le traitement des maladies neurodégénératives et traumatiques du système nerveux central (SNC). Les études in vitro et in vivo antérieures ont montré que le traitement par lysats peut (a) protéger contre la perte progressive ou aiguë de synapses, (b) restaurer l'intégrité neuronale et (c) contrebalancer la neuroinflammation, le stress oxydatif et la perte des fonctions cognitives et/ou motrices [11-14]. Des applications translationnelles de lysats plaquettaires, élaborées à partir d'un pool de concentrés plaquettaires (PCs) de donneurs de sang, sont maintenant envisagées, avec des essais cliniques prévus chez des patients atteints de SLA [15,16].

Les LPH destinés à l'administration cérébrale doivent être de qualité c'est-à dire non toxique et non infectieux et-doivent répondre aux spécifications établies. Les exigences de sécurité nous ont conduit à développer un lysat spécifique, appelé HPPL (pour « Heat-treated human Platelet Pellet Lysate en anglais ») dépourvu de plasma, de teneur relativement faible en protéines pour éviter la surcharge du liquide céphalorachidien, essentiellement exempt de protéines neurotoxiques ou coagulables, et présentant une faible activité pro-thrombogénique, protéolytique et pro-inflammatoire [17,18].

Comme le HPPL est fabriqué à partir de sang humain, une préoccupation essentielle est d'éviter le risque d'infections virales. La sécurité virale est particulièrement critique pour les lysats fabriqués à partir de plusieurs PCs allogéniques pour assurer une cohérence entre lots, car les mélanges de grand nombre de PCs augmente les risques de contamination virale. Il est essentiel de prévenir la contamination par des virus sanguins hautement pathogènes. La nanofiltration est une procédure de biotraitement pour l'élimination des virus dans l'industrie des produits

plasmatiques ; une solution de protéines purifiées est filtrée à travers un dispositif composé de plusieurs fibres de cellulose creuses modifiées, ayant un seuil de coupure de quelques nanomètres, suffisamment petit pour retenir les virus, mais suffisamment grand pour laisser passer les protéines à travers les membranes de taille nanométrique. Dans cette étude, nous avons évalué l'efficacité de la nanofiltration mise en œuvre pour produire un produit sûr contre les virus et leur impact sur la composition et l'activité fonctionnelle du HPPL.

Par ailleurs, nos études préliminaires montrent que le matériel de départ, le PCs, et les lysats plaquettaires contiennent un grand nombre de EVs, soulevant des questions actuellement sans réponse formelle quant à la contribution potentielle de ces EVs plaquettaires (PEV) à l'activité fonctionnelle des LPH. Les EVs sont connues pour jouer un rôle clé dans la communication intercellulaire et la signalisation cellulaire. En particulier, les EVs dérivées des plaquettes et de leurs granules pourraient renfermer d'importants facteurs de croissance, cytokines, et miARN, et exprimer des marqueurs spécifiques des plaquettes. Elles pourraient donc jouer un rôle à des fins thérapeutiques. Les VE de taille nanométrique sont d'importants cargos pour transporter des molécules biologiques encapsulées dans leur bicouche lipidique, capables de traverser les barrières tissulaires.

Objectifs de notre projet

Sur la base des informations de contexte fournies ci-dessus, les objectifs principaux de cette étude sont donc les suivants :

Évaluer (a) la composition et l'activité fonctionnelle de divers LPH, y compris celle apportée par les EVs, destinées à être utilisées pour des indications cliniques spécifiques, (b) l'efficacité de l'élimination des virus par nanofiltration, l'impact de la nanofiltration sur la composition de lysats chauffés et leurs fonctions thérapeutiques neuroprotectrices et neuro-régénératives (c) le profil de certaines préparations de PEVs sélectionnées pour leur caractérisation biophysique, leurs fonctions biologiques et leurs rôles dans la neuroprotection et la neuro-régénération.

Plan de notre travail

Afin de développer des préparations spécifiques les mieux adaptées pour des applications cliniques spécifiques, nous avons préparé et caractérisé diffèrent types de LPH. Nous avons préparé cinq types de lysats à partir des mêmes concentrés de plaquettes. Les produits préparés

sont les suivants : FTPL (Freeze-thaw platelet lysate), SCPL (frozen-thawed platelet lysate serum converted platelet lysate), HSCPL (heated serum converted platelet lysate), PPL (platelet pellet lysate) et HPPL. Ils ont été largement caractérisés par une série de tests pour déterminer et comparer leur composition en protéines, facteurs de croissance, cytokines, profils biochimiques, capacités de génération de thrombine, activités protéolytiques associées à la thrombine, potentiel pro-coagulant associé aux phospholipides, teneurs en VE exprimant la phosphatidylsérine et le facteur tissulaire, et propriétés antioxydantes.

Pour atteindre notre objectif d'évaluation des fonctions des EVs, nous avons d'abord isolé les EVs présents dans le lysat plaquettaire neuroprotecteur (HPPL-EVs) à l'aide d'une colonne de chromatographie d'exclusion stérique (SEC) et une autre préparation de VE a été obtenue à partir du surnageant de concentrés de plaquettes (PCS-EVs), par centrifugation à 20 000 x g pendant 90 minutes. Une fois isolées, la distribution des tailles taille, concentration et activité fonctionnelle de ces EVs ont été analyses en utilisant différentes techniques. Pour mieux comprendre la contribution des EV dans les fonctions du HPPL, une étape d'élimination des virus par nanofiltration sur des filtres de 20nm à l'aide de Planova 20N (Asahi Kasei) a été mise en œuvre, dans le but d'assurer la sécurité vis-à-vis des virus du HPPL pour un usage clinique, et aussi de dépléter les HPPL-EVs. L'efficacité de la nanofiltration pour éliminer les virus a été évaluée en ajoutant des particules virales factices de « Minute Virus of Mice" (MVM) suivies d'une analyse PCR quantitative par test immunologique. L'impact de la nanofiltration sur la composition du HPPL a été évalué. Les VE ont été soumises à une caractérisation physique et biologique pour évaluer le nombre, la distribution des tailles et le contenu fonctionnel (tels que les facteurs de croissance et les cytokines).

L'évaluation de l'activité neuroprotectrice et neuro-régénératrice des fractions d'EVs et du HPPL nanofiltré (NHPPL) a été réalisée en utilisant plusieurs tests in vitro et in vivo. Le NHPPL a été comparé à la fraction brute pour observer l'impact de la nanofiltration sur l'activité fonctionnelle du HPPL. Un modèle cellulaire de la maladie de Parkinson, dans lequel des neurones dopaminergiques non oncogènes différenciés humains (LUHMES) sont exposés à la neurotoxicité de l'érastine, a été utilisé à la fois pour l'évaluation du NHPPL et des PCS-EVs. L'effet de restauration neuronale des PCS-EVs et la capacité du NHPPL à induire la différenciation neuronale ont été évalués en utilisant des cellules de neuroblastome SH-SY5Y. Des cellules microgliales BV-2, soumises ou non à une stimulation par LPS, ont été utilisées pour prédire la capacité des PCS-EVs à moduler la réponse inflammatoire dans le cerveau. Une

étude in vivo utilisant un modèle de souris CCI TBI a été réalisée pour confirmer la capacité du NHPPL et des PCS-EVs à exercer une activité fonctionnelle lorsqu'ils sont administrés par voie intranasale. En particulier, leur potentiel à moduler les cytokines inflammatoires a été vérifié. L'évaluation de l'activité neuroprotectrice des PCS-EVs in vivo dans un modèle de souris MPTP (ULille) a été effectuée. La capacité des PCS-EVs à augmenter la tyrosine hydroxylase (TH) a été examinée par immunohistochimie. L'effet des PCS-EVs sur l'amélioration de la fonction motrice a été évalué par un test comportemental d'actimétrie.

Résultats et discussion

Différentes préparations de lysats de plaquettes humaines (LPH) diffèrent par leur composition et leurs propriétés fonctionnelles

Dans cette étude, nous avons préparé cinq lysats différents à partir de PCs prélevés par aphérèse chez des donneurs de sang sains. Les PCs n'ont pas été soumis à une leuco-filtration spécifique et les plaquettes étaient en suspension uniquement dans du plasma, comme cela se fait pour la plupart des applications en médecine régénérative [19].

Pour préparer le FTPL, le PC a été soumis à des cycles de congélation-décongélation [20] pour libérer le contenu des plaquettes. Ce traitement est utilisé pour produire du LPH pour la propagation ex vivo des cellules humaines en culture [9] et le FTPL est administré pour la cicatrisation des articulations [21,22]. Le SCPL est un LPH converti en sérum préparé par un traitement au sel de calcium qui induit la coagulation sanguine, la formation de fibrine, la dégranulation plaquettaire et la libération de facteurs de croissance. Ce processus est souvent utilisé pour générer un gel de fibrine plaquettaire ou un gel plaquettaire, pour soutenir la cicatrisation des plaies et tissus, ou la croissance osseuse [23-25], en assurant l'activation plaquettaire et la libération de facteurs de croissance ex vivo avant l'administration clinique 198. La séroconversion est également réalisée pour les gouttes oculaires de sérum utilisées pour le syndrome de l'œil sec, car l'élimination du fibrinogène semble préférable [26,27]. Le HSCPL a été évalué ici car le traitement thermique à 56°C pendant trente à soixante minutes inactive les composants immunologiques et améliore l'expansion des cellules de l'épithélium et de l'endothélium cornéens, suggérant des bénéfices cliniques dans le traitement des troubles oculaires [27-29]. Le PPL est fabriqué à partir de plaquettes isolées et est donc dépourvu de compartiment protéique plasmatique. Des préparations similaires ont été évaluées pour le traitement des accidents vasculaires cérébraux chez l'animal [5]. Enfin, le HPPL, également

inclus dans cette étude, est un lysat plaquettaire purifié [30] pour l'administration cérébrale et le traitement des troubles neurologiques ; il a été chauffé à 56°C pendant 30 min pour éliminer davantage le fibrinogène, inactiver les enzymes protéolytiques et améliorer l'activité neuroprotectrice [3,31,32].

Les fractions de LPH diffèrent en termes de profil protéique, de propriétés biochimiques et fonctionnelles : ceci peut avoir un effet sur la sécurité et l'efficacité pour certaines indications cliniques

Nous avons sélectionné un large éventail de tests pour caractériser ces lysats plaquettaires. La teneur en protéines, facteurs de croissance, albumine, IgG, fibrinogène, composants du complément et les études de profilage des cytokines et des protéines liées à l'angiogenèse fournissent une "image" protéomique pertinente de ces LPH. Ces analyses révèlent la présence du plasma par rapport aux protéomes plaquettaires et identifient la présence de facteurs de croissance, de cytokines ou de nutriments considérés comme pertinents pour la fonctionnalité des LPH en médecine régénérative et thérapie cellulaire[19,33-36]. Nos données ont révélé des différences majeures dans la composition et les propriétés fonctionnelles de ces produits. Le PPL et le HPPL, préparés à partir de plaquettes isolées, étaient enrichis en facteurs de croissance, avec des concentrations significativement plus élevées en BDNF, PDGF-AB, EGF, VEGF et TGF-β, que les autres LPH, ainsi qu'un enrichissement très significatif par rapport aux protéines totales, reflétant l'impact de l'élimination du plasma. En revanche, le FTPL et le SCPL, respectivement fabriqués à partir de plaquettes diluées dans du plasma normal ou séroconverti, contenaient des quantités plus importantes d'IGF-1, comme prévu en raison de sa présence dans le compartiment plasmatique [35], ainsi que des quantités détectables d'autres facteurs de croissance. Le traitement thermique a légèrement diminué la présence de tous ces facteurs dans le HSCPL par rapport au SCPL. La diminution était plus prononcée pour le contenu en BDNF, PDGF-AB et EGF dans le HPPL par rapport au PPL, tandis que le rapport VEGF/protéine restait stable et que le TGF- β était enrichi lors du traitement thermique. Les contenus antigéniques de C3 et C4, principales protéines des voies du complément et du système immunitaire [37] dans le FTPL, SCPL et HSCPL, étaient comparables à ceux du plasma normal (C3 : 8044 mg/dL), suggérant aucune élimination substantielle lors de la préparation de ces LPH. En revanche, le PPL et le HPPL avaient de faibles teneurs en C3 et C4, ce qui est cohérent avec leur présence dans le compartiment plasmatique [38] et que les plaquettes ont un contenu relativement faible [39]. Des études récentes ont montré que la surexpression de ces deux

protéines contribue à l'aggravation de l'inflammation, entraînant une perte neuronale dans la maladie d'Alzheimer et d'autres troubles neurologiques [40,41]. Par conséquent, l'utilisation de LPH appauvris en C3 et C4, comme c'est le cas pour PPL et HPPL, peut être préférable pour l'administration cérébrale.

Une analyse de profilage du protéome a détecté des protéines connues pour être présentes dans les plaquettes (telles que BDNF, CCL5 (RANTES), CXCL-5, composant du complément C5, facteur du complément D, EGF, FGF-19, lipocaline-2, MIF, MMP-9, PF-4, PDGF-AA, PDGF-AB, thrombospondine-1, TIMP-1 et VEGF) dans tous les LPH. Des différences dans les profils des cytokines et des protéines liées à l'angiogenèse, BAFF, prolactine et TIMP-4, ont été observées parmi les LPH. L'observation du profil protéique des LPH nécessite une caractérisation supplémentaire avec une analyse protéomique complémentaire telle que la spectrométrie de masse suivie d'un test de quantification ultérieur. La présence de facteurs neurotrophiques, de protéines liées à l'anti-angiogenèse ou de protéines impliquées dans la régénération tissulaire, ainsi que d'autres cytokines connues pour jouer un rôle dans des conditions physiologiques et pathologiques particulières, est importante à connaître pour une meilleure indication de l'utilisation des LPH.

L'analyse biochimique a indiqué que FTPL, SCPL et HSCPL contenaient plus d'albumine, de glucose, d'IgG et de lipides (HDL et LDL) que le PPL et le HPPL, ce qui est cohérent avec l'absence du plasma dans les deux dernières fractions. Le fibrinogène n'a été détecté que dans le FTPL, ce qui est également cohérent avec l'absence d'une étape d'élimination des facteurs de coagulation, et était indétectable (< 0,4 mg/ml) dans SCPL séroconverti et PPL sans plasma, ainsi que dans leurs fractions respectives traitées par la chaleur. La teneur plus élevée en Cl et Ca dans le SCPL et HSCPL est probablement due à l'ajout de $CaCl_2$ pour la conversion en sérum. Des niveaux plus élevés de Cl, K et P dans PPL et HPPL peuvent être expliqués par la suspension du culot plaquettaire dans le PBS (qui contient NaCl, KCl, Na_2HPO_4 et KH_2PO_4).

Notre étude a révélé des différences importantes dans la capacité de générer de la thrombine entre les LPH, telle que déterminé par TGA. En utilisant à la fois une concentration "faible" et "élevée" de micelles de phospholipides contenant du facteur tissulaire humain recombinant et du $CaCl_2$, des quantités plus importantes de thrombine ont été générées dans FTPL, SCPL et HSCPL au fil du temps, mais nettement moins dans PPL, et la génération de thrombine était indétectable dans HPPL. De plus, nous avons évalué toute activité protéolytique de type thrombine en utilisant le substrat chromogénique, S-2238. Le plasma activé par $CaCl_2$ et le

plasma normal ont été utilisés respectivement comme témoins positifs et négatifs. Aucune activité protéolytique n'a été détectée dans FTPL, comme prévu en raison de l'absence d'une étape d'activation. En revanche, l'activité protéolytique était significativement plus élevée dans SCPL ($p < 0,0001$) mais diminuait significativement ($p < 0,0001$) après traitement thermique dans HSCPL, par rapport à PPL et au plasma non activé. Aucune activité protéolytique n'a été détectée dans HPPL. Dans SCPL et HSCPL, l'ajout de $CaCl_2$ a activé les zymogènes des facteurs de coagulation en enzymes protéolytiques, conduisant à la formation de thrombine et de fibrine, car le matériel utilisé pour générer SCPL et HSCPL contenait toute la gamme des facteurs de coagulation présents dans le plasma. En revanche, PPL, qui est dépourvu de la plupart du compartiment plasmatique, contenait significativement moins de thrombine, et le traitement thermique pour produire HPPL a conduit à la précipitation ou à l'inactivation de la thrombine, car la thrombine est sensible à la chaleur [30,42]. Cette observation soutient la préférence pour l'HPPL (lysat de plaquettes à haute concentration en protéines) pour l'administration au cerveau. L'HPPL peut également être préféré pour la réparation des tissus délicats ayant pour origine embryonnaire la crête neurale, tels que l'endothélium cornéen, où les neurotrophines peuvent être précieuses pour la fonctionnalité cellulaire [43], mais pour lequel l'activité protéolytique et le dépôt de fibrine seraient préjudiciables à la cornée [44]. En revanche, la présence de prothrombine ou de thrombine dans le FTPL, le SCPL et le HSCPL peut induire bénéfiquement un maillage de fibrine 3D utile pour la guérison des ulcères cutanés et des brûlures [45-47].

Des dosages dédiés pour déterminer les EV exprimant du PS et du TF ont été effectués pour évaluer un autre aspect de l'activité pro-coagulante des lysats plaquettaires humains. Le PS est un phospholipide anionique coagulant actif capable de se lier à l'acide γ-carboxy glutamique [48] chargé positivement, l'une des protéines de la cascade de la coagulation [49,50]. Les EV des lysats peuvent exprimer du TF et du PS, qui sont des initiateurs puissants de la coagulation [51]. Toutes les fractions de lysat, en particulier PPL, contenaient des VE exprimant du PS. Les teneurs plus élevées en PS dans le PPL sont cohérentes avec sa production à partir de plaquettes isolées, la source de ces EV. De plus, la conversion sérique et la formation de fibrine pendant la préparation du SCPL et du HSCPL peuvent "consommer" et piéger les EV exprimant du PS dans le caillot de [52]. Le traitement thermique à la fois du SCPL et du PPL a diminué l'activité pro-coagulante et le nombre de VE exprimant du PS. Ce résultat est étayé par le dosage STA-procoagulant-PPL qui a révélé des temps de coagulation plus courts du SCPL et du FTPL par rapport au PPL, et une prolongation du temps de coagulation dans les deux fractions traitées à

la chaleur. Il n'y avait pas de VE portant du TF détectables dans l'une des fractions de LPH, soutenant l'absence d'expression de TF par les plaquettes des donneurs de sang sain [53]. L'antioxydation peut contrebalancer un environnement difficile avec un stress oxydatif élevé qui existe dans certaines conditions pathologiques, telles que les troubles neurodégénératifs [54], l'arthrose [55] et les maladies oculaires [56]. Les FTPL, SCPL et HSCPL avaient la plus forte capacité antioxidante absolue, probablement en raison de leur contenu en plasma, qui contient des protéines antioxydantes telles que l'albumine, ainsi que de l'acide ascorbique et de l'acide urique [57-59]. Les PPL et HPPL, préparés à partir de plaquettes purifiées, présentaient également des activités antioxydantes, avec des niveaux similaires à ceux des autres lysats plaquettaires et plus que le contrôle plasmatique lorsqu'ils étaient exprimés par rapport au taux de protéines totales. En conclusion, les cinq préparations de lysats plaquettaires différent considérablement en termes de teneur en protéines, de composants du profil protéique, de compositions chimiques et d'activités fonctionnelles selon le mode de préparation. Ces différences peuvent avoir des impacts biologiques pertinents et doivent être soigneusement prises en compte lors du développement et de la sélection de préparations de lysats plaquettaires pour des objectifs cliniques spécifiques. Des recherches supplémentaires sont nécessaires pour définir quels lysats sont les mieux adaptées à chaque application clinique.

Cette découverte constitue une preuve supplémentaire de sélection du HPPL comme traitement préféré parmi les lysats de plaquettes pour l'administration cérébrale. Le HPPL peut également être préférable pour la réparation de tissus sensibles tels que l'endothélium cornéen, où les neurotrophines pourraient être précieuses pour la fonctionnalité cellulaire [43], mais l'activité protéolytique et le dépôt de fibrine seraient nocifs pour la cornée [44]. En revanche, la présence de prothrombine ou de thrombine dans FTPL, SCPL et HSCPL, peut induire de manière bénéfique un échafaudage de fibrine en 3D utile pour la cicatrisation des ulcères cutanés et des brûlures [45-47].

La mise en œuvre de la nanofiltration pour développer un HPPL non-infectueux (surtout d'origine virale) et depourvu de EVs.

Pour une administration cérébrale sûre, ce HPPL est délibérément déplété du compartiment des protéines plasmatiques et est traité à la chaleur ; un tel traitement élimine les protéines plasmatiques pour éviter la surcharge en protéines du LCR, le fibrinogène neurotoxique et les facteurs prothrombotiques et les enzymes protéolytiques. Il est également vital d'élaborer des

LPH qui répondent aux normes de sécurité virale pour l'application clinique. Étant donné que les lysats de plaquettes sont fabriqués à partir de sang humain, la sécurité virale est obligatoire compte tenu de l'histoire des transmissions virales massives par les produits sanguins en pool, et que la standardisation des lysats nécessite de « pooler » les PCs.

En effet, des études précliniques antérieures ont montré que notre HPPL sur mesure est hautement neuroprotecteur dans un modèle de souris MPTP de la PD [18]. Dans des modèles de souris de TBI léger et modéré/sévère, HPPL a également été trouvé capable de moduler les réponses immunitaires, promouvoir la guérison des plaies et améliorer la fonction cognitive function [60] Ces modèles in vivo ont confirmé les activités neuroprotectrices et neuro-régénératrices in vitro des HPPLs dans les cellules neuronales primaires et les cultures de cellules neuronales [11,32]. Ces données impliquent que HPPL pourrait être une option thérapeutique prometteuse, en particulier pour le traitement des troubles neurologiques.

De plus, notre précédente étude a montré que les fractions de LPH contenaient une population abondante de vésicules extracellulaires (EVs), jusqu'à 10^{11}-10^{12} / mL, y compris dans le HPPL. Elles pourraient être libérées en conséquence du processus d'activation ou du stress de cisaillement lors de la préparation du lysat preparation [61,62]. Les EVs libérées par les plaquettes (PEVs) pourraient agir comme des particules de signalisation entre les plaquettes et d'autres cellules, contenant des substances biologiques dérivées des plaquettes, y compris des facteurs de croissance et des cytokines provenant des granules α, et elles pourraient contribuer de manière significative à la communication intracellulaire de la réponse et de la fonction plaquettaires function [63]. Ainsi, il est suggéré que les PEVs pourraient soutenir le rôle fonctionnel des plaquettes pour la thérapie régénérative. Le nombre élevé de PEVs, en particulier dans le HPPL, soulève la question de savoir quelle peut être la contribution de ces EVs à leur activité neuroprotectrice. La présence de PEV pourrait contribuer à l'action bénéfique de l'HPPL, et s'ils s'avéraient néfastes, leur élimination de l'HPPL serait alors envisagée.

La nanofiltration est connue pour sa robustesse en matière d'élimination d'un nombre important de virus et permet donc améliorer la sécurité des produits dérivés du plasma sanguin. Selon la taille des pores, les filtres capturent à la fois les virus enveloppés et non enveloppés [64,65]. Dans cette expérience, nous avons utilisé un filtre dénommé Planova-20N (ASAHI Kasei, Japon) composé de fibres de cellulose creuses, avec une taille de pore de ±19 nm. Il est suffisamment

petit pour retenir les virus et est encore considéré comme suffisamment grand pour permettre aux protéines de passer à travers les membranes nanométriques. D'autre part, ce filtre pourrait potentiellement éliminer d'autres particules, y compris les EVs.

Ainsi, dans la deuxième partie de notre travail, nous avons évalué la faisabilité et l'efficacité de la nanofiltration mise en œuvre pour assurer la sécurité virale du HPPL. Nous avons également évalué son impact sur les compositions du HPPL, y compris leur contenu en protéines et en EVs et plus important encore, leur activité neuroprotectrice et neuro-régénérative. De plus, bien que les EVs aient été éliminés tout au long du processus de filtration, cela nous pousse à déterminer le rôle neuroprotecteur de ces EVs seuls en menant une expérience pour isoler et évaluer leur activité séparément

La faisabilité de la nanofiltration et la valeur de réduction des virus.

Notre étude a identifié pour la première fois que HPPL pourrait être soumis à un processus de nanofiltration dédié à l'aide de cartouches de taille de pore de 19 nm. Le HPPL à faible teneur en protéines a été préparé à partir de PC centrifugés pour précipiter les plaquettes et éliminer le plasma. Le HPPL a été préfiltré à l'aide de filtres de 0,2 et 0,1 µm pour réduire tout risque de colmatage lors de la nanofiltration, un problème courant avec les solutions protéiques complexes. Dans cette étude, plus de 20 mL de HPPL ont pu être filtrés à travers le système Planova-20N de 0,001 m² en environ 3,5 h à un débit constant de 0,1 mL/min et à faible pression, correspondant à plus de 20 L de HPPL à l'échelle industrielle en utilisant une cartouche commerciale Planova-20N de 1 m² (et plus de 80 L en utilisant une cartouche commerciale Planova-20N de 4 m²). Nous nous attendons, sur la base de données précliniques data[15,18,60] et en considérant le volume du liquide cérébrospinal chez l'homme, qu'un lot de 20 L permettrait de traiter environ 80 patients par an en utilisant une dose de traitement de 5 mL par patient par semaine.

La capacité d'élimination virale, évaluée par la détection immuno-qPCR de MVP, fut supérieure à 5 unités logarithmiques, démontrant ainsi l'efficacité de la nanofiltration pour éliminer même de petits virus. La nanofiltration peut éliminer une large gamme de virus et a contribué à améliorer la sécurité des produits dérivés du plasma industriel grâce à un mécanisme d'élimination déterminé par la taille du virus par rapport à celle de la membrane [64,65]. Dans l'industrie des produits biologiques, y compris les produits dérivés du plasma

sanguin, la nanofiltration s'est en effet avérée être une méthode robuste d'élimination virale [65,66]. Les filtres utilisés pour les produits mis sur le marché ont généralement une taille de pore moyenne de 35, 19 ou 15 nm [66,67]; la sélection du seuil de coupure de la nanofiltration dépend des caractéristiques (en particulier la taille) des protéines à soumettre à la nanofiltration afin d'éviter l'obstruction du filtre (la taille des protéines sanguines varie approximativement de 3 à 15 nm) [67]. Une revue complète indique que le nanofiltre Planova 20N avec une taille de pore moyenne de 19 ± 2 nm est capable d'éliminer tous les virus connus transmis par le sang, y compris le petit parvovirus B19 non enveloppé (B19V) d'une taille de 18 à 26 nm et le virus de l'hépatite [65]. A d'une taille de 26 à 29 nm, de divers produits fractionnés du plasma humain industriel. La capacité de Planova 20N à éliminer de manière robuste le B19V a également été démontrée par des observations microscopiques du nanofiltre [68]. Enfin, un autre petit virus non enveloppé transmis par le sang, le virus de l'hépatite E [5], d'une taille de 27 à 34 nm, a également été démontré être éliminé par Planova 20N.[69]

Par conséquent, tous les virus transmis par le sang connus et cliniquement pertinents sont éliminés par Planova 20N, offrant une grande marge de sécurité à NHPPL. Ainsi, Planova-20N devrait éliminer de manière robuste tous les virus transmis par le sang, qu'ils soient enveloppés ou non enveloppés.

L'impact de la nanofiltration sur le contenu de HPPL : élimination des VE et des protéines associées

Comparé au produit non-nanofiltré, le NHPPL était dépourvu de VE, y compris les PEV exprimant le PS pro-coagulant, tout en préservant largement la composition en protéines, comme révélé par la protéomique LC/MS-MS. Plus important encore, l'étape de nanofiltration n'a pas altéré les propriétés neuroprotectrices, neurorestauratrices ou anti-inflammatoires de HPPL dans des modèles cellulaires in vitro de la maladie de Parkinson et du TBI, et lors d'une administration i.n. chez un modèle de souris de TBI. Ces données sont essentielles pour les futures évaluations cliniques, l'approbation réglementaire et l'octroi de licences de préparations de LPH virales sûres et fonctionnelles produites à partir de pools de PCs humains. Les données de quantification des protéines et les évaluations ELISA ont identifié des diminutions de protéines totales et de facteurs de croissance, tels que PDGF-AB et VEGF, qui pourraient refléter une dilution survenue pendant la nanofiltration et/ou une adsorption non spécifique sur les membranes en fibres creuses de Planova-20N. Ces facteurs de croissance ont été

sélectionnés car ce sont des neurotrophines importantes que nous avons évaluées dans nos études précédentes pour caractériser HPPL[14,18,32,60,70]. De plus, leur masse moléculaire (VEGF : env. 40 kDa ; PDGF : env. 30 kDa ; et EGF : env. 6 kDa) est représentative de celle des facteurs trophiques HPPL, un paramètre pertinent pour évaluer une technologie de réduction de virus basée sur l'exclusion de taille. De plus, ces facteurs de croissance pourraient potentiellement être associés à des PEV et à d'autres vésicules lipidiques présentes dans HPPL et éliminées par la séquence de filtration. De plus, nous avons restreint la détermination ELISA à ces trois facteurs de croissance car une caractérisation plus étendue des impacts du processus de nanofiltration a été réalisée par la protéomique. L'analyse protéomique a identifié que le traitement thermique précédemment trouvé pour améliorer ou normaliser la sécurité et l'efficacité de HPPL[18,32], a conduit à une élimination encore plus prononcée du fibrinogène et des facteurs thrombogènes. Une diminution du nombre total de protéines était détectable après la nanofiltration, mais plus de 80% d'entre elles étaient communes. Les protéines contribuant aux fonctions essentielles de HPPL pour la thérapie cérébrale, telles que les antioxydants, les cytokines et les facteurs neurotrophiques, étaient bien préservées dans le NHPPL, avec une grande similitude dans les processus biologiques impliqués. La base de données KEGG a montré que la séquence de filtration/nanofiltration a retiré des protéines associées à des voies pathologiques, principalement liées aux infections bactériennes/virales/parasitaires et aux pathologies cancéreuses. Cette diminution peut refléter la suppression de PEVs, comme discuté ci-dessous. En effet, les PEVs sont associés à des réactions biologiques lors d'infections ou lors de la progression du cancer [71]. De plus, les plaquettes dans la circulation sanguine contribuent aux mécanismes de défense contre divers pathogènes et peuvent subir une activation qui déclenche de multiples voies de signalisation via leurs produits de sécrétion et le recrutement de cellules immunitaires [72,73]. De plus, l'analyse des voies KEGG a révélé une diminution de l'abondance de certaines protéines impliquées dans la coagulation par filtration. Cette observation soutient que le NHPPL devrait avoir un risque de thrombogénicité encore plus faible que le HPPL lorsqu'il est administré au cerveau.

Un autre aspect informatif fut l'impact de la nanofiltration sur la suppression des EVs. La plupart des protéines éliminées étaient associées aux exosomes extracellulaires. Les EVs peuvent être classés en "petites", "moyennes" ou "grandes" selon leur taille [74]. Dans les lysats de plaquettes, les EVs ont une taille comprise entre environ 50 et 300 nm 300 nm [75]. Planova 20N, avec une taille de pore moyenne de 19 nm, a supprimé les particules plus grandes que cette taille. Les protéines associées aux EVs encore détectées après la nanofiltration peuvent

suggérer leur présence sous forme soluble ou une possible disruption des EVs en entités plus petites lors du processus de nanofiltration. La suppression des EVs a été confirmée par des analyses de DLS, NTA et des tests fonctionnels d'EVs prothrombotiques et procoagulants. L'analyse de DLS a montré une diminution de la distribution de taille des particules d'environ 280 nm dans le HPPL à environ 12 nm dans le NHPPL. La séquence de filtration a diminué le nombre d'EVs de près de 99% (2 logs), comme indiqué par NTA. La valeur peut être sous-estimée en raison de la présence de protéines dans la plage de 5~12 nm qui ne sont pas supprimées par la nanofiltration et réactives par DLS et NTA. De plus, le test fonctionnel MP-PS, un test de capture qui quantifie les EVs fonctionnelles exprimant du PS, a été utilisé pour évaluer l'impact de la nanofiltration sur ces EVs spécifiques. Une étude précédente a montré que le traitement du HPPL à 56 °C pendant 30 minutes réduit la teneur en EVs exprimant du PS fonctionnel [70]. Nous avons trouvé ici que la quantité d'EVs portant du PS dans le NHPPL était significativement diminuée par rapport au HPPL. L'essai STA-procoagulant-PPL, qui est un test de temps de coagulation dépendant de phospholipides procoagulants, a suggéré la suppression de PEV procoagulantes, comme l'indique une prolongation marquée du temps de coagulation du NHPPL par rapport au HPPL. La diminution des PEV exprimant le PS due à la nanofiltration devrait encore limiter les risques de coagulation et donc améliorer davantage la sécurité du NHPPL pour l'administration au cerveau.

Le HPPL nanofiltré conserve ses potentiels neuroprotecteurs et neuro-régénératifs

Une étude in vitro a été réalisée en utilisant des cellules LUHMES comme modèle de maladie de Parkinson pour déterminer l'impact de la nanofiltration sur l'activité neuroprotectrice du HPPL. Le NHPPL à une dose de 5% (v/v) n'était pas toxique et a maintenu sa capacité à protéger les cellules contre l'érastine neurotoxique. Les cellules sont restées viables 24 heures après le traitement, similaire à ce qui a été observé avec le HPPL dans nos études précédentes [18,76]. De plus, nous avons évalué la capacité du NHPPL à stimuler la maturation cellulaire, comme cela avait été observé précédemment avec le HPPL [32,76].

Notre étude utilisant la lignée de neuroblastomes SH-SY5Y a révélé qu'après une semaine de traitement avec 2% de NHPPL, les cellules exprimaient fortement le marqueur de différenciation β-III tubulin, similaire à ce qui avait été observé avec le HPPL et les contrôles RA positifs. Ainsi, le NHPPL a maintenu sa capacité à favoriser la différenciation et la maturation cellulaire, ce qui est essentiel pour compenser la dégénérescence neuronale progressive.

Nous avons réalisé un modèle *in vivo* de traumatisme crânien léger (« TBI ») [77], pour évaluer la capacité du NHPPL à moduler les marqueurs inflammatoires après une commotion, comme cela avait été trouvé précédemment avec le HPPL non-nanofiltré [60]. Le HPPL et le NHPPL ont été administrés par voie intranasale sur trois jours consécutifs et leurs actions anti-inflammatoires dans les tissus corticaux ipsilatéraux ont été évaluées sept jours après la lésion. Les deux ont été administrés à une dose de 60 µL / jour pour une dose totale de 180 µL sur trois jours. Cette posologie quotidienne a été sélectionnée sur la base de nos études in vivo précédentes utilisant le HPPL dans des modèles de souris PD [18] and TBI [60]. De plus, l'activité fonctionnelle in vitro des lots de HPPL et NHPPL utilisés ici était cohérente avec celle observée avec le HPPL dans nos études précédentes [14,18,32]. Les données d'expression des gènes ont montré que la surexpression des marqueurs inflammatoires chez les souris atteintes de TBI non traitées était significativement régulée à la baisse chez les souris traitées avec le HPPL et le NHPPL. Ce résultat suggère que, après la nanofiltration, le HPPL a conservé son potentiel anti-inflammatoire dans les modèles de TBI. De plus, par rapport à notre étude précédente où des administrations topiques et intranasales étaient effectuées, nos résultats actuels démontrent que dans ce modèle de souris TBI, l'administration intranasale seule du NHPPL était efficace.

Ceci est cliniquement vital pour le traitement des TBI où il n'y a pas d'accès au cerveau et l'administration intranasale serait la seule option de livraison envisageable [60], Nos données indiquent que l'élimination des PEV de l'HPPL par nanofiltration n'affecte pas l'activité neuroprotectrice, suggérant que ces EV ne sont pas essentielles à ce biomatériau plaquettaire. Cependant, les EV d'autres lysats plaquettaires favorisent la croissance et la migration des cellules neuronales et stimulent la formation de réseau dans les cultures neuronales primaires [75].

L'évaluation des potentiels neuroprotecteurs et neuro-régénérateurs des PEVs

Afin de confirmer l'activité fonctionnelle des EV dans le HPPL (HPPL-EVs), nous les avons d'abord analysés séparément. Ces EV ont été isolés par chromatographie SEC-Izon et leur concentration a été déterminée en utilisant NTA.

Une évaluation utilisant un modèle de cellules LUHMES in vitro exposé à l'erastin a été réalisée. Un nombre total d'environ $4x10^{10}$, $1x10^{11}$ et $2x10^{11}$ d'EVs dérivées de HPPL n'a pas affecté de manière significative la viabilité cellulaire après 24 heures, suggérant une absence

de toxicité a court terme. Cependant, ils n'ont pas pu protéger les cellules LUHMES de la neurotoxicité de l'erastin. Cela confirme notre découverte selon laquelle après l'élimination des EV et des virus dans HPPL en utilisant la nanofiltration, HPPL conserve encore son potentiel neuroprotecteur. Cependant, une autre préparation de PEV isolée à partir du surnageant de concentré plaquettaire (PCS-EVs) a été testée dans le même temps et a pu exercer une activité neuroprotectrice. Cela montre que différents types de préparations de EVs peuvent exercer une activité fonctionnelle différente. Il est probable que cela soit dû à des facteurs de déclenchement différents. Les HPPL-EVs ont été produites par des étapes de congélation-décongélation et ont donc exprimé une PS [78] plus élevée. De plus, comme cela a été noté précédemment, l'élimination des EV dans HPPL après la nanofiltration a été accompagnée d'une diminution de la PS pro-coagulante, reflétant leur activité fonctionnelle. En fait, les PCS-EVs sont des vésicules naturellement présentes dans le surnageant de plasma. Une étude a montré que les EV isolées à partir du plasma sans stimulation ne présentent pas de conjugaison avec l'annexine - montrant une PS [79] nulle ou faible, ce qui suggère que cette préparation de EV est moins pro-coagulante et plus adaptée à l'administration cérébrale. Nous avons donc procédé à une caractérisation plus poussée des PCS-EVs sur leur profil biophysique et leurs activités fonctionnelles.

Notre analyse a montré que les PCS-EVs isolées présentent un profil de distribution de taille cohérent avec les études précédentes sur les EV dans le plasma ou le sérum humain serum [80,81]. Déterminées par DLS, les PCS-EVs avaient une population hétérogène avec une taille de population majeure d'environ 200 nm et une plage de tailles allant de 70 à 350 nm. Les mesures de NTA et TRPS ont révélé que la concentration en EVs dans cette préparation était comprise entre 10^{10} et 11^{11} particules/mL.

Le profil protéique des PEVs issues des PCS a été caractérisé par ELISA et une analyse protéomique. Les données ont montré que les PEVs des PCS contiennent une quantité substantielle de BDNF, PDGF, EGF et VEGF. Le PDGF, le BDNF, l'EGF et le VEGF sont des facteurs de croissance particulièrement abondants dans les plaquettes, et donc leur abondance relative dans les PEVs n’est pas très surprenant. expected [3,82]. L'analyse protéomique a également confirmé la présence de ces facteurs et a révélé d'autres facteurs, notamment des cytokines et des antioxydants plaquettaires : PDGF-A, PDGF-B, VEGF, HGF, TGF-β1, IGF, protéine kinase dépendante de cAMP, catalase, glutathion S-transférase, glutathion

peroxydases, SOD 1,2, protéine riche en glutamate, VTI1A, glutathion réductase, facteur de maturation des cellules gliales.

L'analyse d'enrichissement à l'aide des ressources bioinformatiques DAVID 6.8 a montré que la dégranulation et l'activation des plaquettes, l'adhérence cellulaire, la réponse immunitaire et l'endocytose médiée par les récepteurs faisaient partie des processus biologiques impliqués par les composants protéiques dans les PEVs des PCS. Le cluster hautement enrichi trouvé dans l'analyse d'annotation fonctionnelle était surtout lié à l'endopeptidase de type sérine et à son inhibiteur, aux protéines intégrine et de liaison à l'antigène, et à la liaison cadhérine impliquée dans l'adhérence cellulaire. Les protéines associées aux microparticules sanguines (MVs), aux granules alpha plaquettaires, à la protéine kinase dépendante de cAMP ont été confirmées comme faisant partie des composants abondants majeurs dans les PEVs des PCS.

Notre travail initial visait à confirmer l'activité neuroprotectrice des PCS-EVs en utilisant des cellules LUHMES. Les résultats ont montré qu'un nombre d'environ 2x 10^{11} PCS-EVs étaient capables d'exercer une activité neuroprotectrice significative contre la neurotoxicité de l'erastin. Les PCS-EVs ont été démontrés leur capacité à exercer une neuroprotection avec une viabilité cellulaire de 65 % comparée à 17 % sans traitement. Les PCS-EVs dérivés des plaquettes elles-mêmes sont connus pour transporter une pléthore de molécules fonctionnelle qui proviennent à l'origine des granules denses et α, expliquant leur activité protectrice. De plus, les molécules antioxydantes trouvées dans les PCS-EVs telles que les glutathion peroxydases, SOD1 et SOD2, pourraient être impliquées dans la baisse de l'augmentation des espèces réactives d'oxygène lipidiques nocives induites par la ferroptose après un traitement à l'erastin [83-85].

De plus, en prenant en compte le contenu des facteurs de croissance régulant de nombreux processus dans la cicatrisation cellulaire et des plaies, la capacité des PCS-EV à favoriser la croissance et la réparation neuronale in vitro a été évaluée. Des cellules de neuroblastome humain SH-SY5Y ont été utilisées en conjonction avec un test de blessure par égratignure établi. Nous avons révélé que les PCS-EV augmentaient significativement la capacité de réparation neuronale en favorisant la reconnexion neuronale. Ceci est cohérent avec la découverte selon laquelle une variété de facteurs de croissance, notamment le PDGF, le BDNF, l'IGF-1, sont capables de stimuler la différenciation et d'augmenter la survie cellulaire des SH-SY5Y [85-87].

Nous avons également testé les effets du traitement sur l'activation microgliale avec des cellules BV-2. Le marqueur pro-inflammatoire TNF-α, qui est l'une des principales cytokines libérées par les cellules microgliales lors de l'activation par LPS, a été mesuré [88,89]. Nos résultats ont démontré que les PCS-EV, à la dose utilisée, exercent des activités anti-inflammatoires et réparatrices favorables chez les BV-2 activees es par LPS. Cependant, avec une double concentration, il y a eu une augmentation de l'expression de TNF-α, indiquant que la dose plus élevée de PCS-EV était inefficace pour inhiber l'activation de BV-2 causée par l'induction de LPS. L'élévation de TNF-α est probablement due à une accumulation de protéines plus importante qui conduit à une réponse suractive de BV-2 causée par LPS. Dans des conditions normales (c'est-à-dire sans stimulation par LPS), les PCS-EV dans les deux doses utilisées n'ont pas déclenché d'expression significative de TNF-α par rapport au témoin, ce qui montre qu'ils n'ont pas induit l'activation des microglies BV-2, confirmant la sécurité du traitement par PCS-EV.

Effet anti-inflammatoire et neuro-protecteur in vivo des PCS -EV

Dans la présente étude, nous avons examiné pour la première fois l'efficacité des EV-PCS administrées par voie intranasale pour moduler les actions inflammatoires en utilisant un model murin de TBI. Le modèle CCI bien établi a été utilisé pour induire une faible lesion en avec des paramètres contrôlés. Les EV-PCS administrées pendant trois jours consécutifs après la blessure ont contribué à exercer un effet anti-inflammatoire après la lesion. Les marqueurs inflammatoires tels que TNF-α, GFAP, CCL4, TLR2 et TREM2, initialement surexprimés après la blessure, ont montré une tendance à diminuer avec le traitement par les EVs.

De plus, dans nos expériences avec un modèle de PD, des souris MPTP ont été soumises à une administration i.n. de PCS-EVs. MPTP est un modèle animal validé et fiable de la maladie de Parkinson utilisé pour cibler spécifiquement les neurones dopaminergiques. Dans cette étude, nous avons utilisé un modèle aigu classique de souris MPTP où 4 doses ont été utilisées en une journée. Les PCS-EVs ont été administrées par voie intranasale un jour avant l'intoxication. Nos résultats ont montré que le traitement par les PCS-EVs améliorait la fonction locomotrice après la détérioration chez les souris MPTP. Cela a été démontré en particulier par l'augmentation du nombre de redressements chez les souris traitées par les PCS-EVs à certaines doses (4×10^{10} particules d'EVs). Suite à nos résultats comportementaux, l'analyse IHC a confirmé nos résultats antérieurs in vitro avec LUHMES. La thérapie par les PCS-EVs a

augmenté le nombre de cellules positives à la TH après MPTP, démontrant un impact protecteur sur les neurones dopaminergiques. Cependant, en utilisant une dose plus élevée, nous n'avons pas observé un impact similaire, ce qui indique qu'une étude supplémentaire est nécessaire pour déterminer la dose la plus efficace pour un résultat thérapeutique optimal.

Dans l'ensemble, notre étude a montré que l'activité neuroprotectrice, neuro-régénératrice et anti-inflammatoire de nos PCS-EVs, démontrée in vitro et in vivo, semble être régulée par plusieurs facteurs de croissance, composés antioxydants et cytokines présents dans ces EVs. Certains facteurs de croissance également présents dans les PCS-EVs ont été démontrés pour protéger les neurones dopaminergiques, favoriser leur survie et leur croissance, et moduler l'inflammation post-lésion. Le BDNF associé à la PDGF-BB a favorisé la génération de nouvelles cellules dans la substance noire et le striatum chez un modèle de rat [90]. L'IGF-1 protège les neurones dopaminergiques et augmente la survie globale des cellules progénitrices neuronales humaines in vitro et après greffe dans un modèle de rat de PD [91]. Le TGF-β1 exerce un effet anti-apoptotique et anti-inflammatoire, prévient la dégénérescence des neurones hippocampiques chez des rats ischémiques. Il a également été démontré que les TGF-β sont capables de protéger les cellules dopaminergiques contre le MPTP et le 6-ODHA dans un modèle In vivo de PD [92,93]. De plus, l'épuisement de ces facteurs de croissance est souvent associé à une augmentation de la vulnérabilité due au stress oxydatif résultant de la lésion [94,95].

Le prétraitement avec le PDGF-AA ou le PDGF-BB a réduit le stress oxydatif associé à une augmentation de l'activité des antioxydants tels que la catalase, la glutathion peroxydase et la SOD. Les antioxydants ont des propriétés anti-inflammatoires et aident à réduire l'inflammation dans le cerveau, ce qui explique probablement l'activité des PCS-EVs pour réguler l'inflammation après une lésion cérébrale traumatique. L'activation de la catalase, de la SOD et du glutathion supprime la quantité de radicaux libres dans les cellules, empêche la libération intracellulaire de Ca ++ et arrête la signalisation apoptotique subséquente, protégeant finalement la perte de neurones dopaminergiques dans le modèle animal MPTP. [96,97]

La taille nanométrique des EV pourrait expliquer leur capacité à atteindre le cerveau et ainsi à délivrer leurs facteurs thérapeutiques. En effet, l'un des avantages de l'utilisation des EV comme vecteurs est qu'ils sont capables de surmonter les barrières tissulaires, y compris la barrière hémato-encéphalique. Une étude a montré que les EV de plaquettes peuvent être

internalisées par les cellules endothéliales du cerveau humain par endocytose, ce qui soutient cette hypothèse [98].

En fin de compte, nous concluons que les EV isolées du surnageant de concentrés de plaquettes humaines, abrégées en tant que PCS-EVs, riches en facteurs neurotrophiques, cytokines et antioxydants, ont un effet neuroprotecteur solide dans un modèle in vitro établi de la maladie de Parkinson, de la neuro-restauration sur des cellules différenciées de neuroblastome (modèle TBI) et n'induisent pas l'activation de cellules microgliales, confirmant leur sécurité. Notre étude in vivo a confirmé l'effet anti-inflammatoire chez les souris atteintes de lésion cérébrale traumatique. Les PCS-EVs ont exercé une activité neuroprotectrice sur les neurones dopaminergiques et ont été capables d'améliorer les déficits locomoteurs dans un modèle animal de la maladie de Parkinson induit par la MPTP. Cette découverte ouvre des perspectives intéressantes dans le développement de biothérapies à base d'EV neuroprotectrices.

Perspectives

Nous avons élaboré que les propriétés biochimiques et fonctionnelles des préparations de LPH varient considérablement en fonction de leur mode de production, avec des impacts potentiels sur la sécurité et l'efficacité. Des recherches supplémentaires sont nécessaires pour définir les LPH les plus adaptés à des applications cliniques spécifiques. De plus, la caractérisation du profil protéique du LPH, par exemple par analyse protéomique et quantification des composants individuels, est nécessaire pour le développement de modèles précliniques *in vitro* et *in vivo* adaptés.

La technologie de nanofiltration peut être mise en œuvre pour produire des LPH de qualité clinique, sûres pour les virus, avec une sécurité et une tolérance améliorée sans affecter leurs fonctions neuroprotectrices et anti-inflammatoires.

Des EV isolés du surnageant de concentrés plaquettaires humains ont démontré des effets neuroprotecteurs robustes dans des modèles précliniques de la maladie de Parkinson et de traumatismes crâniens lorsqu'ils sont administrés par voie intranasale. Des études supplémentaires sont nécessaires pour déterminer l'effet dose-dépendant et les effets à long terme du traitement avant une éventuelle application clinique. Cela ouvre une perspective précieuse pour le développement de biothérapies à base d'EV neuroprotectrices qui peuvent

contenir des facteurs neurotrophiques, des cytokines antioxydantes et anti-inflammatoires pour soutenir la croissance et la survie neuronales.

.

ENGLISH ABTRACT

Human platelet lysates (HPLs)-based biotherapies, manufactured from clinical grade of platelet concentrates (PCs) are currently emerging as a novel and translational therapeutic strategy in regenerative medicine. The scientific rationale supporting the clinical benefits of HPL is their richness in bioactive molecules and healing factors. Moreover, recently gaining attention is their content and functional contribution of platelet-extracellular vesicles (EVs). Various modes of HPLs manufacturing have been reported, depending on the intended application, a specific preparation method might be needed. Heat-treated Platelet Lysate (HPPL) was customized to be enrich in neurotrophic factors and free from unwanted proteins, dedicated for the brain administration. HPPL shown to provide a robust neuroprotection and neuro-restoration in Parkinson's disease (PD) and traumatic brain injury (TBI) models *in-vitro* and *in-vitro*. However, little is known about how modes of HPL preparation, including in tailor made-HPPL, affect their composition and functional properties especially when they are intended to be used for a particular therapeutic purpose. The virus safety was also a concern especially in fact, HPL prepared from blood product when pooling donations statistically increase the viral risk transmission. Nanofiltration has known for its robustness in the removing wide range of viruses and improved the safety manufactures of plasma-derived products. Depending the pore size, it entraps both enveloped and un-enveloped viruses.

Our current project is intended to assess (a) the composition and functional activity, including that contributed by proteins and EVs, of various HPLs intended for specific clinical indications (b) the virus removal efficacy and impact of 19-nm nanofiltration on the HPPL compositions and their neuroprotective and neuro-regenerative therapeutic functions (c) the bio-physical characterization, biological functions, and neuroprotective and neuroregenerative roles of selected PEVs preparations.

.

We received the Platelet Concentrates (PCs) from Taipei Blood Center located in Guandu, Taiwan, and processed them into five distinct platelet lysates - PPL (Platelet Pellet Lysate), HPPL (Heat-treated Platelet Lysate), SCPL (Serum-Converted Platelet Lysate), and HSCPL (Heat-treated Serum-Converted Platelet Lysate). To evaluate the characteristics of these HPLs, we analyzed them for their total protein content, growth factor content, biochemical compositions, thrombin activity, PEVs functional activity, and anti-oxidative properties. Our research findings from this initial phase showed that all five HPL preparations had detectable

levels, ranging from approximately 0.1 to 350-ng/ml, of supraphysiological levels of all growth factors, except for insulin-like growth factor-1 (IGF-1), which was only detected in HPLs containing plasma. Significant differences were observed among the HPLs in terms of total protein, fibrinogen, complement components C3 and C4, albumin, and immunoglobulin G, as well as in their functional coagulant and procoagulant thrombin activities and antioxidative capacities. These findings highlight the impact of the production method on the biochemical and functional properties of HPL preparations. Therefore, the mode of preparation of HPLs should be carefully designed, and the product properties should be evaluated based on the intended therapeutic use to ensure optimal clinical outcomes. Our *in vitro* analysis led us to select HPPL, which was prepared from isolated platelets and enriched in growth factors, depleted of plasma proteins, and low in generated thrombin and pro-thrombogenic activity, as a suitable preparation for administration to the brain.

Furthermore, future clinical application of HPPL will require a large-scale preparation and a viral-safe product. Thus, a virus removal step by nanofiltration using 19-nm pore size Planova 20N (Asahi Kasei) was implemented and in the same time to understand further the EVs contribution in HPPL functions. The virus reduction value was evaluated by spiking experiments using non-infectious small virus of mice-mock particles followed by Immune-quantitative PCR analysis. The impact of nanofiltration to the HPPL proteins compositions and including EVs was determined. The functional activity of the nanofiltered HPPL (NHPPL) was evaluated *in vitro* and *in vivo*. The results of spiking experiments demonstrated the efficacy of nanofiltration with >5.30 log of virus removal. This filtration induced removal of some proteins including some associated with pro-thrombin and coagulation as well as EV, but preserved a range of neurotrophic factors. Our assessment on their functional activity showed that NHPPL (a) maintain a strong neuro-protective and anti-inflammatory activity *in vitro* in LUHMES cells against erastin neurotoxicity (b) stimulated the differentiation of SH-SY5Y cells (c) they preserved anti-inflammatory function in a mouse model TBI. Thus, showing that nanofiltration step were not affecting the neuroprotective and anti-inflammatory functions in HPPL.

Moreover, as shown, HPPL maintained their functions even after depletion of EVs, suggesting that EVs did not play a role in HPPL neuroprotective effects. In addition, separated experiment confirmed that HPPL-EVs did not show any functional activity at the dose used in LUHMES dopaminergic neuron cell model of PD against erastin. Nevertheless, EVs isolated from platelet concentrate supernatant (PCS-EVs) did exhibit a neuroprotective effect in the same model. Our

characterization showed that PCS-EVs consisted of a heterogeneous population from 70 to 350 nm, with a main population size of ~200 nm, and the concentration was in the range of 10^{10}-10^{11}/mL, as found previously in serum and plasma. They contain an substantial growth factors, cytokines and antioxidants revealed by ELISA and proteomic analysis. More in their functional assessments, *In vitro* data using SH-SY5Y revealed that PCS-EVs support the restoration neuronal cells after scratch assay, show anti-inflammatory activity in BV2 stimulated with lipopolysaccharides (LPS). PCS-EVs exert anti-inflammatory function in a mouse model TBI. PCS-EVs intranasal administration protected TH expression and improve the rearing motor activity in the MPTP mouse model.

Our study highlights the significance of the differences in the profile of HPLs and emphasizes the importance of considering these differences when developing and selecting HPLs for specific clinical purposes. In order to increase viral safety and reduce the risks associated with prothrombotic and procoagulant properties, nanofiltration technology can be readily implemented to manufacture clinical-grade virus safe HPPLs without compromising the neuroprotective and anti-inflammatory functions of the product. We also found that EVs isolated from the supernatant of human platelet concentrates exhibit robust neuroprotective properties. These findings provide intriguing perspectives in the development of neuroprotective EV-based biotherapies.

INTRODUCTION

1.1 Platelets

1.1.1 Platelets structure and functions

Platelets are anucleated blood cells derived from the fragmentation of megakaryocyte's cytoplasm in the bone marrow. Megakaryocytes supply up to $\sim 10^{11}$ platelet daily to the bloodstream through a process called thrombopoiesis [1]. In human, platelet have a lifespan until about 7-10 days. Platelets cytoskeleton consist of a bundle of microfilament and microtubules maintain their discoid shape [2]. They are the smallest compared to the other blood cells component, with a diameter approximately 2 – 3 µm and play a critical role in the hemostasis and thrombosis. Platelets are the first time response when there is a site injury in the tissue/vessel, this event thus initiating their activation which is characterized by the changing of their morphology and expanding of their cellular structures known as pseudopods [3]. Reorganization of the cortical actin cytoskeleton in the platelet structure during activation promotes firm adhesion and aggregation of platelets with each other, followed by a release of important mediators regulating blood coagulation and leading to the formation of an hemostatic fibrin-based plug [4]. Normal range of platelet number circulating in human body are 150,000/µL to 400,000/ µL. Insufficient amount of platelet results in a medical condition called thrombocytopenia which can induce a bleeding disorder [5], and excessive number will lead to thrombocytosis [6]. Platelets do not have nuclei, but they do carry genetic components like as messenger RNAs (mRNAs) and microRNAs (miRNAs), which are known to be transmitted from megakaryocytes [7]. Platelet membrane include ribosome complexes, canalicular system, dense tubular system, and endoplasmic reticulum. Platelets also feature mitochondria, which, despite their simple structure, play an important role in providing platelet energy [7]. Moreover, platelets are also a significant reservoir of hundreds of bioactive proteins, thus extending their roles not only in the blood coagulation and hemostasis but also in such events like the healing process and regeneration, immune cells recruitment, and pathogens defense [8,9]. These proteins are stored mainly in their granules, there are three majors granules that has been characterized such as alpha granule, dense granule, and lysosome [10], as described below :

α-granule

α-granule is the most abundant secretory granule in platelet, accounting for about 10% of platelet volume and storing hundreds or most of the platelet content [11]. There is around 50–80

α-granule in one platelet preserving important biomolecules such as cytokines chemokines, growth factor, coagulation factors, chemokines and immunological molecules as shown in Figure 1 [12,13].

Those content are stored and released when a respond is needed to a particular physiological event is required including a variety of cytokines, chemokines, growth factors that are important for platelet functions in tissue regeneration. Growth factors such as platelet-derived growth factor isoforms (PDGF-AA, BB, AB, and C), epidermal growth factor (EGF), transforming growth factor-β1 (TGF-β1), insulin-like growth factor-1 (IGF-1), vascular endothelial growth factor (VEGF), brain-derived neurotrophic growth factor (BDNF), basic fibroblast growth factor (b-FGF or FGF-2), hepatocyte growth factor (HGF), bone morphogenetic protein 2, -4 and -6 (BMP-2, -4, -6), and connective tissue growth factor (CTGF) are contributing to promote cellular growth and initiating the physiological events leading to wound healing and tissue remodeling [14]. Proteins and/or membrane bound protein that are originally in α-granule are also expressed on the platelet surface or released into the outer space as a soluble protein upon platelet activation. There are including adhesion and activation molecules such as vWf, GPIbα-IX-V, integrin αIIb β3, P-selectin, and the collagen receptor [15,16]. Platelets are able to sense an injury that happens at the vessel endothelium and eventually act as an anti-microbial host defense via some chemokines such as platelet factor 4 (PF4), chemokine ligand 5 (CCL-5), and thymosin-β4 [11].

Dense granule

Dense granules appear 10-fold less than the α-granule in platelet and they stored mainly signaling molecules such as adenosine diphosphate (ADP), adenosine triphosphate (ATP), calcium ions, polyphosphate, pyrophosphate and some neurotransmitters are stored that act as a platelet signaling factors including serotonin, dopamine, glutamate, epinephrine, and histamine [17].

Lysosome

Furthermore, lysosomal granules are much less abundant. There are about 1-3 lysosomes in one platelet 116. Lysosome carry essentially proteases and hydrolases. There are acid phosphatase, chaptesin D and E, and some Figure 2. Content of platelet secretory

cargoesenzymes play a role in growth/angiogenesis regulators such as n-acetylglucosaminidase, α-arabinosidase, β-galactosidase, and β -glucoronidase [18].

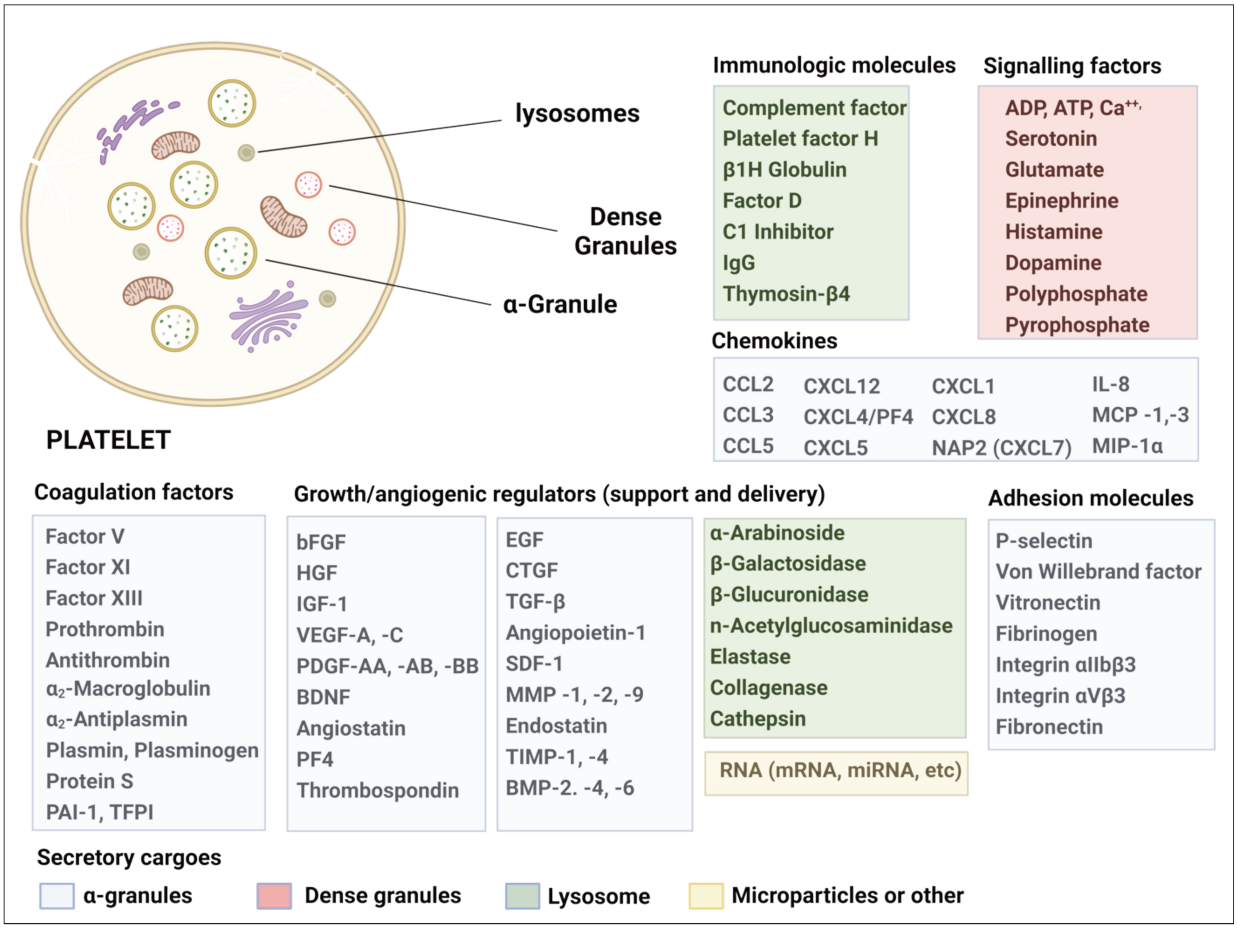

Figure 1. Content of platelet secretory cargoes

(Adapted from Li, J. L., et al., 2017 and Burnouf et al., 2018)[13,19]

Abbreviations: *ADP, adenosine diphosphate; ATP, adenosine triphosphate; BDNF, brain derived neurotrophic factor; bFGF, basic fibroblast growth factor; BMP, bone morphogenetic protein; C, complement; CTGF, connective tissue growth factor; EGF, epidermal growth factor; HGF, hepatocyte growth factor; IGF-1, insulin-like growth factor-1; IgG, Immunoglobulin; VWF, Von Willebrand Factor; IL-1 β, interleukin 1 β; CLCX1, chemokine (C-X-C motif) ligand 1; CLCX12, chemokine (C-X-C motif) ligand 12; CLCX5, chemokine (C-X-C motif) ligand 5, CLCX8, chemokine (C-X-C motif) ligand 8; CCL2, Chemokines ligands-2; CCL3 Chemokines ligands-3;CCL5, Chemokines ligands-5; MMP, matrix metalloproteinase; CXCL7/NAP2 neutrophil-activating protein-2); PAI-1, plasminogen activator inhibitor-1; PDGF, platelet derived growth factor; CXCL4/PF4, platelet factor 4); TFPI, tissue factor pathway inhibitor; TGF-β, transforming growth factor- β; TIMP, tissue inhibitor of metal-loproteinases; VEGF, vascular endothelial growth factor.* "This figure was created with BioRender.com"

1.1.2 Platelet growth factors

Numerous investigations have shown the importance of growth factors in physiological and pathological disease conditions. They are associated mostly to tissue modeling and repair, and also to inflammatory response. In addition, in the nervous system some of platelet trophic factors have been recognized to play key roles in the neuronal viability, development and function [20]. These factors include BDNF, PDGF, b-FGF, IGF-1, VEGF, EGF, and TGF-β, involved in neuroprotection and neurogenesis are briefly described below:

Brain derived-neurotrophic factor (BDNF)

BDNF is one of the most studied neurotrophic factors. Through the activation of its main receptors, such as (tropomyosin-related kinase B) TrkB or neurotrophin receptor p75, BDNF plays key roles in neuronal development, neurite outgrowth and survival, as well as the promotion of some crucial events such as and synaptic development, maturation, and neurogenesis [21-25].

BDNF together with PDGF-BB promoted newly generated cells in the *substantia nigra* and *striatum* in a Parkinson's disease (PD) rat model [26]. It is known to play a dual role as a neuroprotective agent that inhibits the neuronal loss and also as a neuromodulator that upregulates the expression of protein related with dopaminergic neuron [27]. It is well studied that the mitogen-activated protein kinase (MAPK) pathway, specifically the extracellular signal-regulated kinase (ERK) pathway, is involved in cell proliferation and differentiation as a response to BDNF. The phospholipase Cg (PLCg) and phosphoinositide 3-kinase (PI3K) pathways have also been found as being implicated [20,28]. Furthermore, in a response to neuronal damage, BDNF aids in neuronal restoration, which is known to be regulated via a complex network of signaling pathways linked to cell survival, inhibition of cell death, anti-inflammation, and synaptic plasticity [20,29]. BDNF promotes neuronal survival after injury by blocking pro-apoptotic receptors such as Forkhead, Bad, GSK-3, and JNK-p53-Bax via Akt pathway mediated by TrkB [30,31]. Pre-incubation of BDNF in a culture of hippocampal neurons 24 hours before a glutamate shock lower the number of apoptotic cells and the lethal effect by roughly 60% is mediated by ERK and PI3-kinase pathways [32]. In rats with ischemic stroke, intranasal administration of BDNF improves neuroprotection against ischemic insult through immunomodulatory action. It increases the activation of NF-κB DNA-binding activity and suppresses the expression of TNF-α [33]. The activation of NF-κB has been identified as a

critical factor in protecting cells from a range of insults, such as glutamate toxicity and hypoxia, and promoting neuron survival. This activation leads to an increase in the expression of Bcl-xl, an antiapoptotic protein, possibly via the TrkB-PI3-kinase-Akt pathway [34,35].

Platelet-derived growth factors (PDGF)

PDGFs are functional factors with five different isoforms : PDGF-AA, PDGF-AB, PDGF-BB, PDGF-CC, and PDGF-DD which are formed by their four different polypeptide chains [36,37]. They are major mitogens for many cell types such as endothelial, smooth muscle cell, as well as neuronal progenitor cells [38-40]. PDGF is important factor needed for myelin formation during oligodendrocytes development [41,42].

The PDGFs involvement in some cellular signaling pathways is known to be medicated by their tyrosine kinase receptors, receptor α, and PDGF receptor β [43]. The MAPK/ERK pathway, which is linked with gene regulation and cell cycle development eventually promotes neuronal differentiation and proliferation [44,45], and the PI3K/Akt pathway, which is associated with neuronal growth and development in response to PDGF [46,47]. PDGF-BB for instance together with BDNF promotes the expression of TH in dopaminergic neuronal cells against neurotoxin MPP+ via the activation of ERK/Akt *in vitro*. It also able to stimulate TH expression in MTPT mice model by inducing the nucleus translocation of CREB, which functions as a transcriptional activator of TH genes [47]. PDGF act to increase the production of anti-apoptotic proteins by PI3K/Akt activation and rescued neuronal cells from glutamate-induced excitotoxicity in cell study [48].

It also has been demonstrated to act in a protective role by modulating the cellular stress response, ultimately protecting cells from oxidative damage injury. PDGF protects the cell from H_2O_2-induced cytotoxicity in primary cultured neuron via signaling mechanism involved against oxidative stress [49]. Pretreatment with PDGF-AA or PDGF-BB reduced glucose deprivation and oxidative injury-induced neuronal degeneration in hippocampus neurons, which was associated with increased activity of antioxidants such catalase, glutathione peroxidase, and superoxide dismutase (SOD) [50].

Basic-fibroblast growth factor (bFGF)

bFGF is essential for the early development of neurons in the nervous system, as well as the proliferation and differentiation of neuronal progenitor cells [51-53]. Numerous experimental

studies in neuronal cell cultures and animal models have demonstrated the dependency of cells proliferation levels with the presence of b-FGF. It play a role in neuron and axonal growth formation both under normal and pathological conditions by the binding of their receptor [54]. b-FGF is identified in the CNS, including in the hippocampus, and is known also to help neurite extension [55,56]. bFGF administration to postnatal rats resulted in an increase in total DNA, as well as increased the formation of neurons, cell mitosis, and survival [57]. Additionally, in bFGF-knockout mice, there was a significant decrease in hippocampal DNA content and the number of glial fibrillary acidic protein (GFAP)-positive cells [58]. In a PD model, b-FGF promotes dopaminergic graft survival *in vitro* and *in vivo* [59,60]. Their administration also was able to protect neurons by reducing endoplasmic reticulum stress caused by 6-OHDA, increase monoamine neurotransmitter in the corpus striatum, promote TH expression and reduce motor impairment in PD rats [61]. bFGF adequately protected the BBB from damage via binding of FGFR1 and the activation of the ERK signaling cascade, enhanced the formation of new neurons, improved the cognitive recovery following in rats model of TBI [62,63].

Insulin-like growth factor I (IGF-I)

IGF-I is involved in the body growth, tissue development and modulates adult neurogenesis and angiogenesis [64,65]. IGF-1 acts by binding to its glycoprotein receptor (IGF1R), a membrane-bound glycoprotein with two subunits α and β chains [66]. They play an important role in CNS development and maturation, as well as cellular neuroplasticity known to be associated to some signaling pathways such as PI3K-Akt, Ras-Raf-MAP, and MAPK/ERK pathways [67,68]. In TBI rats, treatment with IGF-1 showed significantly reduced the expression of Hsp70 and TUNEL-positive cells in the peritraumatic area and improved the motor activity after injury [69]. Exogenous IGF-1 administered by various methods, including intranasal and intravenous, prior to and after the shock, was able to reduce cerebral damage and reverse behavioral impairments in ischemic rodent model. Their neuroprotective role is suggested link to the inhibition of glutamate-induced neurotoxicity via activating the β-subunit of IGF-1R causing calcium influx, subsequently through IRS-2 activating survival downstream MEK/ERK and PI3K/Akt signaling pathways [70,71]. IGF-1 protects dopaminergic neurons and increases the overall survival of human neural progenitor cells *in vitro* and after grafting in a rat model of PD [72].

Vascular endothelial growth factor (VEGF)

The VEGF family and their associated receptors are important regulators of angiogenesis and vascular permeability. The VEGF family includes VEGF-A, placenta growth factor (PlGF), VEGF-B, VEGF-C, VEGF-D, and VEGF-E [73]. In CNS, VEGF is a crucial factor for early neurovascular development, a transgenic mice with low levels of VEGF develop motor neuron degeneration in the later set similar to amyotrophic lateral sclerosis (ALS)[74-76]. VEGF levels dropped in the CSF of ALS patients with a chronic hypoxemic known to be associated with (hypoxia inducible factor 1α) HIF-1 pathway, thus suggest that VEGF depletion involved in the pathology of ALS [76-79]. In the SOD1 mouse model of ALS, a single injection of VEGF protected brain stem motor neurons and slowed down the progression of motor impairment [80]. Moreover, some other preclinical studies in rodent models of PD and ischemia as well as the hippocampus in normal rats showed the neuroprotective and neuronal development roles of VEGF. In an ischemic rats induced by middle cerebral artery occlusion (MCAO), VEGF were able to promote neurogenesis, protect the neurons and reduce cerebral infarcts [81]. The neuroprotective effect of VEGF is suggested by their involvement in the regulation of cell-death pathways mediated caspase-3 and via VEGFR-2 modulating the PI3K/Akt signal transcription system [82,83]. Treatment with VEGF rescued the dopaminergic neuronal fibers from 6-OHDA toxicities and preserved the number of TH-positive neurons in striatum and SN in rats PD model. VEGF promote the neuroprotective activity possibly via an indirect mechanism that enhances glial proliferation and angiogenesis [84-86]. VEGF-treated rats had twice as many BrdU+ cells in the hippocampus subgranular zone (SGZ) as controls, and resulting in improvement of locomotor activity and learning memory, implying their role in neurogenesis[87]. In an ischemic rats induced by middle cerebral artery occlusion (MCAO), VEGF were able to promote neurogenesis, protect the neurons and reduce cerebral infarcts [81]. The neuroprotective effect of VEGF is suggested by their involvement in the regulation of cell-death pathways mediated caspase-3 and via VEGFR-2 modulating the PI3K/Akt signal transcription system [82,83]. Treatment with VEGF rescued the dopaminergic neuronal fibers from 6-OHDA toxicities and preserved the number of TH-positive neurons in striatum and SN in rats PD model. VEGF promote the neuroprotective activity possibly via an indirect mechanism that enhances glial proliferation and angiogenesis [84-86].

Transforming growth factor beta (TGF-β)

TGF-β is a cytokine that is involved in a variety of biological processes such as cell growth, differentiation, apoptosis, and inflammation [88,89]. TGF-β is expressed by neurons and glial cells in CNS. It plays a role in various brain development including astrocyte differentiation, neuronal migration, and cortical lamination. TGF-β interaction is mediated mainly by its two serine threonine kinase receptors, TGFRI and TGFRII [90]. TGF-β1 is able to prevent the degeneration of hippocampal neurons in ischemic rats. The protective impact is suggested linked to its anti-apoptotic and anti-inflammation properties as well as their involvement in the preservation of Ca2+ neuronal homeostasis [91]. It has also been demonstrated that TGF-βs able to protect dopaminergic cells against MPTP and 6-ODHA in *In vivo* model of PD, it mediated astroglia cell activity and increased cell proliferation, ultimately leading to dopaminergic neurons survival [92,93].

1.2 Extracellular vesicles (EVs)

1.2.1 EVs biogenesis and function

EVs or “extracellular vesicles", is a generic term to define a lipid bilayer-enclosed structure which are released by the cells and do not replicate [94]. They are heterogenous nanometer-size particles shedding from the plasma membrane of essentially all cells. There are microvesicles (MVs), exosomes, and apoptotic bodies in the EVs population [95,96]. Their number increases in some pathological conditions such as cancer, and systemic inflammation [97-99]. The classification of EVs is made according to their size, cellular origin and content as showed in Table 1. MVs size ranges from ca. 100 nm to 1000 nm. Exosomes are typically smaller, around 20 – 100 nm, while the apoptotic bodies are >1 μm. However, there is an overlapping in size among them, therefore they cannot completely be distinguished based on the size [94]. Exosomes are released in the late endosomal stage by the fusion of multivesicular bodies (MVBs) to the plasma membrane. MVs “pinch out” as a result of membrane phospholipid redistribution due to the contraction of the protein cytoskeletal initiated by amino-phospholipid translocases (floppase and scramblase) [100], as shown in Figure 2. Thus, some of the enzymes, such as extracellular signal-regulated kinase [101], and myosin light-chain kinase, function as signaling mediators triggering the release of MVs. Exosomes, which were released during reticulocytes formation, were at first only recognized as a cellular garbage bag throwing away unwanted protein [102]. However, recent studies now have evidenced that MVs and exosomes can play a

role as signaling particles that carry several important biomolecules cargoes, such as proteins and genetic materials, mRNA, and miRNA into the cells at a distance [103,104].

Table 1: Characteristics of EVs

	Exosome	**Microvesicle**	**Apoptotic Body**
Approximate Size	20-100 nm	0.1 – 1 μm	> 1 μm
Origin	Multivesicular Bodies	Plasma membrane	Cellular fragmentation
Markers examples	Tetraspanin CD 63	- Phosphatidylserine - CD9, CD81	- Fragment DNA - PS

Abbreviation: Phosphatidylserine (PS)

1.2.2 Platelet Extracellular vesicles (P-EVs)

EVs released from platelets were first discovered by Peter Wolf in plasma and serum and were regarded as only "platelet dust" [105]. Platelets release EVs during the physiological activation process, shear stress, or apoptosis taking place in the blood circulation [106,107]. This phenomenon leads to the exposure of anionic phospholipids on the outer layer of the membrane during the formation of MVs. These anionic phospholipids, such as phosphatidylserine (PS) and phosphatidylethanolamine, present on the surface of platelet microvesicles (PMVs) are known to exert a pro-coagulant activity as they can bind with the cationic surface of the proteins of the coagulation cascade such as coagulation factor VII (FVII), FIX, FX, and prothrombin. The release of PMVs bearing tissue factors (TF) may also contribute to enhancing the coagulation activity since TF is a receptor at the initiation of the coagulation cascade [108,109]. However, the evidence shows that despite an abundant number of platelets EVs circulating in the blood, the pro-coagulant role is not always the case. Depending on the triggering factors, when there is an activation step mechanism such as by ADP, or epinephrine their procoagulant activity decreases [110,111]. PMVs isolated from plasma without any stimulation failed to bind to the annexin-V, demonstrating a lack of phospholipid procoagulant expression [112].

Platelet-EVs know to exhibit specific surface properties as expressed in platelets, distinguishing them from EVs released from the other cells type. They could express trans

membrane protein for a specific targeting P-selectin (CD62p), and other various integrins, and adhesion receptor such as PF4, CD63, CD31, and membrane glycoproteins GPIIb/IIIa (CD41/CD61), GpIba (CD42b), Gp1a [106,113]. Most importantly, PEVs contain other platelet-derived biological substances such as growth factors and cytokines, as well as miRNA and mRNA [108]. They are considered to be the most abundant (60-80%) type of EVs circulating in the blood [114,115], and act as signaling particles between platelets and other cells with substantial contributions in the intracellular communication of platelet response and functions [116]. P-EVs contain a number of growth factors and cytokines such as BDNF, PDGF, EGF, bFGF, TGF-β, FGF2 and VEGF that are contributing to their biological activity, including facilitating tissue repairs and regeneration [117,118]. Moreover, P-EVs are suspected to contribute to the functional role of platelets in regenerative medicine or can be used as a stand-alone treatment [119-121]. Previous study in our lab showed that P-EVs isolated from PC supernatant, comprised in multiple of growth and trophic factors, able to promote corneal endothelial cells repair and regeneration [117]. PMVs were also found to exert anti-inflammatory properties in the macrophages activated by Lipopolysaccharide (LPS) endotoxin, as showed by a decrease in TNF-α and IL-10 levels [122]. Moreover for their potential use in CNS treatment, PMVs enhance the proliferation and differentiation of neural stem cells (NSC) *in vitro*, as well as promotes the angiogenesis, survival and neurogenesis in ischemic rats which result in behavioral improvement [123,124]. These functions appear to be regulated by multiple of growth factors found in PMVs including FGF2, VEGF, and PDGF, and the downstream pathways discovered are also linked to the pERK/pAkt [124]. Furthermore, the nanoscale size of EVs bring the advantages of their use as a carrier that able to cross tissue barriers, including the blood-brain barrier (BBB). For instance, MSC-derived MVs exhibit enhanced BBB passage, contributing to the reduction of inflammation and promotion of neurogenesis following TBI [125,126]. *In vitro* studies have shown that PEVs can be internalized by human brain endothelial cells by endocytosis [127]. Dopamine-loaded blood exosomes administered intravenously exhibit therapeutic efficacy in a PD mice model and reduced systemic toxicity compared to free dopamine, indicating that they also can transport drugs passing through the BBB [128].

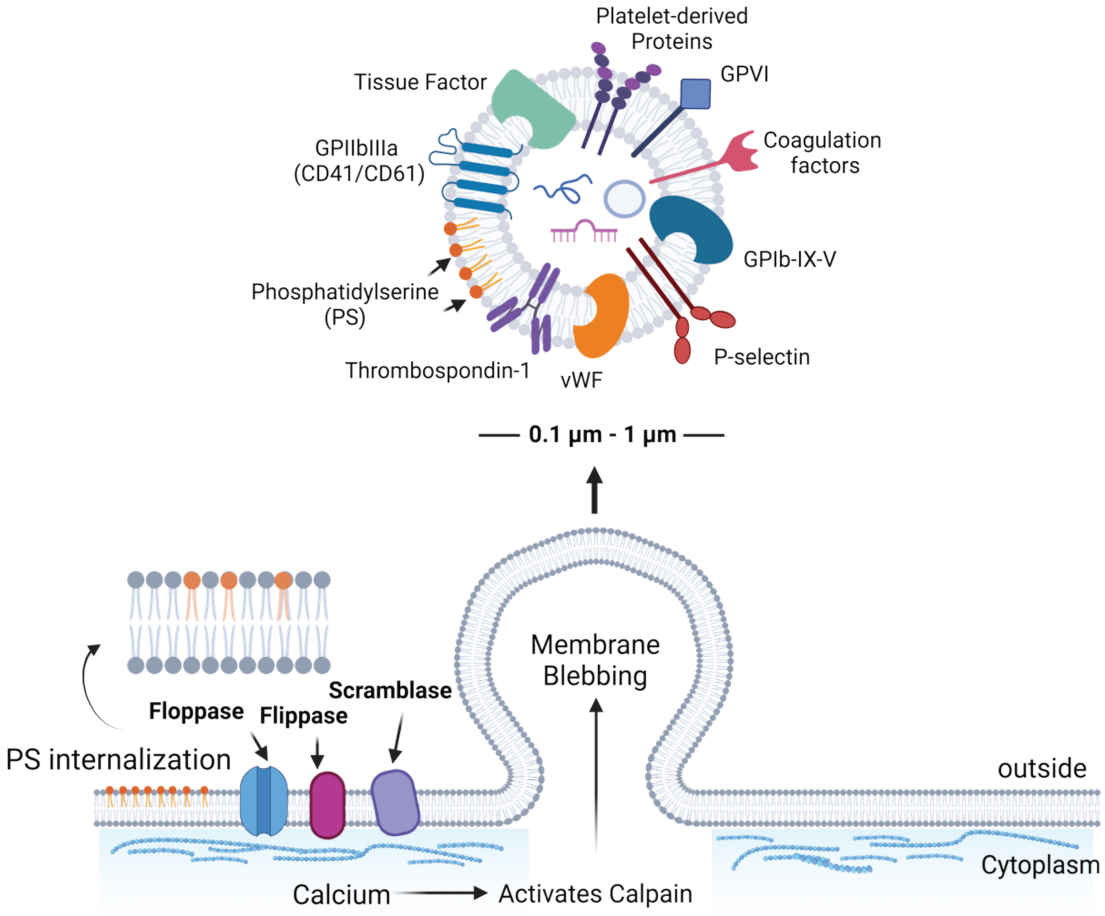

Figure 2. Platelet-MVs releasing mechanism. PMVs formed as a response to activation, and intracellular calcium increases. This inhibits flippase and activates floppase and scramblase, leading to the externalization of negatively charged of PS. The cytoskeleton is reorganized and calpain cleaves PMVs, releasing them into the circulation. PMVs could bear proteins like growth factors, cytokines/chemokines, and apoptotic proteins, as well as nucleic acids and mitochondria. They share surface proteins with platelets and their characteristics depend on the environment and agonist(s) triggering their formation. Abbreviations: Microvesicles (MVs). Phosphatidylserine (PS). "This figure was created with BioRender.com".

(Adapted from Zaldivia, Maria TK, et al. (2017)[129]

1.3 Platelet Concentrate (PC)

1.3.1 PC collection

The donation and collection of PC are crucial steps in fulfilling medical needs of platelet transfusion. Approximately 2 million units of platelets are transfused in the US each year [130]. Platelet donations collected as platelet concentrates (PC) are used to help patients with severe bleeding disorder or thrombocytopenia and severe injury, or patients undergo surgery where they suffer with a major blood loss. Conditions such as bone marrow failure and auto-immune disease can cause platelet production impairment or platelet destruction, eventually leading to platelet deficits or dysfunction [131]. PC are listed in the World Health Organization's (WHO) "Model List of Essential Medicines" [132]. Platelets have only a 5 to 7 day shelf life after collection, therefore there is continuing need for new donations.

PC can be obtained from a whole-blood donation or by an apheresis method [133,134]. From the whole-blood, low-speed centrifugation processes are performed to remove red blood cells, followed by separation steps to generate buffy coat or platelet rich plasma (PRP). In the buffy coat method, the first step involves centrifuging whole blood to separate its components. Four units of buffy coat and one unit of plasma, obtained from four different donors, are combined. After another round of centrifugation platelet concentrate is generated. In the PRP method (typically 4-6) of PC from whole blood are collected and combined to create a unit of approximately 200 mL [19]. Meanwhile, dedicated apheresis technology connects a cell separator to a centrifuge in order to recover platelets while returning the remaining of blood components to the donor. Apheresis yields a greater volume of PC (approximately 230-250 mL) from a single donor [134,135] (Figure 3). PC are collected in a presence of an anti-coagulant such as acid-citrate or acid-phosphate dextrose, and then stored at a regulated temperature of 22 ± 2°C with continual agitation. This procedure is used to keep platelets from activating and clotting [134]. Platelet storage buffer and compartment used to store the PC also could affect their quality after collection. The PC must be stored in a bag with a good permeability for adequate oxygen (O2) and carbon dioxide (CO2) therefore the PH is maintained [136]. Furthermore, PC for transfusion are usually suspended in plasma or can be stored in the presence of platelet additive solution (PAS) at the proportion 60 -70% [137]. In this case, the plasma itself can be used for the

other purpose such as to prepare plasma derivative products for therapeutic purposes, for instance factor VII, albumin, immunoglobulins, and von Willebrand factor [138,139].

Furthermore, for addressing the safety of PC donations, the viruses and bacterial testing need to be done to reduce the possibility of pathogens transmission. Only healthy blood donors only are selected, and screening step need to be done afterward, such as by an antigen marker testing at least for some well-known blood borne transmitted viruses such as human immune deficiency virus (HIV), hepatitis B virus (HBV), and hepatitis C virus (HCV). However, there is still risk of potentially pathogens infection, that possibly happens during the window period donation or untested viruses [140,141], also increases when pooling. Thus, to ensure the safety of PC, pathogen reduction strategies are being implemented [142-144].

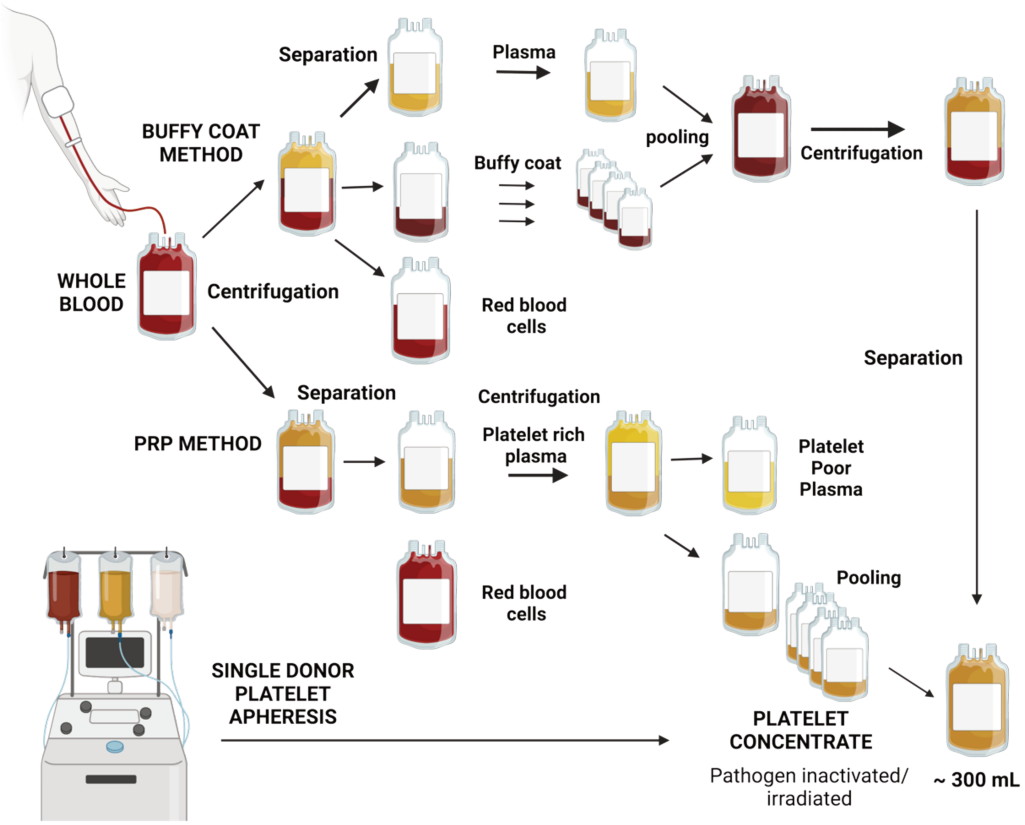

Figure 3. PC preparations. Whole blood derived PCs are prepared either by the buffy coat method or by the PRP method. The buffy coat method was done by pooling four buffy coats and one plasma unit, then followed by centrifugation step, PRP method (pooling four to six units). Single-donor of PC is produced by apheresis technology. Pathogen inactivation or gamma irradiation usually implemented as a virus reduction step. Abbreviations: platelet concentrate (PC), platelet-rich plasma (PRP). "This figure was created with BioRender.com".

(Adapted from *Burnouf et al., 2018)*[13,19]

1.4 Human platelet lysates (HPLs)

Human platelet lysates (HPL) are platelet-derived biomaterials produced through a step that leads to the releasing of platelet contents including their growth factors, cytokines, antioxidant and other bioactive compounds. The preparation methods are such as by freeze/thaw-mediated platelet lysis, sonication or chemical treatment, thrombin activation and clotting (Figure 4), and as described below [19]. HPLs can be obtained from either single or pooled, autologous or allogeneic of PC, and either from whole blood donations or apheresis collection. There is usually a need for making pool of PCs in order to produce HPLs with minimum variations resulting from different donors [145].

Standard freeze-thaw method

This is a straightforward and widely used method for producing platelet lysate. The PC is centrifuged to pelletize the platelets. The pellet is then collected for freezing and thawing cycles. This step is to break the platelets membrane and stimulates the release of platelet factors. Three cycles of freezing at -80 °C and thawing at 37 °C were characterized as sufficient to complete release of platelet content.

Sonication

Sonication is performed to disrupt the platelets membrane, where at the frequency of 20 kHz for 30 min is known to be efficient. This is followed by centrifugation to eliminate cellular debris.

Calcium chloride activation methods

Calcium chloride ($CaCl_2$) is added to stimulate to stimulate endogenous thrombin and eventually forming the fibrinogen clot. Centrifugation step is performed and supernatant is recovered as HPL.

Solvent/detergent (S/D) treatment

S/D treatment is used to initiate platelet lysis and in the same time as a virus inactivation step especially lipid-enveloped virus. After, centrifugation step is performed to remove cell debris. Furthermore, when there is no additional process to eliminate fibrinogen, an anticoagulant is usually used to prevent coagulation.

Depend on the preparation step, HPLs content is usually also contain some proteins that are originally presence in plasma. Moreover, due to their richness of bioactive compounds, cytokines, growth and healing factors, HPLs is becoming an important resource in regenerative medicine and cell therapy. HPLs have been used as a promising alternative, supplement to growth media for human cells expansion replacing fetal bovine serum (FBS), used in transplantation, cell therapy, and tissue engineering such as cultures of mesenchymal stromal cells (MSC) [19,146].

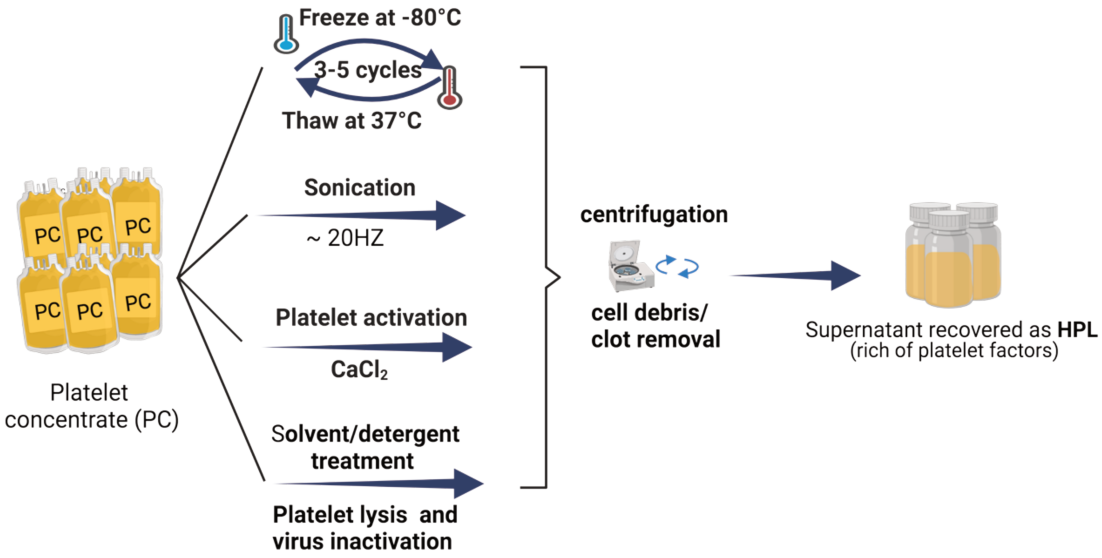

Figure 4. Human platelet lysate (HPL) preparation methods. Several methods are available for preparing HPL including freeze/thaw steps to induce platelet lysate, CaCl2-induced platelet activation, sonication, and solvent/detergent (S/D) treatment. After cell lysis, the debris is removed through centrifugation and discarded, while the resulting supernatant is recovered as HPL. Abbreviations: human platelet lysate (HPL), calcium chloride ($CaCl_2$); platelet concentrates (PC) platelet-rich plasma (PRP). "This figure was created with BioRender.com".

1.4.1 HPLs as regenerative medicine

There has been a surge of interest in platelet-derived biomaterials, including PRP or HPL, in recent years. These biomaterials, which can be obtained from either autologous or allogenic sources, have shown promising therapeutic potential in the areas of regenerative medicine, cell therapy, and tissue engineering [147]. They are currently being utilized in a wide range of regenerative medicine applications. These include the treatment of recalcitrant skin ulcers, orthopedic surgeries, dry eye syndrome, and certain musculoskeletal disorders. Additionally, ongoing evaluations are being conducted to explore their potential in several other areas [148-150].

However, there is a large variability in the modes of preparation of HPL currently used and therefore there is a need to better understand their composition and functional properties to develop dedicated preparations best suited for specific clinical indications. For the direct clinical use of HPL as regenerative medicine, it is increasingly considered important to control and document the quality of the starting PC material, as well as the mode of preparation. Both can indeed affect substantially the protein composition of the HPL and, therefore, its functional activity as well as the clinical outcomes, including efficacy and potential side-effects [151]. The starting PC specifications as indicated previously in this section such as the presence of PAS and/or plasma, as well as the mode of activation or lysis of the platelets can have a direct impact on the content and extent of release of growth factors and other platelets biomolecules, as well as the presence of procoagulant proteins, such as thrombin and fibrinogen coagulation factors, or the generation of thrombogenic and proteolytic activity [152]. Platelet lysates, which contain fibrinogen and adhesive plasma proteins, can be converted into a potent fibrin-based scaffold for tissue regeneration and healing. These components can be converted into a potent fibrin-based scaffold that is capable of triggering cell attachment and tissue formation, thereby enhancing the healing process [153,154]. On the other hand, fibrinogen can be undesirable for the use in central nervous system (CNS) [155] or ophthalmologic applications due to its neurotoxicity and involvement in neuroinflammation, as well as its potential role in the pathogenesis of dementias [156,157]. Additionally, there is a risk of fibrin gelification when applied to the eyes, further limiting its use in ophthalmologic applications [158]. Heat treatment of platelet lysates at 56 °C for 30 minutes has shown potential benefits in the treatment of corneal diseases in patients with autoimmune disease, possibly due to a reduction in [159,160]. Similarly, heat treatment of purified HPL intended for brain administration has been found to decrease cellular toxicity and promote neuroprotection in various neuronal cell models [155,161]. Thus, to optimize a manufacturing process of HPL for dedicated clinical uses, it is best to combine complementary analytical tools allowing to characterize the composition of the preparation and explore the functional activity. Such assays, not much used yet in the characterization of HPL, can include assessment of proteolytic activities, [162,163] thrombin generation activity [164], pro-coagulant activity [165], antioxidant activity [166], metalloproteinase activity [167], as well as inhibitors of metalloproteinase activity [168].

1.4.2 HPLs for a treatment of neurological disorders

Despite significant therapeutic advances in treating various pathologies, there is still a lack of effective pharmacological treatments that can address the complex cognitive and motor functional decline associated with neuronal disorders [169-171]. Therefore, there is a growing need for an efficient, safe, and affordable therapy for brain diseases [120]. HPL has been shown to be neuroprotective and beneficial in studies in *in vitro* and animal's models of several brain pathologies such as stroke, Parkinson's disease (PD), Alzheimer's disease (AD), and also Traumatic brain injury (TBI). In our laboratory, we have conducted pre-clinical studies that demonstrate the potential of a customized purified and heat-treated HPL, obtained from platelets isolated from high-quality platelet concentrates, to provide strong neuroprotective activity in a MPTP mice model of PD [155]. We also have found that this HPL formulation can modulate immune responses, enhance wound healing, and ameliorate cognitive dysfunction in mice models of mild and moderate/severe TBI [172]. HPL components were found to exert a biological activity involving the activation of the Akt-MKT pathway to protect the neurons from apoptosis in a study with dopaminergic neuronal cells [173]. Moreover, in line with the previous study, another type of HPL was able to stimulate the neurogenesis and angiogenesis in a rat model of stroke and reduce the injury leading to the decreasing of movement decline [174]. It has been shown, that HPL, through intranasal administration, exerted neuroprotective activity by reducing the accumulation of β-amyloid and cognitive deficit in a mice model of AD [175,176], also preventing degeneration of dopaminergic neurons in a mice PD [177]. Current considerations include conducting clinical trials involving patients diagnosed with Amyotrophic Lateral Sclerosis (ALS) [178,179]. HPL rich in a physiologically balanced combination of trophic factors, therefore may offer a promising functional biotherapy for the treatment of neurological disorders. HPL comprised in neurotrophic growth factors, cytokines, antioxidants, anti-inflammatory molecules, and neurotransmitters able to involve in some biological pathways promote cells survival and counterbalance pathological environment resulting from brain disorders and trauma [176,177,180]. Overall, these accumulating findings suggest that HPL therapy has the potential to provide a promising treatment approach for various diseases of the CNS.

1.4.3 The need for pathogen-free HPLs and dedicated virus reduction treatments

An optimal safety and quality of HPLs is crucial, especially when it is proposed to be applied for the brain administration. There is a vital concern to avoid the risk of transfusion-transmitted infections since HPPL is manufactured from human blood. Virus removal step will be very critical especially when HPPL are prepared from a multiple allogeneic PCs to ensure quality consistency. Pooling donations of PCs increases the risks of contamination by pathogens [181-183]. Measures aimed at prevention involve strict screening of potential blood donors and individual donations through serological and nucleic acid testing for viral presence [184]. However to achieve an optimal margin of viral safety, it is necessary to employ rigorous virus-inactivation or removal procedures that do not compromise the therapeutic safety and efficacy of the products [185,186], and therefore such treatments can be administered to pooled platelet biomaterials [181,182]. Pathogens reduction technology (PRT) is being implemented and available in some countries such as Mirasol, and FDA approved INTERCEPT and THERAPLEX. These pathogen reduction technologies use a combination of riboflavin or amotosalen with ultraviolet light to inactivate pathogen genetic materials [187,188]. However, these PRT methods in the same time have a potential to affect platelet viability and functions eventually their therapeutic efficacy, in addition, they may not be effective toward all types of pathogens [189,190].

1.4.4 Nanofiltration technology

Nanofiltration is a commonly use virus removal technology in the plasma product industry [191] that consists in passing a purified protein solution through a device composed of modified, hollow cellulose fibers with a cutoff of a few nanometers. This allows the nanosized membranes to trap viruses while allowing proteins to pass through, resulting in a virus-free protein solution. The virus-removal efficiency, while mitigating the risk of filter clogging by large proteins, need to be ensured. This implies selecting a nanofilter with a pore size large enough (19±2 nm) to allow protein filtration but entraping the smallest blood-borne viruses such as parvovirus B19. We hypothesized that this filter would effectively remove blood-borne viruses, including the neurotoxic flaviviruses such as HCV, Dengue virus (DENV), Zika virus (ZIKV), and West Nile virus (WNV) and coronaviruses, as well as the herpes simplex virus HSV [191,192], which is approximately 150 nm in size. However, we were uncertain about the

impact of this virus-removal step on the proteome and extracellular vesicle (EV) content of HPPL products and, consequently, their neuroprotective properties.

1.5 Central nervous system (CNS) disorders

Some of the most common CNS disorders are AD, PD, stroke, epilepsy, TBI, multiple sclerosis and ALS [193]. One of their hallmarks is an accumulation of abnormal protein aggregation such as beta-amyloid, tau proteins, α-synuclein, TDP-43 proteinopathy, and huntingtin. These aggregated proteins form clumps and interfering the normal neuron, eventually leading to the neuronal cell death [194,195]. Some other common overlapping features are including chronic inflammations, oxidative stress, mitochondrial dysfunction, impairment of glial cells, which as the consequence disturb the neuronal activity and result in a devastating behavioral impairment [196,197].

1.5.1 Parkinson's disease (PD)

PD is the second most common neurological pathology associated with aging, affecting about 1% of people over 60 [198]. The pathology is characterized by a movement disorder caused by a degeneration of dopaminergic neurons in the *substantia nigra pars compacta* region of the brain [199,200]. A patient with PD experiences typical automatic movements failures, such as slow movement (bradykinesia), rigidity, rest tremor, and postural imbalance as a progressive loss of the neuron happens [201]. PD is a multifactorial disease involving many genetic and environmental causes even for a given individual [202]. The physiopathology is involving an accumulation of iron and of insoluble protein (α-synuclein) fibrils in the brain into Lewy bodies. The presence of Lewy body in the *substantia nigra* is the histological hallmark of PD [203,204]. Lewy bodies interfere with the signaling between neurons, and their accumulation is associated with neurological pathological impacts resulting a high oxidative stress that is eventually leading to neuroinflammation and ultimate progressive loss of the dopaminergic neurons [205,206]. Interestingly, a new type of regulated cell death, ferroptosis, seems prevalent in the PD models and could offer new therapeutic options [207]. This complex pathological process of PD is progressive and worsens over time. There are many very effective symptomatic treatments (Levodopa/L-Dopa, rehabilitation, dopaminergic agonists, deep brain stimulation) but currently no disease modifying treatments [208-211]. An effective treatment, particularly for

neuron restoration, is therefore still crucially needed. Cellular therapies relying on the transplantation of cells able to counter-balance neuronal loss are currently gaining much attention [212,213]. In addition, cellular and animal studies have found some benefits in the administration of neuroprotective growth factors like PDGF-BB, b-FGF, and BDNF [213-215]. However, engineered stem cells failed onto clinic, probably due to the extensive CNS damage not accessible with local and single site of transplantation [216].

1.5.2 Traumatic brain injury (TBI)

TBI is a physical harm to the brain tissue that impairs brain function temporarily or permanently [217]. The severity is depending on the mechanism of the injury happens, forces and the damage following after. The consensuses of mild injury may not be obvious at the time it is happened. Surprisingly, epidemic data collection showed that TBI is a leading cause of death and disability in the some countries such as, United States with a number of case reaching 1.6 millions in 2003 [218]. The burden of disease has an impact on individuals' quality of life, as well as their families, and the society. The injury can lead to physical disability, cognitive deficits, as well as psychiatric problems such as memory impairment and lowered capacity to regulate emotions. Moreover, the heterogeneity and complexity of the damages induced, make predicting the long-term implications even more difficult. The classification of TBI and improvement of diagnostic tools are important to provide a better treatment. Injuries are typically classified as open or closed. Open refers to an involvement of sharp object that may reach scalp and skull. Closed injuries occurred due to collides or crash of the head causing trauma or inflammation.

TBI-related brain injury physiopathology is defined by two major events regardless of the degrees. There are an initial insult (primary injury) and a secondary event (secondary injury). The early stage of primary injury is characterized by brain tissue destruction due to initial forces from the trauma. Furthermore, the secondary injury occurs when the effects of an initial insult propagate to the cellular level, such as neuron degeneration and, eventually, axons and glial cells. The severity and diversity of the secondary impacts are complimentary to the initial insult. It is a genuine secondary neurodegenerative process that will continue to progress on its own. The cell function and the spreading events encompass disruption of the blood-brain barrier, immune response depolarization, excitotoxicity primarily at the glutamate, free-radical generation, ischemic, and neuronal cell death [219]. Following the injury, there is a rapid

activation of glial cells such as microglia activation producing inflammatory mediators, eventually astrocytes responses and affect the surrounding neurons. There is also leucocytes recruitments and upregulation of inflammatory cytokines and chemokines post cerebral injury. The glial inflammatory mediators are common to be studied such as Glial fibrillary acidic protein (GFAP), nestin, vimentin, and ionized calcium-binding adaptor molecule 1 (IBA1) [220-222]. Furthermore, cytokines such as interleukin-1 (IL-1) interleukin-6 (IL-6) interferon-, and TNF-α, Chemokine ligand-3 (CCL3), CCL4, and CCL5, the monocyte chemoattractant protein Macrophage inflammatory protein-1 (MCP-1), (CCL2), MIP-1, MIP-2 are commonly produced during the inflammation process [223] .

1.6 *In-vitro* and *In-vivo* experimental models used in this study

1.6.1 PD models

LUHMES as a cell model of PD

Lund human mesencephalic (LUHMES) cells are non-carcinogenic dopaminergic neuronal cells that was established from the sub clone of mesencephalic (MESC2) cell line [224]. V-myc retro virus was used to stimulate their cellular growth continuously. Furthermore, N2 media containing tetracycline was utilized to block v-myc synthesis and the cell proliferation via prevention of transcription activation by tTA (tetracyclineK controlled transactivator). Thus in the presence of dibutyryl-adenosine-cyclic monophosphate (db)-cAMP and Glial cell derived neurotrophic factor (GDNF) the cell was differentiated into a post-mitotic stage producing dopaminergic neurons [224]. This cell has been widely studied for robustness, complete phenotype and highly uniform post-mitotic neurons with conversion rate >99% considered to be the most suitable cellular model of PD [225-227].

Neurotoxic drugs

There are several neurotoxic agents that are commonly used in cellular and animal experiments of PD as the below section. Each drug employs a specific mechanism to cause dopaminergic neuronal cell death, thus which is often be used to investigate a various underlying mechanism link to PD and their therapeutic approach.

MPP+ and rotenone

Oxidative damage known has been associated to PD progression. Rotenone and 1-methyl-4-phenyl pyridinium (MPP+) known work in a similar mechanism via inhibits complex I of the mitochondrial electron transport chain, resulting in ROS accumulation and, eventually, mitochondrial failure and neuronal cell death [228-230].

.

Rapamycin

Rapamycin induces autophagy, a process in which cells break down and recycle their own cellular components notably via mTOR. mTOR is a protein that regulates cell growth, proliferation, and survival. Rapamycin binds to a protein FKBP12 intracellular receptor, forming a complex that interacts with mTORC1 [231].

Erastin

Recent studies show that ferroptosis is a crucial triggered cell death of dopaminergic neurons. Ferroptosis induces cell death by the iron metal accumulation, which eventually causes a rise in lipid peroxidation, resulting in a non-apoptotic programmed cell death [232,233]. Erastin induces ferroptosis by inhibition of the system xc− via a stress sensor activating transcription factor 3 (ATF3) eventually distrub the cystine import and glutamate exchange resulting void of intracellular glutathione synthesis (GSH), thus promoted lipid peroxidation accumulation [234].

MPTP mice model of PD

Various *in vivo* models of PD have been developed to understand the disease pathology as well as to develop therapeutic strategies. MPTP abbreviated for (1-methyl-4-phenyl-1,2,3,6-tetrahydropyridine) toxin, able to initiate PD pathology has been validated and widely used [235,236]. In CNS, MPTP is transformed by glial cells into the final toxic metabolite, MPP+ targeting selectively dopaminergic neurons in substantia nigra (SN) and striatum areas of the brain [235]. Depending on the dose and protocol implemented, MPTP eventually induces nigral cell and striatal dopamine loss [237]. Single dose of 20 mg/kg MPTP (relatively high dose), administered by intraperitoneal injection is able to lead to a significant loss of dopaminergic neurons in the SN identified by a decrease of tyrosine hydroxylase (TH) positive cells and a total neuron number [21]. The classical acute MPTP mouse model is using 4 doses over one day. TH-positive neurons are found throughout the striatum, as are TH co-positive fibers of the classic dopaminergic projection from the SN to the striatum. Thus, TH is commonly used as a marker to study the striatal dopaminergic loss [238-241]. Moreover complementary with cellular

destruction due to the neurotoxin, animals exposed to MPTP indeed demonstrated obvious motor impairment, including lowered bursts of movement and the early stages of behavioral deficits [237,242].

1.6.2 TBI models

In vitro study of TBI

SH-SY5Y neuroblastoma cell line

The SH-SY5Y cell line was originated from a bone marrow biopsy of a female patient with neuroblastoma. These cells are a well-established cell line and are frequently utilized in neuroscience research due to their resemblance to adult neurons in the differentiation stage. SH-SY5Y can be differentiated into a mature neuronal phenotype under selected growth condition[243]. Retinoic acid (RA), a vitamin A derivative is by far the most commonly used to induce differentiation and inhibit the cell proliferation [244]. Differentiated SH-SY5Y is characterized by the expression of differentiation markers such as tubulin beta-III (TUBB3), neurofilament proteins, microtubule-associated protein 2 (MAP2), microtubule associated protein Tau (Tau, MAPT) and the reduction of non-differentiation marker such as nestin [245,246]. Differentiated SH-SY5Y cells can also be characterized by their morphology, which includes a decrease in cellular proliferation rate and formation of substantial neurite outgrowth [246]. An experiment using a scratch assay *in vitro* using SH-SY5Y cells has been done to evaluate the wound healing and neuronal recovery after injury [247-249].

BV-2 microglia cell line

The BV-2 microglial cell line was isolated from the brain of C57BL/6J mouse. The cells were cloned using the v-raf/v-myc oncogene-carrying retrovirus (Raf/Myc) resulting an indefinitely proliferation activity in culture [250]. BV-2 cells have been widely used to study neuroinflammation, neurotoxicity and microglia interaction and function. They have a persistent phenotype and respond to many of the same stimuli as well as expressing cell surface receptors and cytokines as primary microglia [251]. Depending on the study purpose, two most common stimuli has been used to initiate the BV-2 cells activation are gram-negative bacteria LPS and cytokine interferon-gamma (IFN-γ), other stimuli are such as protein aggregates and cytokines induced-oxidative stress and hypoxia [251-254].

***In vivo* study of TBI**

There are several types of TBI animal models which are commonly used, as below:

***Weight-drop model**:*

The weight drop model is performed by using a heavy object to be dropped onto an exposed/closed skull of the rodents, resulting in mechanical damage, contusions, and hemorrhages in the brain tissue [255]. The consequences of close head weight-drop consider to represent closely neurotrauma from injury which occurs in the majority of people. The degree of severity can be adjusted by the weight and height used, however there is possibly variation between experiment when the experiment performed without stereotaxis device [256].

The fluid percussion injury (FPI)

This model is used to generate trauma in the brain without creating any fracture to the skull. A fluid-filled chamber is implanted through a tiny craniotomy and the fluid is delivered with a controlled pulse which generate a rapid increase of the intracranial pressure and eventually induces TBI [257,258].

Model of blast injury:

In this model, animals are exposed to a blast wave produced by a shock tube. As a consequence, the shock wave delivers a complex set of pressure that spread to the brain and causing a range of traumas. The blast was reported to induce a spread of injury including a diffuse axonal damage [259,260].

Controlled cortical impact model (CCI) of TBI

CCI models are widely used in pre-clinical TBI research to understand the cellular and molecular mechanisms as they are widely considered to be close to clinical TBI [261]. The device equipped with compressed air-driven metallic pistons and tips can produce impacts on brain tissue, which can result in contusions, edema, high intracranial pressure, cortical and axonal injury, and even coma [262-264]. The secondary event as the impact of injury applied also observed in CCI mice, there are temporal changes in cell marker expression related to inflammation and cellular infiltration [265]. CCI model of TBI has been used to assess the anti-inflammatory activity, neuronal repair and behavioral impairment of human platelet lysate and growth factors such as IGF-1 [266-269].

1.2 Objectives of this study

In order to develop dedicated preparations that are best suited for specific clinical applications, it is crucial to evaluate the compositions and functional activity of different HPLs prepared by different methods. This evaluation will enable the development of customized platelet material preparations, which are clinically recommended to optimize the healing mechanism of each tissue, while eliminating any undesired blood components. Our primary objective is to analyze the composition and functional activity of HPLs, specifically also to confirm the selection of the most suitable HPL for brain administration.

Moreover, a large-scale preparation of HPPL is needed for clinical use, which involves pooling multiple allogeneic PCs. Since this increases the risk of viral contamination, a robust virus elimination step is critical to ensure safety and efficacy of the product. Nanofiltration is known for its effectiveness in removing viruses and enhancing safety of plasma-derived products [191,270]. For this purpose, we proposed to use Planova-20N filter, consisting of hollow cellulose fibers with a pore size of ±19 nm, which is small enough to trap viruses yet large enough to allow protein flow. Moreover, this filter may also remove some other protein composition and particles, including EVs. Therefore, in the second part of our study, we aim to evaluate the feasibility and effectiveness of nanofiltration to ensure virus safety of HPPL, and its impact on the composition and functional activity of HPPL, including proteins and EVs content.

Moreover, our previous study revealed that HPLs fractions, including HPPL, contain a substantial population of EVs, ranging from 10^{11}-10^{12}/mL. They might be released during the activation process or the lysate preparation due to shear stress [106,107]. Platelet-EVs can act as signaling particles, containing platelet-derived biological substances such as growth factors and cytokines from the α-granules, and contribute significantly to platelet response and function [116]. Thus, PEVs may play a supportive role in platelet regenerative therapy. The high number of PEVs in HPPL raises questions regarding their contribution to its neuroprotective activity. In addition of EVs removal from HPPL during nanofiltration, we propose to assess separately the neuroprotective activity of (HPPL-EVs) to further understand their function. In the same time we are also evaluating the neuroprotective activity of EVs that are presence in the PC supernatant. We aim to do further characterization of PEVs profile in their bio-physical, biological functions, and their neuroprotection and neuro-regeneration roles.

Our study therefore has been targeting 3 mains objectives:

To assess (a) the composition and functional activity of various HPLs, including that contributed by EVs, intended to use for specific clinical indications and most particularly confirm the selection of the most suitable HPL for brain administration (b) the efficacy of virus removal by nanofiltration, the impact of the nanofiltration on the heated-HPL compositions and their neuroprotective and neuro-regenerative therapeutic functions (c) the profile of selected PEVs preparations bio-physical characterization, biological functions, and their neuroprotection and neuro-regeneration roles.

CHAPTER II: MATERIALS AND METHODS

2.1 Overall experimental design

1. In order to develop dedicated preparations best suitable for specific clinical applications, the composition of HPLs preparations that impacts their functional activity was evaluated. We prepared five types of HPL from the same platelet concentrates (FTPL, SCPL, HSCPL, PPL, HPPL) that we extensively characterized by a range of assays to determine and compare their content including:
    - proteins, cytokines, and growth factors
    - biochemical compositions
    - thrombin-generating capacities,
    - thrombin-associated proteolytic activities,
    - phospholipid-associated procoagulant potential,
    - presence of EVs expressing phosphatidylserine and tissue factor,
    - antioxidative capacity

2. The conclusion of our first work led us to confirm the selection of HPPL as a suitable preparation for administration to the brain. However, the virus safety was a concern especially in fact, HPPL prepared from blood product when pooling donations statistically increase the viral risk transmission. A virus removal step by nanofiltration using 19-nm pore size Planova 20N (Asahi Kasei) was implemented. The purpose was to verify its technical feasibility and efficiency as a virus reduction step of HPPL for clinical use. The efficacy of nanofiltration to remove the virus was evaluated by spiking experiments using non-infectious small virus of mice-mock particles followed by Immune-quantitative PCR analysis. The impact of nanofiltration to the HPPL proteins compositions and including EVs was determined by a range of assays. More importantly, the understand the impact of nanofiltration on the functional activity of HPPL, especially in its neuroprotective and anti-inflammatory activity was assessed. *In vitro* and *In vivo* study was performed such as using LUHMES dopaminergic neurons, SH-SY5Y neuroblastoma cell, and TBI-CCI mice model.

3. To further confirm the contribution of EVs in HPPL (HPPL-EVs) to its neuroprotective activity, an *in vitro* study using LUHMES cells were performed. Thus, HPPL-EVs were isolated by SEC chromatography column and the number were determined by NTA.

   Moreover, another selected preparation of EVs, isolated from PC supernatant (PCS-EVs) by using ultracentrifugation (20,000 x g for 90 minutes), was evaluated. The PCS-EVs were characterized to assess number, size distribution and functional content (such as growth factors, cytokines, antioxidant). LUHMES and SH-SY5Y neuroblastoma cells were used to confirm their neuroprotective and neuro-regenerative activity, respectively. BV-2 microglia cells subjected or not to LPS stimulation were used to predict the capacity of PCS-EVs to modulate the inflammatory response in the brain. *In vivo* study using a TBI mouse model was performed to confirm the capacity of PCS-EVs to exert a functional activity when administered intranasally and their potential to modulate pro-inflammatory cytokines was tested. The assessment of the neuroprotective activity of PCS-EVs *in-vivo* was done in a MPTP mice model, by examining their capacity to protect tyrosine hydroxylase (TH) expression and improve motor function. The experimental design is shown in Figure 5.

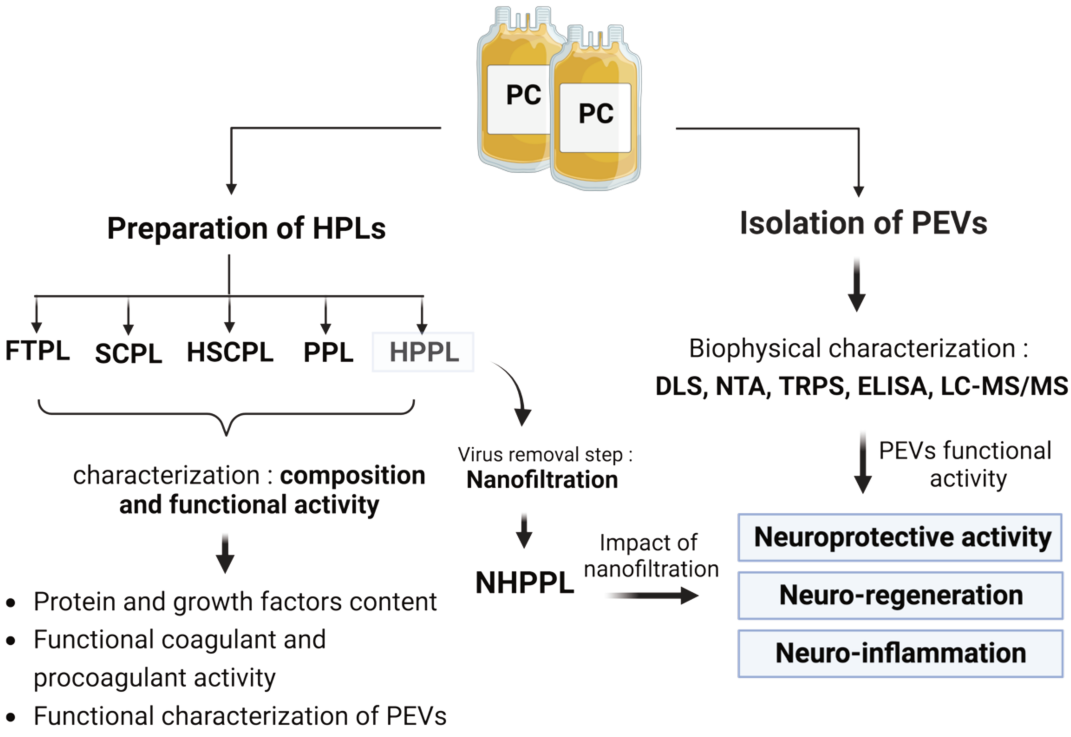

Figure 5. Overall experimental design. PC resuspended in plasma and collected in the presence of an anticoagulant was used to produce HPLs. Five types of HPLs were prepared from the same PC and their composition and functional activity was characterized. HPPL was subjected in to nanofiltration virus removal step. PEV was prepared from the supernatant of PC. *Abbreviations: platelet concentrate (PC); human platelet lysates (HPLs), frozen-thawed platelet lysate (FTPL), serum converted platelet lysate (SCPL), heated serum converted platelet lysate (HSCPL), platelet pellet lysate (PPL), heated platelet pellet lysate (HPPL), nanofiltered HPPL (NHPPL), dynamic light scattering (DLS); nanoparticle tracking analysis (NTA); tunable resistive pulse sensing (TRPS); Liquid Chromatography with tandem mass spectrometry (LC-MS/MS). "This figure was created with BioRender.com".*

2.2 Platelet biomaterials preparation

2.2.1 Source of PC

The study received approval from the Institutional Review Board of Taipei Medical University (TMU-JIRB N201802052). The study utilized clinical-grade, non-leukoreduced, allogeneic PCs. These PCs were suspended in 100% plasma and anticoagulated with citrate-phosphate-dextrose. The platelets were collected from voluntary non-remunerated donors who had given informed consent using MCS+ platelet collection system (Haemonetics, Braintree, MA, USA) at Taipei Blood Center (Guandu, Taiwan). Upon reaching their expiry date, 5 days after collection, the PCs were transported to the laboratory at Taipei Medical University within approximately 90 minutes in an insulated box at a controlled temperature. The PCs were then placed on a slow-speed platelet agitator at 22 ± 2 °C and were processed into different HPL fractions on the same or next day. Prior to processing, an aseptic sample was collected and used to determine the blood cell count using the ABC Vet blood cell count system (ABC Diagnostics, Montpellier, France)

2.2.2 Preparation of HPLs

Five different types of HPL were prepared from three PCs donation. One PC was used to prepare each type of HPL, which was then subsequently pooled (n = 3) for further analysis. All procedures were performed under sterile and aseptic conditions (Figure 6), as described below in details:

Frozen-thawed platelet lysate (FTPL) preparation

PC was subjected to three freeze (-80 ± 1 °C) and thaw (37 ± 1 °C) cycles to lyse platelet membranes and release platelet contents [271]. The suspension was centrifuged (6000 ×*g* for 15 minutes at 22 ± 2 °C), and the supernatant was recovered as FTPL.

Serum-converted platelet lysate (SCPL) preparation

10% of 1M $CaCl_2$ was added into 25 mL of PC at the dose of 30 µL/mL (final concentration : 23 mM $CaCl_2$) in the presence of 0.5 g/mL autoclaved glass beads at 30 ± 2 °C to activate and degranulate the platelets. The mixture was then shaken gently until the formation of a solid fibrin clot, typically for 60 minutes. The fibrin clot and the glass beads were then removed by

centrifugation of the suspension at 6000 x g for 30 minutes at 22 ± 2°C. The pellet was discarded, the supernatant (SCPL) was recovered and aliquoted and stored at -80 °C until use.

Heated SCPL (HSCPL) preparation

To obtain HSCPL, SCPL was subjected to a heat treatment process by incubating it at a temperature of 56 ± 1 °C for 30 minutes, followed by rapid cooling in an ice bath for 5 minutes. The resulting mixture was then centrifuged at 10^4 x g for 15 minutes at a temperature of 4 ± 2 °C to remove any precipitates. The resulting supernatant, now referred to as HSCPL, was collected, aliquoted and stored at a temperature of -80 °C until use.

Platelet pellet lysate (PPL) preparation

To prepare PPL, 250 mL of PC was centrifuged at 3000 x g for 30 minutes at 22 ± 1°C to pelletize the platelets. The platelet pellet surface was washed gently with sterile PBS twice, then re- suspended in the PBS using a volume of 10% that of the initial PC. The resuspended pellet was subjected in to three freeze (-80 ± 1 °C) and thawed (37° ± 1 °C) cycles, and centrifuged at 4500 x g for 30 minutes at 22 ± 2 °C. Supernatants (PPL) were aliquoted and stored at -80 °C until use [155].

Heat-treated PPL (HPPL) preparation

HPPL was produced by heat-treatment of PPL at 56 ± 1 °C for 30 minutes in a dry bath (Basic Life, Taiwan) then immediately cooled down on ice for 5 minutes, followed by centrifugation at 10^4 x g for 15 for 15 minutes at 4 ± 2 °C to remove any precipitate. The supernatant (HPPL) was recovered, aliquoted and stored at -80 °C until use [155].

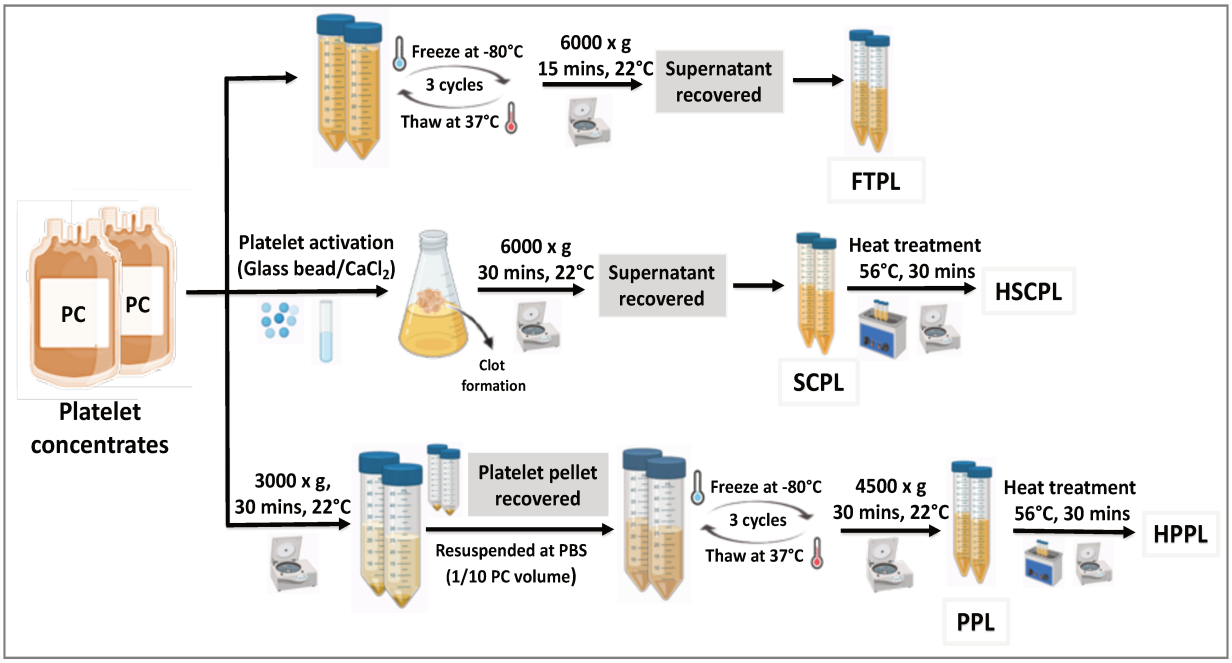

Figure 6. HPLs preparation procedure. Five types of HPLs were prepared from the same source of PC. Pooled PCs was divided into three parts: One part was directly subjected to freeze-thaw cycles to produce FTPL. The second part, PC was added by $CaCl_2$ and in the presence of glass beads induce the formation of fibrin clot. The supernatant was recovered as SCPL and heat treatment was done to prepare HSCPL. The third part, PC was centrifuged, and the pellet obtained was subjected in to freeze-thaw cycle to prepare PPL and HPPL. Abbreviations: platelet concentrate (PC), phosphate buffer saline (PBS), calcium chloride ($CaCl_2$), frozen-thawed platelet lysate (FTPL), serum converted platelet lysate (SCPL), heated serum converted platelet lysate (HSCPL), platelet pellet lysate (PPL), heated platelet pellet lysate (HPPL). "This figure was created with BioRender.com"

2.3 Characterization of HPLs composition and functional activity

2.3.1 Total protein quantification

The total protein content was assessed by bicinchoninic acid protein assay kit (BCA, Pierce Biotechnology, Rockford, IL, USA). FTPL, SCPL, and HSCPL were initially diluted 500 times, and PPL and HPPL were diluted ten times. 25 uL of diluted samples were mixed with 200 uL BCA working reagent (1:50) in 96 plate-well, shaken immediately for 30 seconds. After an incubation for 30 minutes at 37 °C, a purple color was generated and measured at 562 nm using Biotek EPOCH 2, microplate reader (Santa Clara, CA, USA). Bovine serum albumin (BSA) in the range of 25-2000 ug/mL concentrations were used as a standard.

2.3.2 Growth factors determination by ELISA

The levels of BDNF, PDGF-AB, EGF, VEGF, IGF-1, and TGF-β growth factors present in HPL were quantified using a sandwich enzyme-linked immunosorbent assay (ELISA) kit (DuoSet ELISA; R&D Systems, Minneapolis, MN, USA), as previously described following the manufacturer's protocol [161,272]. To determine the concentrations of VEGF, EGF, BDNF, and PDGF, FTPL, SCPL, and HSCPL were diluted 2-, 50-, 100-, and 200-fold, respectively. For PPL and HPPL, the dilutions used were 5-, 100-, and 500-fold for VEGF, EGF, and PDGF determinations, and 500- and 50-fold for BDNF. To create the standard reference curves for the growth factors studied, a range of concentrations was used, specifically 0-1500 pg/mL for BDNF, 0-250 pg/mL for EGF, 0-2,000 pg/mL for recombinant human IGF-1 and VEGF, 0-1,000 pg/mL for recombinant human PDGF-AB, and 1971 pg/mL for TGF-β. Initially, 96-well plates were coated with 100 µL of capture antibody, which had been diluted in Phosphate buffer saline (PBS), covered with an adhesive strip, and incubated at room temperature (RT) overnight. o perform the ELISA assay, the plate was washed three times with washing buffer (0.05% Tween 20 in PBS). The next day, 30 µL of blocking buffer (reagent diluent RD, 1% BSA in PBS, w/v) was added to each well and incubated for 1 hour to eliminate non-specific binding. After another washing step, 100 µL of standard (prepared using serial dilutions in reagent diluent) and samples were added to the wells and incubated at room temperature for 2 hours. Following this incubation period, 100 µL of detection antibody (diluted in reagent diluent) was added and incubated for an additional 2 hours. After three washes, 100 µL of Streptavidin horse-radish peroxidase (HRP) diluted in reagent diluent (1/200) was added to the ELISA plate and incubated for 20 minutes. During this step, the plate was wrapped in aluminum foil to protect it from direct light. Afterward, 100 µL of tetramethylbenzidine (TMB) substrate solution (1:1 ratio of solution A and solution B, v/v) was added to each well and incubated in the dark for 20 minutes. The reaction was halted with 50 µL of 2N H_2SO_4, and the absorbance was measured at 450 nm using an Infinity M200 Tecan spectrophotometer. The concentrations of growth factors were then estimated using the standard curves.

2.3.4 Proteome profiling cytokine and angiogenesis array

All HPL samples were diluted 40- and 80-fold for TGF-β and IGF-1 analyses, respectively. The levels of cytokines and angiogenesis-related proteins in different HPL samples were

evaluated using a proteome profiling cytokine kit (ARY022) and an angiogenesis array kit (ARY007) from R&D Systems, following the manufacturer's instructions. In brief, the manufacturer spotted duplicates of chosen capture antibodies on the array nitrocellulose membranes. Each spot then added with the HPL samples mixed with cocktail of Cytokine Array Detection Antibody as followed: 500 μL of PPL and HPPL and 200 μL of SCPL and HSCPL were incubated on cytokine array membranes. 250 μL of each HPLs was incubated on angiogenesis array membranes. Any antibody complex that is present in the samples is bound to the membrane by the related immobilized capture antibody. After, streptavidin-HRP and chemiluminescent detecting solutions are applied successively after a wash to eliminate free molecules. Each location emits light in accordance to how much cytokine is bounded. In order to detect and quantified the level of each detected cytokine, the membranes were imaged for 1-10 minutes with the UVP imaging system (Analytic Jena, Upland, CA, USA). The manufacturer's list and coordinates for analytes and controls were used to identify each cytokine.

2.3.5 Complement determination

The analysis was performed according to the manufacturer recommendation. The concentration of complement components C3 and C4 in the HPLs was quantified by an ADVIA® Chemistry XPT analyzer (Siemens, Munich, Germany) based on a polyethylene glycol [159]-enhanced immunoturbidimetric reaction.

2.3.6 Clinical chemistry and immunochemistry analysis

Glucose, cholesterol, triglycerides, HDL, LDL, Cl, Na, K, Ca, P, Mg, and Fe, and the total iron-binding capacity (TIBC) levels were measured by Roche Cobas c702 (Roche Diagnostic, Rotkreuz, Switzerland); the unsaturated iron-binding capacity (UIBC) and ferritin were determined by Roche Cobas e602. The concentrations of vitamin B12 and folate were measured by Roche Cobas e601; and hemoglobin and fibrinogen were analyzed using Beckman DXH1601 (Beckman Coulter, Brea, CA, USA) as previously described [161,273]. The concentration of IgG was analyzed by an Abbott i1000SR Auto analyzer of immunology tests (Chicago, IL, USA). All these quantifications were performed at Taipei Medical University (TMU) Hospital according to their established and clinical standardized procedures.

2.3.7 Functional coagulant and procoagulant activity in HPLs

Thrombin generation

For this test, we used the thrombin generation trigger agents "RC-low" and "RC-high" reagents, with low and high quantities of phospholipid micelles, respectively. 40 µL of HPL samples were mixed with 10 µL of TGA Reagent (phospholipid micelles containing recombinant human tissue factor and $CaCl_2$ in Tris-Hepes-NaCl buffer). Then 50 µL of TGA substrate was added to initiate the coagulation cascade. Moreover, immediately the reading was done at 1-min intervals for 60 minutes at 37 °C by Thermo Varioskan Flash (Vantaa, Finland). The amount of thrombin generated was detected by fluorescence and the results was quantified by a comparison to a thrombin calibration standard curve. The lag phase, thrombin generation peak, and inactivation phase were collected as variables and then processed by the TECHNOTHROMBIN® TGA evaluation software.

Thrombin proteolytic activity

Pre-existing proteolytic potential of thrombin, was measured by a Chromogenix S-2238 assay (Diapharma, Bedford, MA, USA). S-2238 substrate is a short peptide conjugated with pNA (4-nitroaniline) functional group and acts as a specific substrate for thrombin. The serine protease activity of thrombin induces the cleavage of the pNA and leads to the formation of free pNA, which absorbs light at 405 nm. The thrombin activity determination is based on the difference of absorbance between that of the original substrate and of pNA generated. The increasing rate of pNA formation per second is proportional to the enzymatic activity of thrombin. The reaction is performed at a constant temperature (37 °C). 100 µL of HPL samples were added to each well of a preheated microplate to 37 °C and incubated at 37 °C for 10 minutes in the Thermo VARIOSKAN FLASH. 100 µL of substrate was preheated and added to each well and incubated for 3 minutes at 37 °C. The activity of thrombin was then determined by kinetic examination at 405 nm wavelength every 30 s 22 times. Human plasma and $CaCl_2$-activated plasma were both used as experimental controls.

STA-procoagulant-phospholipid assay

The experiment was conducted at TMU hospital following their established procedures. To evaluate the presence of procoagulant phospholipid activity, an STA-procoagulant-phospholipid assay (Diagnostica Stago, Asnières, France) was utilized. In this assay, 25 µL of reagent 1, which contained citrated human plasma depleted of phospholipid, was added to 25

µL of HPL samples and allowed to incubate for 120 seconds at room temperature. Following this, 100 µL of activated factor X (FXa) (Reagent 2) was added to initiate the reaction. Coagulation occurred due to the presence of phospholipids in the HPLs, and the clotting time was measured using an STA Compact automatic coagulometer. Additionally, positive and negative control samples provided in the kit were also evaluated.

2.3.8 Antioxidative activity assay

The total antioxidative capacity was determined by a Zen-Bio ORAC (oxygen radical absorbance capacity) antioxidant assay kit. This assay is necessary to understand the antioxidant properties of HPL that may contribute to their activity and maintaining the conditions under harsh environment with high oxidative stress. The assay measures the loss of fluorescein fluorescence over time due to peroxyl-radical [274], formation from the breakdown of AAPH (2,2'-azobis-2-methyl-propanimidamide, dihydrochloride). The oxidation of fluorescein due to the peroxyl-radical generates a product without fluorescence. Antioxidants agent in the sample suppress this reaction by a hydrogen atom transfer, inhibit the oxidative degradation of the fluorescein. 150 µL of fluorescein solution was added to each well of a 96-well assay plate that had been preheated to 37 °C. Positive control plasma, FTPL, HSCPL, SCPL, and pre-diluted PPL and HPPL samples (at 300-fold and 100-fold dilutions, respectively), as well as Trolox standard and buffer as negative controls, were added (25 µL per well) and incubated at 37 °C for 10 minutes. Subsequently, a peroxyl radical, AAPH solution was added to each well using a multi-pipette channel, and the mixture was immediately analyzed for antioxidative activity by measuring the fluorescence signal at 485-nm wavelength at 1-minute intervals for 30 minutes. After incubation for 2 hours at 37 °C, 50 µL of a stop solution was added, and the absorbance was measured at 405 nm following a 10-minutes incubation using a microplate reader (Thermo Varioskan Flash, Vantaa, Finland).

2.3.9 Functional characterization of platelet EVs in HPLs

Phosphatidylserine (PS) expression

To evaluate the procoagulant effects linked to the presence of PS on EV surfaces, we employed a functional Zymuphen-MP activity assay. This assay produces a chromogenic substance that absorbs light at 405 nm, and its intensity is directly proportional to the amount of PS present. For conducting the assay, 100 µL of FTPL, PPL, and HPPL (previously diluted 1000 times),

along with SCPL and HSCPL (pre-diluted 200 times using sample diluent), were introduced to an Annexin-coated microplate. Subsequently, the microplate was incubated at 37 °C for 60 minutes. Afterward, 100 µL of a factor Xa-Va mixture, in the presence of calcium, along with 50 µL of prothrombin, were introduced to the microplate. The mixture was then incubated for 10 minutes at 37 °C, facilitating the activation of prothrombin into thrombin. The microplate was washed five times with 300 µL of washing solution, and subsequently, 50 µL of a chromogenic substrate was added. Following a 3-minute incubation at 37 °C, a colored substance was generated, and its absorption was measured using a microplate reader (Thermo Varioskan Flash, Vantaa, Finland) after adding 50 µL of 2% citric acid as a stop solution. The assay identified procoagulant activity in HPL by measuring the formation of a chromogenic substance that absorbs light at 405 nm.

Tissue factor (TF) expression

The procoagulant activity of EVs that express TF was measured using the Zymuphen MP-TF activity assay from Hyphen BioMed, Paris, France. To capture the TF-expressing EVs, 25 µL of HPL samples were added to a pre-coated plate with a specific murine monoclonal antibody for human TF. 200 µL of an MP-TF assay enhancer was then added, and the plate was incubated overnight at 25 ± 2 °C. Following the five washes with 300 µL of washing solution, the next step involved adding 25 µL of activated factor VII (FVIIa) and 25 µL of factor X (FX) to the microplate. After incubating for 2 hours at 37 °C, the TF-FVIIa complex formed, which then activated FX into FXa in the presence of calcium. A substrate specific for FXa (50 µL) was added, resulting in the formation of a chromogenic color. After 10 minutes, 50 µL of 2% citric acid was added as a stop solution, and the absorbance was read at 405 nm using a microplate reader, Thermo Varioskan Flash (Vantaa, Finland).

2.4 Virus removal treatment of HPPL

2.4.1 Preparation of HPPL for nanofiltration purpose

A single PC pool comprising of 50 donations was made to prepare HPPL. Prior to each evaluation, samples were thawed at 37 ± 1 °C and centrifuged at 10^4 x g for 15 minutes at 4 ± 1 °C to remove any insoluble proteins.

2.4.2 Nanofiltration processes in HPPL

Approximately 25 mL of HPPL was initially subjected to pre-filtration using 0.2-µm PN 4612 and 0.1-µm PN 4611 filters (Pall Life Science, Ann Arbor, MI, USA). Subsequently, 20 mL of the pre-filtered sample was directly filtered through a 0.001-m^2 Planova-20N filter (with a pore size of 19 ± 2 nm; Asahi Kasei, Tokyo, Japan). The Planova 20N filter is commercially available and extensively utilized for virus removal from biotherapeutic drugs. The nanofiltration process was conducted at a controlled temperature of 22 ± 0.5 °C, employing an AKTA PRIME PLUS chromatographic system (GE Healthcare Life Sciences, Freiburg, Germany), which ensured a constant flow rate of 0.1/minute. During this process, the protein adsorption at 280 nm of the Planova-20N filtrate and the transmembrane pressure were continuously monitored. The filtrate was collected, aliquoted, and then stored at -80 °C for subsequent characterization and evaluation of its functional activity [272,275].

2.4.3 Virus-removal assessment during nanofiltration

To assess the effectiveness of virus removal through the nanofiltration process using Planova-20N, an immuno-qPCR-based assay was employed. The assay utilized a Minute virus of mice-mock virus particle (MVM-MVP) kit, along with Mock-V solution (Cygnus Technologies, Southport, NC, USA). This method allowed for the detection and quantification of any potential residual viruses after the nanofiltration step. MVM, composed of small, stable, non-enveloped parvovirus-like particles (20~22 nm), was spiked into 4 mL of HPPL, pre-filtered with 0.2- and 0.1-µm filters, to a final total concentration of 10^{10} MVPs/mL. A small aliquot of the spiked HPPL was taken as a positive control and either immediately frozen at -80 °C after spiking or kept on the bench for the duration of nanofiltration. The MVP-spiked HPPL was then passed through a nanofilter consisting of a single hollow-fiber Planova-20N 0.0001-m^2 membrane that was specially manufactured for these experiments by Asahi-Kasei. Nanofiltration was conducted at a constant pressure of 0.08 MPa using compressed air. The non-nanofiltered HPPL, the 0.2~0.1-µm pre-filtered spiked HPPL control, and the nanofiltered HPPL (NHPPL) were stored at -80 °C prior to further analyses. The spiking experiment was conducted in duplicate to evaluate the log reduction clearance of MVM-MVPs using an immuno-qPCR analysis. The procedure for the analysis is described below.

2.4.4 Immuno-qPCR and MVP clearance factor

The manufacturer's (Cygnus Technologies) instructions for the immuno-qPCR test were followed as previously mentioned [276]. Reagents were briefly warmed up to RT for thirty minutes before to the beginning of the assay. The MVP stock (10^{12} MVPs/mL) was serially diluted and used as references. A 96-well coated with a monoclonal antibody was first rinsed with 400 µL of washing solution and left to soak for ten minutes. 100 µL of the samples and the reference solution were added into the wells and they then underwent incubation at 37 °C for 30 minutes. The wells were rinsed out and a 100 µL of an MVP detection antibody, was added and incubated for 30 minutes at 37 °C. Following incubation step, the supplier's buffers 1 and 2 were used to wash the plate. 50 µL of the recovering buffer were then added and it was let to incubate at the room temperature for 5 minutes. After thoroughly mixing the recovered materials, 5 µL were added to a qPCR plate. Oligomers, the 6-FAM probe, and DNase/RNase-free water were utilized in the preparation of the TaqMan master mix in accordance with the provider's instructions. The qPCR-well plate was subsequently filled with twenty microliters of the master mix, sealed, and centrifuge at 10^3 x g for 2 minutes. The StepOneTM Real-Time PCR device was used to run the samples in accordance with Cygnus Technologies' advice. The cycles threshold (Ct) obtained at the end of the amplification were then plotted against the exponential standard curve [277]. The log reduction value (LRV) was quantified using the following formula: LRV = [(Cl*Vl)/(Cf*Vf)], where Cl is the loaded concentration, Vl is the volume loaded, Cf is the final concentration after nanofiltration, and Vf is the final volume.

2.4.5 Evaluation of total protein and trophic factors in NHPPL

We determined the total protein concentration of the NHPPL by a Pierce™ BCA assay (ThermoFisher Scientific, Waltham, MA, USA), using a range of 25~2000 µg/mL of BSA as a standard. Contents of PDGF-AB, EGF, and VEGF were quantified by an ELISA (DuoSet R&D Systems, Minneapolis, MN, USA) following the manufacturer's protocol and as previously described in section 2.3.2.

2.4.6 Determination of functional properties of the EVs in NHPPL

The procoagulant activity of EVs in HPPL before and after nanofiltration was determined using an STA-procoagulant-phospholipid assay (Diagnostica, Stago, Asnières, France) [278]. Meanwhile, the presence of EVs expressing functional PS and their pro-thrombogenic activity

was assessed using the functional Zymuphen MP-activity assay from Hyphen BioMed, Paris, France, as detailed in the section 2.3.7 [279].

2.4.7 Proteomic and bioinformatics analyses of NHPPL

Liquid chromatography-tandem mass spectrometry (LC-MS/MS) was used to conduct a proteomics study to better understanding of the fraction's composition after filtrations. The samples underwent treatment with pre-cooled acetone at -20 °C using a ratio of 1/4 for sample/acetone (v/v). The mixture was left to settle overnight at -20 °C, followed by centrifugation at 15,000 x g for 10 minutes at 4 °C. The resulting pellet was washed twice using a cold acetone in water solution with a ratio of 1/4, and centrifuged at 13,000 x g for 10 minutes at 4 °C. The supernatant was discarded, and the pellet was air-dried before being re-suspended in 6 M urea. The protein content was measured using a BCA protein assay kit, and 20 µg of protein was used for proteomics analysis, as described before [172,280]. Peak lists were generated for each raw data file recorded by MS using Data Analysis version 4.3 (LC-quadrupole time of flight (QTOF); Bruker Daltonics, Billerica, MA, USA) and Proteome Discoverer version 2.2 or 2.4 (LTQ Orbitrap; ThermoFisher Scientific). The study utilized the human UniProt Swiss-Prot database (release 2019.07), which consists of 20,431 annotated proteins. To maintain accuracy in the analysis, a false discovery rate (FDR) of 1% was applied for both spectrum and protein matching. For functional annotation and enrichment of corresponding genes, we employed the DAVID (The Database for Annotation, Visualization, and Integrated Discovery) tool. This annotation process included Gene Ontology (GO) and Kyoto Encyclopedia of Genes and Genomes (KEGG) pathways. To visualize the results, a Venn diagram was generated using the Python matplotlib-venn package, allowing for a clear representation of the overlapping or unique elements in the datasets.

2.5 PEVs preparations

2.5.1 Preparation of PEVs from HPPL

Size-exclusion chromatography (SEC) column

500 µL of HPPL were loaded onto a 10 mL EV original SEC (75 nm, Izon Science), then freshly filtered (0.1µm) PBS was immediately added slowly, a fraction of 0.5 mL sample that

passed through the column was collected continuously (25 fractions in total). Thus, these PEVs fractions were then stored at 80 °C until further assessment.

Ultra 50K filter

400 uL of each Izon sub-fractions containing PEVs were pooled and re-concentrated using Amicon Ultra 50K device with 50 kDa filter and centrifuged at 4,000 x g for 25 minutes. PEVs which are bigger than 50 kDa was retained and recovered.

2.5.2 Preparation of PEVs from PC supernatant (PCS-EVs)

PC were agitated slowly at the temperature 22-24 ℃ when they are received. All the procedure was done under sterile conditions. PC were centrifuged (Centrifuge model FRESCO17, Thermo, Whatman, MA, USA) at 3,000 x g for 30 minutes at 25 ± 2 °C to pellet the platelets. The supernatant was kept and subjected to a second centrifugation (FRESCO17, Thermo, Whatman, MA, USA) at 6,000 x g for 10 minutes at 25 ± 2 °C to remove the remaining cell debris. The supernatant then was centrifuged (Ultracentrifuge J-25 BECKMAN Avanti Germany) at 20,000 x g for 90 minutes at 18 ± 2 °C to isolate the PCS-EV. The pellet recovered was washed by 0.1 um filtered PBS buffer to make sure no contaminant of plasma protein. PEVs pellet was resuspended using 0.1 um filtered PBS with volume ratio 1/100 mL of the starting PC and was aliquoted and stored at -80 °C until use.

2.6 Determination of physical and functional properties of the EVs

2.6.1 Dynamic light scattering (DLS)

Dynamic light scattering (DLS, Zetasizer, Malvern, Malvern, UK) was used to determine the main size distribution of EVs and zeta potential of particles in a population under a Brownian motion. The fluctuation of light scattered from each particle depending upon the size collected by a detector gives the information about the size distribution. 100 µL of each sample was placed in a low volume disposable sizing cuvette designed for DLS measurement. The analysis was done using Zetasizer Nano ZS (Malvern, UK) which allows to obtain curves with population of EVs size distribution.

2.6.2 Nanoparticles tracking analysis (NTA)

The size distribution and concentration of nanoparticles can be determined by NTA. Particles were visualized due to their movement under the Brownian motion using an illumination with incident laser light (Blue 488). The scattered light was captured by detector and processed in to detect the size and the number of particles. NTA allows a determination of the size of each nanoparticle in a population with a range 10-1000 nm. Samples were diluted in 0.1 μm filtered PBS to disperse the particles and allow for reliable tracking and measurement of individual particles. NTA analysis was done by Nano-sight NS300 system (Malvern Instruments, UK) at the service center of DKSH (Neihou, Taiwan) and core facility TMU (Taipei, Taiwan). 1 mL sample was injected with a syringe pump and recorded at 60 seconds. HPPL was diluted 2 x 10^3-fold, and both 0.2-0.1 μm-filtered and NHPPL were diluted 100-fold using 0.1 μm filtered PBS. PPL-PEVs, HPPL-PEVs, and PCS-EVs were diluted 10^3-fold. The EVs size distribution and number of EVs per mL were counted and analyzed NTA software (Malvern Panalytical, UK).

2.6.3 Tunable resistive pulse sensing (TRPS)

TRPS is a technique allowing to determine the size of individual particles and also to quantify nanoparticles. A single particle was measured while passing through a nanopore under electro-kinetic and fluid forces. Size and concentration of particles is determined by comparing the resistive pulses of tested particles with a known number of calibration particles of known diameter. TRPS analysis was done by qNano (Izon, New Zealand) with 400 nm pore size of nanopore membranes and 210 nm (CPC200) particle size calibrating beads. 40 μL of pre-diluted PCS-EVs (10-fold) were introduce to the upper fluid cells. The particles rate was recorded for 10 minutes. The data were processed by qNano software.

2.6.4 Proteomic and bioinformatics analyses of PCS-EVs

A proteomics analysis of PCS-EVs was performed using LC-MS/MS described in details as previous section 2.4.7. Functional annotation and gene set enrichment analysis was done by DAVID, the cellular component (CC), biological functions (BF), and molecular functions (MF) of the proteins were determined by GO (https://david.ncifcrf.gov/).

2.7 Cell cultures

2.7.1 LUHMES cells culture

LUHMES cells were provided by Dr. Devos's Laboratory, Université de Lille, France. 4 x 10^6 cells were seeded in Advance DMEME/F12 culture medium (Thermo Fisher) containing N_2 supplement (Thermo Fisher), 2 mM l-glutamine (Thermo Fisher), and 40 ng/mL recombinant bFGF (R&D System, USA) in the flask pre-coated with 50 µg/mL poly L-ornithine (Sigma-Aldrich) and 1 µg/mL fibronectin (Sigma-Aldrich). Cells were incubated in an environment with 5% of CO_2 at 37 °C humidified incubator to let the cells proliferate. The cells differentiation was performed by seeding 2.5 x 10^6 T75 flask with the proliferation medium and incubated for 24 hours with 5% of CO_2 at 37 °C humidified incubator. The medium was then changed into differentiation medium Advance DMEME/F12 (cat. 12634010, Thermo Fisher) supplemented with N_2 supplement, 2 mM L-glutamine and 1 mM db-cAMP (cat. D0627, Sigma-Aldrich), 1 µg/mL tetracycline (cat.T-7660, Sigma-Aldrich) and 2 ng/mL recombinant GDNF (cat.212-GD, R&D Systems) for two days. The cells were next transferred into 24-well plates in order to complete the differentiation process for an additional three days.

Neuroprotective assessment of NHPPL, HPPL-EVs, and PCS-EVs in LUHMES cells against erastin

On the fifth day of differentiation, LUHMES cells were treated with 5% (v/v) of HPPL, 0.2-0.1 µm pre-filtered HPPL, or NHPPL, followed by a dose of 1 µM erastin for neurotoxic stimulation. For HPPL-EVs, cells were treated with approximately 4 x 10^{10}, 1 x 10^{11}, or 2 x 10^{11} EVs. HPPL containing ~1 x 10^{11} EVs was used as a positive control. PCS-EVs were used at a concentration of ~1 x 10^{10} or 5% (v/v), and HPPL was used as a positive control. After 1 hour of treatment, cell viability was assessed using the CCK-8 assay (Cat. 96992, Sigma-Aldrich) after 24 hours of incubation. The absorbance of the samples was measured at 450 nm. The cell viability was then determined and expressed as a percentage, representing the number of viable cells relative to the untreated cells, which were used as the 100% viability control.

2.7.2 SH-SY5Y neuroblastoma cells lines

Ability of NHPPL to stimulate cell maturation in SH-SY5Y

The neuroblastoma cells were grown in high-glucose DMEM in the presence of 100 U/mL penicillin, 100 U/mL streptomycin (Gibco, Life Technology, Carlsbad, CA, USA), and 10% fetal bovine serum (FBS, Gibco). Cells were cultured at 37 °C in a 5% CO2 incubator. The cells were grown at a density of 4 x 10^4 cells per well in a six-well plate to provide enough space for their differentiation. After one day of incubation, the buffer was renewed, and 1 µM RA (positive control), 2% (v/v) HPPL, and 2% (v/v) NHPPL were added to the new medium accordingly. The media was replaced every three days, and the cells were analyzed on day seven. Fluorescence labeling with β-III tubulin (Abcam, Cambridge, UK: cat no. Ab18207; 54 kDa, 1:500 dilution) was used to assess the ability to promote SH-SY5Y cell differentiation. In brief, the media was withdrawn, and the cells were washed with PBS before being fixed in 2% paraformaldehyde for 30 minutes at room temperature. Cells were then permeabilized for 20 minutes at room temperature with 0.2% PBS-Triton X-100, and non-specific binding was blocked for 1 hour with 1% BSA in PBS. The treated cells were incubated with primary anti-β-III tubulin (cat. Ab18207, Abcam) overnight at 4 °C. The following day, wells were rinsed with PBS, followed by incubation for 1 hour with Alexa Fluor-488-conjugated goat anti-rabbit IgG antibody (Abcam). DAPI was used to stain the nuclei. A Leica DMi8 fluorescence microscope (Sage Vision, West Chester, PA, USA) was used to acquire fluorescence pictures. Using Image J software (1.6, NIH, Bethesda, MA, USA), the fluorescence intensity of β-III tubulin was measured by the integrated fluorescence density for each treatment in three separate trials.

Neurorestorative capacity of PCS-EVs in SH-SY5Y cells

The ability of PCS-EVs to stimulate neuronal restoration was performed using the scratch assay on the differentiated SH-SY5Y cells. SH-SY5Y cells were first maintained before being subjected to differentiation procedure under RA treatment. After, the cells monolayer was wounded using 100 uL tips, then (5% (v/v) or 1.25 x 10^{10} particles of PCS-EVs was applied. The same dose of HPPL was used as positive control. The wounded zone free of cells was examined under microscopy (Leica DMi8 microscope, Wetzlar, Germany) over two days.

2.7.3 BV-2 microglia cell culture

The immortalized mouse microglial cells BV-2 was used to evaluate PCS-EVs ability to modulate the activation of these cells under LPS treatment. BV-2 cells were cultured and maintained in T75 flask in DMEM supplemented with 10% FBS (100 U/mL penicillin). The incubation conditions were at 37 ± 1 °C and 5% CO2 humidified incubator. When they reached 80-90% confluence the cells were passaged. A total of 2.10^4 cells were grown per well in 24-well plates to be used in the present study. The buffer was supplemented with 10% FBS until confluent. Then, cells were treated with two concentrations (5 and 10%) of PCS-EVs and HPPL, 1 hour prior to a 100 ng/mL LPS (cat. L4130, Sigma) addition.

2.8.4 Cell viability assay

50 µL of Cell counting-8 (CCK-8) solution with WST-8 (water-soluble tetrazolium salt) was added into 500 µL medium with cells. NADH and NADPH generated by the cell's activities initiate the reduction of WST-8 by atom H through 1-methoxy PMS into orange-colored WST-8 formazan. The amount of WST-8 formazan represents the number of living cells in the medium. The plate was incubated for 4 hours in a 37 ± 1 °C humidified incubator with 5% CO_2. WST-8 absorbs a color at 450 nm wavelength, and the absorbance value was determined using a microplate reader Tecan Infinity M200. The viability was then expressed as a percent of the untreated cells (control) using the formula: (O.D samples - O.D blank)/ (O.D control-O. D blank) *100.

2.8 Animal studies

2.8.1 TBI mouse model CCI model

Study approval of animal experiments

The study involving animals was carried out following ethical guidelines and under a protocol approved by the animal facility center located at TMU, Taipei, Taiwan (application no. LAC 2020-0042). Male C57/BL6 mice, aged between 8 to 12 weeks and weighing 20 to 30 g, were purchased from the Taiwan National Laboratory Animal Center in Nangang, Taipei, Taiwan.

The mice were housed in the TMU animal facility under controlled lighting conditions, with a 12-hour light-dark cycle.

Anesthesia and surgical preparation

In the present investigation, Zoletil 50 and xylazine were combined to create the anesthetic solution, which was then prepared prior to the surgical operation. The animals were subsequently given an intraperitoneal injection of 10 µL/g body weight to make them unconscious. After shaving the area of operation, the animal was put in a stereotaxic apparatus. The ear bars kept its head from moving. Before cleaning the area of surgery, the sterilized cotton swabs were dipped in ethanol and betadine.

CCI model

A controlled cortical impactor (eCCI-6.3, Custom Design & Fabrication, Sandston, VA, USA), was used to generate a mild TBI in mice as previously reported [172]. A mouse's head was quickly secured in a stereotaxic frame utilizing ear bars after being completely anesthetized with a combination of zoletil and xylazine. A 4 mm-diameter hole was carefully carved over the right side between the bregma and lambda after an incision along the midline was made to reveal the skull. The next step was to produce a mild injury by utilizing an impactor with a 3-mm tip, an actuator moving at 3 m/s, a deformation depth of 0.2 mm, and a dwell period of 250 ms. The cortex's surface was hit perpendicularly, which caused the damage. After that, the skin was sutured, and an antibiotic cream was used to prevent infection. At the end of the procedure, the animals were return in new clean cages.

Treatment procedure

Approximately 2 hours after the injury, the HPPL, NHPPL, and PBS (control) therapies were given via intranasal route. In brief, with a 20 µL pipette, 60 µL of each compound were administered while preserving 5-minutes breaks between each 20 µL delivery. Every animal received 180 µL of the therapy over the course of three days in a row. On the seventh day, mice were sacrificed by cervical dislocation. The brains were rapidly removed and rinsed in cold PBS. A 4.0-mm biopsy punch was then used to capture the affected region of the corresponding cortex. After then, samples were immersed in liquid nitrogen until they were used for analysis.

Genes expressions analysis by quantitative reverse transcription PCR (RT-qPCR)

RNA purification

The RNeasy Lipid Tissue Mini Kit (cat. no. 74084, Qiagen, Genomic, Taiwan) was used to extract RNA from the obtained tissue in accordance with the manufacturer's instructions. The frozen samples were mixed with 1 mL of Qiazol. Then, the samples were homogenized using a tissue homogenizer. 5 minutes after, 200 µL of chloroform were added and shook. The resulting solution was centrifuged at 12,000 x g for 15 minutes at 4 °C, after which the RNA-present in upper aqueous phase was transferred to a separate tube and an equivalent amount of 70% ethanol was added. Then, 700 µL of each sample were placed on an RNeasy Mini Spin column placed on a 2-mL collection tube, and they underwent a 15-second 8000 x g centrifugation. The flow-through was removed, and the spin column was put back on to the 2 mL tube. The spin column was then filled with 700 µL of RW1 and spun for 15 seconds at 8,000 x g. The flow-through was discarded once more, and 500 µL of RPE was transferred to the spin column. For 15 seconds, the column was spun at 8,000 x g. The flow-through was subsequently eliminated and the process was repeated. Finally, the spin column had been moved to a new 1.5 mL tube, and the total RNA drained by centrifugation at 8,000 x g for a minute with fifty microliters of RNase-free water. The total quantity of RNA was then determined using the NanoDrop2000 (Thermo Fisher Scientific, Waltham, MA, USA).

RT-qPCR for inflammatory markers

Total RNA (1 µg) was subjected to reverse transcription, converting it into cDNA, using the Applied Biosystems High-Capacity cDNA reverse transcription kit (ref 4368814).The reverse transcription was carried out using the following program: 5 minutes at 25 °C, 10 minutes at 37 °C, 2 hours at 85 °C, and 5 minutes at 4 °C. The resulting cDNA was stored at -20 °C until use in qPCR. Validated primers were used for qPCR. For each reaction, the following components were combined: 5 µL of Power SYBR Green PCR Master Mix (cat. 4367659, ThermoFisher Scientific, Waltham, MA, USA), 0.1 µL of forward primer, 0.1 µL of reverse primer, 2 µL of cDNA pre-diluted 20 times, and 2.8 µL of RNase-free water. The StepOneTM Real-Time PCR System (ThermoFisher Scientific, Watham, MA, USA) was used with an amplification profile of 50 °C for 2 minutes, 95 °C for 10 minutes, 40 cycles of 95 °C for 15 seconds and 60 °C for 1 minute. The melt curve analysis was performed to confirm the specificity of the amplification.

2.8.2 Animal model of PD

MPTP mice experiment

This experiment was at Professor David Devos's laboratory (Inserm U1172, Lille, France). The mice were housed together in groups of 4-5 in an enriched environment that was kept at a constant temperature of 19-24 °C and humidity level of 60-70%, with a 12-hour light and dark cycle. Prior to any experimental interventions, the animals were given a period of 7 days to adjust to the laboratory setting. All experiments performed in this study adhered to the guidelines specified in the European Union Directive 2010/63/EU for the ethical treatment of animals in research. Additionally, the study was granted authorization by both the National Ethical Committee in Animal Experimentation (Comité d'éthique en Expérimentation Animal Nord-Pas de Calais CEEA no. 75) and the French Ministry of Education and Research (agreement number: 2018060818218219 v4). The results of this research were reported according to the ARRIVE criteria for reporting animal experiments.

In our study, 8-week-old male C57BL/6 mice were used. They were divided in to 4 groups: sham group (n = 7) and MPTP groups with at least 17 mice in each. There was a MPTP mice treated only with PBS group as negative control. On the other hand, two different groups of MPTP mice were treated with two doses (4×10^{10} and 8×10^{10}) of PCS-EVs. These treatments were given one day before MPTP injections. At day 0, mice were subjected to intraperitoneal injection, receiving either 20 mg/kg of MPTP (Sigma-Aldrich) to induce intoxication or saline as a control (sham). The open field behavior test was performed at the day 7 and after mice was sacrificed for further analysis.

Mice brain tissue preparation for immunohistochemistry (IHC) staining

Mice were perfused intracardially with cold saline containing heparin (5 mg/mL) followed by cold 4% paraformaldehyde (PFA). Whole mice brain then was collected and immediately stored in 4% PFA overnight. After, they were transferred into 30% sucrose overnight before freezing at -80 °C for cryo-sectioning. Frozen brains then were cut in a coronal section with 20 μm of thickness and collected in a coated glass slide.

TH staining

IHC was performed to stain TH markers as described below. First, brain tissues collected were incubated with primary antibodies for TH from Genetex (USA). This was followed by

incubation with anti-rabbit goat secondary antibodies (1/500) and avidin-biotinylated horseradish peroxidase (HRP) complex from Vectastain Elite, and 3,3'Kdiaminobenzidine (DAB). Multiple brain slices were examined using optical microscopy from ZEISS AXioskop2 (Germany), which was coupled with a CCD camera from Optronics (USA) to capture the images. Subsequently, ZEISS ZEN lite software was used to analyze and process the obtained images.

Open field test

The open field test was utilized in conjunction with an open-field infrared actimeter to evaluate spontaneous locomotor activity. Actimetry device (Panlab, Barcelona, Spain), an open field apparatus made from transparent Plexiglas a with a size (45 cm × 45 cm × 35 cm) integrated with two frames of infrared beams, was used. This test is based on mice natural tendency to explore a new environment. The activity was recorded over a 10-minutes. The major result was the total distance walked (in cm), rearing numbers, resting time, velocities, movements and distance, which was captured by two rows of infrared photocells and analyzed using the ACTi track software.

2.9 Statistical analysis

The statistical analyses were conducted using GraphPad Prism software version 6.0 (La Jolla, CA, USA), and the data were presented as the mean ± standard deviation (SD) or standard error of the mean (SEM). The significance of differences was assessed using a one-way analysis of variance (ANOVA) followed by Fisher's least significant difference (LSD) test, with $p < 0.05$ considered statistically significant. The legends of the figures provide information on the number of independent values (n), the method of comparison, and the statistical significance. Image J software (NIH, USA) was used to analyze the intensity of fluorescents in the cell study.

CHAPTER III: RESULTS

We present our results into three main sections as follow:

1. Extensive characterization of the composition and functional activities of five different HPLs preparations. This section provides an in-depth analysis of the composition and functional activities of five different HPLs preparations. Through this evaluation, we aimed to identify the most suitable HPL for brain administration.
2. The impact of nanofiltration on the composition and functional activity of HPPL. We discuss the feasibility and the effectiveness of virus removal of nanofiltration as well as its impact on the HPPL proteins, including EVs, and more importantly HPPL functional activity.
3. The assessment of neuroprotective and neuro-regenerative potential of PEVs. The final section discusses the assessment of the neuroprotective and neuro-regenerative potential of PEVs. We aimed to determine the functional effects of different EV preparation, particularly the neuroprotective potential of PCS-EVs, which are naturally occurring vesicles found in PC supernatant.

3.1 Extensive characterization of the composition and functional activities of five different HPLs preparation

We first performed a range of assays on the five HPLs prepared by different modes to have a comprehensive understanding on their compositions and functional activities and help determine their application for specific clinical uses.

5 HPLs were prepared by our lab following our standardized methods. FTPL was prepared by subjecting the PC into three freeze (-80 ± 1 °C) and thaw (37 ± 1 °C) cycles to release the platelet content. A centrifugation was then performed to pellet cells debris, and the supernatant was recovered. SCPL is a serum-converted HPL prepared by the addition of $CaCl_2$ to the PC in the presence of glass beads to induce fibrin formation and platelet degranulation eventually to release the growth factors. The clot then was removed, and the supernatant was recovered. HSCPL was prepared by heat-treatment at 56 °C for 30 minutes of the SCPL. PPL was made from isolated platelets and is therefore depleted of the plasma protein compartment. The

platelet pellet was then subjected to three freeze (-80 ± 1 °C) and thaw (37 ± 1 °C) cycles to release the platelet content. Finally, HPPL was obtained by 56 °C-30 minutes treatment of PPL.

3.1.1 Blood cell count

Starting PCs had platelet counts ranging from (408~570) x 10^3 cells/mm^3 or in the range number of 2.4 ~3.8 10^{11} per PC unit. The residual red blood cell (RBC) and white blood cell (WBC) levels were under the respective limits of detection (< 0.7 × 10^6/mm^3, and < 0.8 × 10^3/mm^3, respectively).

3.1.2 Five HPLs significantly differed in their protein contents

The total protein content was evaluated by BCA assays. There is a significantly higher protein concentration in FTPL compared to what found in SCPL ($p < 0.01$) and PPL ($p < 0.0001$). Furthermore, in the heat-treated fractions, HPPL and HSCPL, the protein content was decreased compared to their unheated counterparts 1.0- and 1.7-fold, respectively (Figure 8).

3.1.3 PPL and HPPL were enriched in growth factors content

The data revealed significantly higher levels ($p < 0.01$~0.0001) of growth factors: BDNF, PDGF-AB, EGF, VEGF, and TGF-β in PPL and HPPL fractions that were prepared from isolated platelets, compared to the other HPLs where platelets were suspended in plasma. Meanwhile in FTPL that was prepared from platelet suspended in plasma, and SCPL, IGF-1 was found higher compared to what measured in PPL ($p < 0.05$~ 0.0001). Heat treatment resulted in a slight decrease in the levels of all these factors in HSCPL compared to SCPL. However, in HPPL, significantly lower amounts ($p < 0.0001$) of BDNF, PDGF-AB, and EGF were observed in comparison to PPL. Moreover, IGF-1 was found to be undetectable (< 62.5 pg/mL) in HPPL samples. Concentration of growth factors in ng/mL is shown in Figure 7A-F. The content of selected growth factors relative to total protein in a ratio ng/mg are shown in Figure 8A. The content of VEGF per total protein (ng/mL) did not show any significant difference between the two groups. However, a relative enrichment of TGF-β was observed in HPPL when compared to PPL.

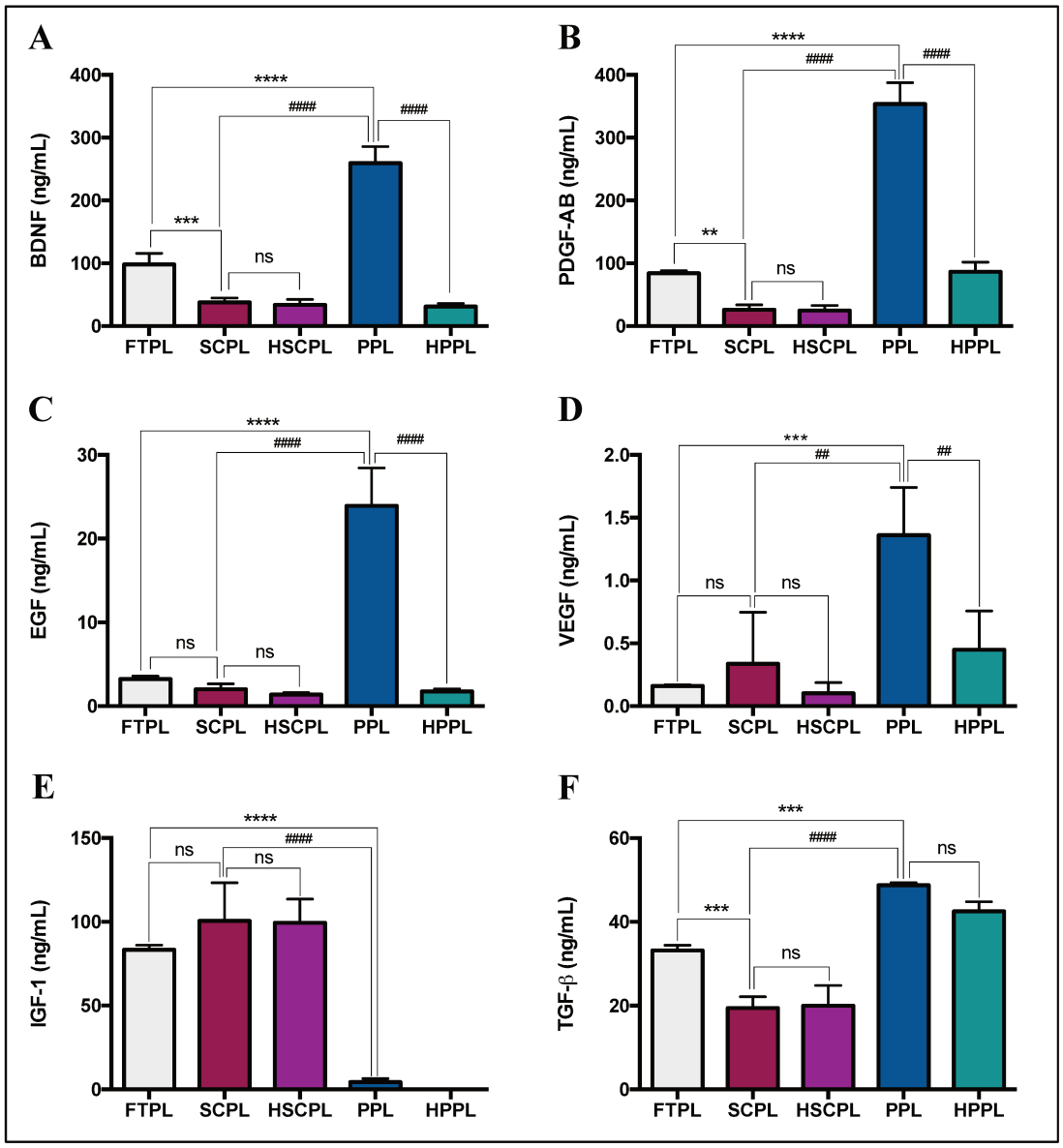

*Figure 7. Growth factors and complement determination in HPL fractions. (A) BDNF (ng/mL) (B) EGF (ng/mL) (C) PDGF-AB (ng/mL) (D) VEGF (ng/mL) (E) IGF-1 (ng/mL) (F) TGF-β1 (ng/mL) (G) Complement C3 (ng/mL) (H) Complement C4 (ng/mL). Results expressed as a mean ± SD. (** $p < 0.01$), (*** $p < 0.001$),), (**** $p < 0.0001$) as compared to FTPL, ($^{\#\#}$ $p < 0.01$), ($^{\#\#\#\#}$ $p < 0.0001$) as compared to PPL, ns: not significant. Statistical evaluation was performed by one-way ANOVA followed by dunnett's multiple comparisions test. Abbreviations: brain-derived neurotrophic factor (BDNF), platelet-derived growth factor-AB (PDGF-AB), epidermal growth factor (EGF), vascular endothelial growth factor (VEGF), insulin-like growth factor-1 (IGF-1), TGF-β: transforming growth factor-β, frozen-thawed platelet lysate (FTPL), serum converted platelet lysate (SCPL), heated serum converted platelet lysate (HSCPL), platelet pellet lysate (PPL), heated platelet pellet lysate (HPPL). Copyright © 2021 by Taylor & Francis Group.*

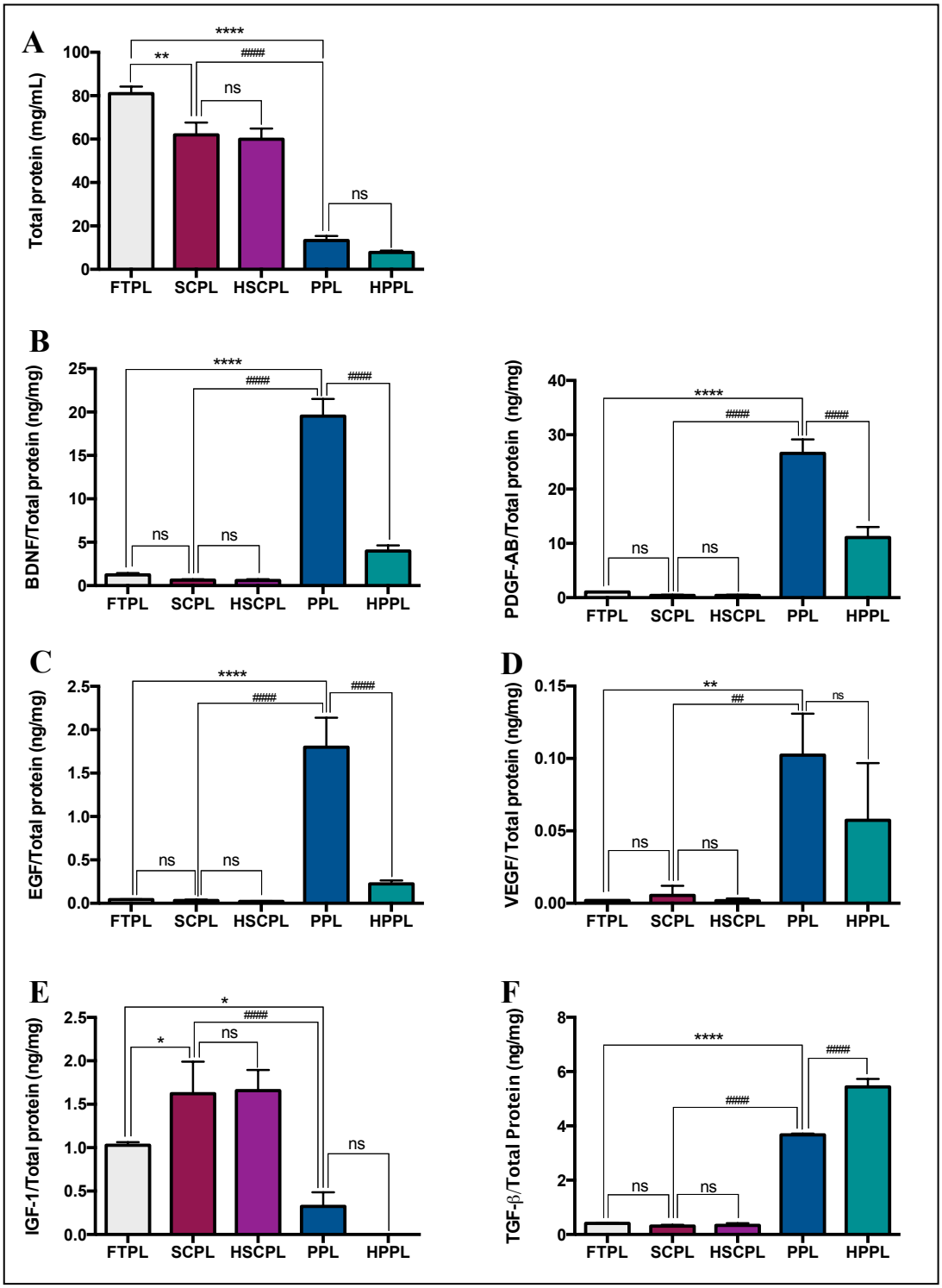

Figure 8. Growth factors per total protein content in HPL fractions.(A) Total protein (mg/mL) (B) BDNF (ng/mg) (C) PDGF-AB (ng/mg) (D) EGF (ng/mg) (E) VEGF (ng/mg) (F) IGF-1 (ng/mg) (G) TGF-β1 (ng/mg) Results expressed as a mean ± SD. ($p < 0.05$), (** $p < 0.01$),), (**** $p < 0.0001$) as compared to FTPL, (## $p < 0.01$), (#### $p < 0.0001$) as compared to PPL, ns: not significant. Statistical evaluation was performed by one-way ANOVA followed by dunnett's multiple comparisions test. Abbreviations: brain-derived neurotrophic factor (BDNF), platelet-derived growth factor-AB (PDGF-AB), epidermal growth factor (EGF), vascular endothelial growth factor (VEGF), insulin-like growth factor-1 (IGF-1), TGF-β: transforming growth factor-β, frozen-thawed platelet lysate (FTPL), serum converted platelet lysate (SCPL), heated serum converted platelet lysate (HSCPL), platelet pellet lysate (PPL), heated platelet pellet lysate (HPPL). Copyright © 2021 by Taylor & Francis Group.*

3.1.4 Complement factors presence higher in FTPL and SCPL

The presence of complement components C3 and C4 in HPLs was evaluated using an immunological method (Figure 9). In both FTPL and SCPL, the result shown that the amounts of these two complement factors were significantly higher ($p < 0.0001$), compared to in PPL. The analysis revealed that there were no significant differences in the levels of complement components C3 and C4 between HSCPL and SCPL, as well as between HPPL and PPL. This suggests that the heat treatment had no detectable impact on the concentrations of these complement components.

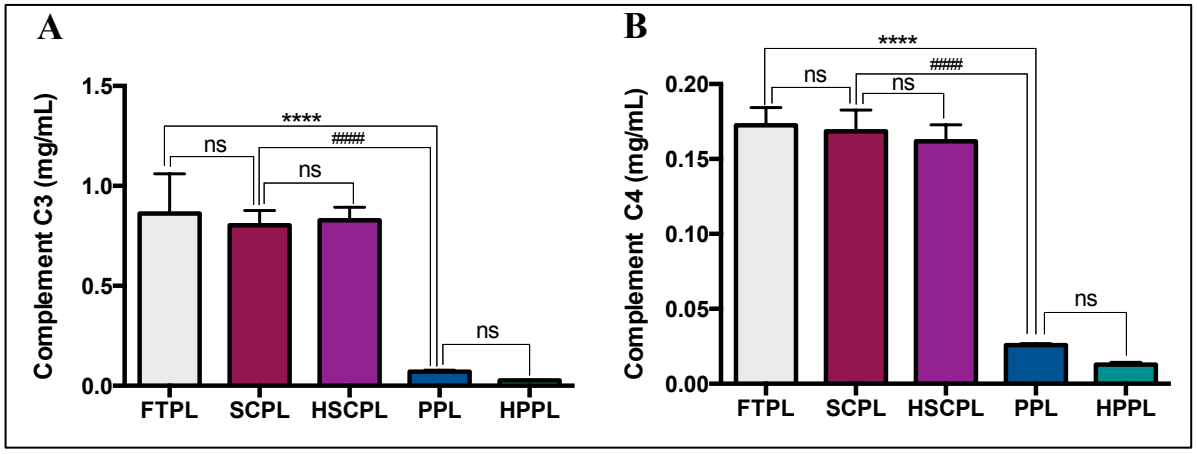

*Figure 9. Complement determination in HPL fractions. (A) Complement C3 (ng/mL) (B) Complement C4 (ng/mL). Results expressed as a mean ± SD. (** $p < 0.01$), (*** $p < 0.001$), (**** $p < 0.0001$) as compared to FTPL, (## $p < 0.01$), (#### $p < 0.0001$) as compared to PPL, ns: not significant. Statistical evaluation was performed by one-way ANOVA followed by Dunnett's multiple comparisons test. Abbreviations: frozen-thawed platelet lysate (FTPL), serum converted platelet lysate (SCPL), heated serum converted platelet lysate (HSCPL), platelet pellet lysate (PPL), heated platelet pellet lysate (HPPL).*

3.1.5 Proteome profiling assay: variety of protein known to be present in platelets detected in all HPLs

The relative expression of protein profiles in SCPL, HSCPL, PPL, and HSCPL was assessed using a cytokine and profiling array kit. The cytokines and proteins that were analyzed are illustrated in Figure 10. The results of the study confirmed the presence of various proteins known to be associated with platelets. These include BDNF, chemokine ligand 5 (CCL5), chemokine (C-X-C motif) ligand-5 (CXCL-5), complement component C5, complement factor D, EGF, fibroblast growth factor-19 (FGF-19), lipocalin-2, macrophage migration inhibitory

factor (MIF), metalloproteinase-9 (MMP-9), platelet factor-4 (PF-4), PDGF-AA, PDGF-AB, serpin, thrombospondin-1, tissue inhibitors of metalloproteinase-1 (TIMP-1), and VEGF. The analysis of the HPLs samples revealed distinct relative protein profiles among them, with CXCL-16, prolactin, and TIMP-4 detected exclusively in SCPL and HSCPL, and B-cell activating factor (BAFF) and myeloperoxidase found only in PPL and HPPL. Moreover, extracellular matrix metalloproteinase inducer (EMMPRIN) and leptin were not detected in HSCPL, while endostatin and endoglin were absent in HPPL but detectable in SCPL and PPL.

A

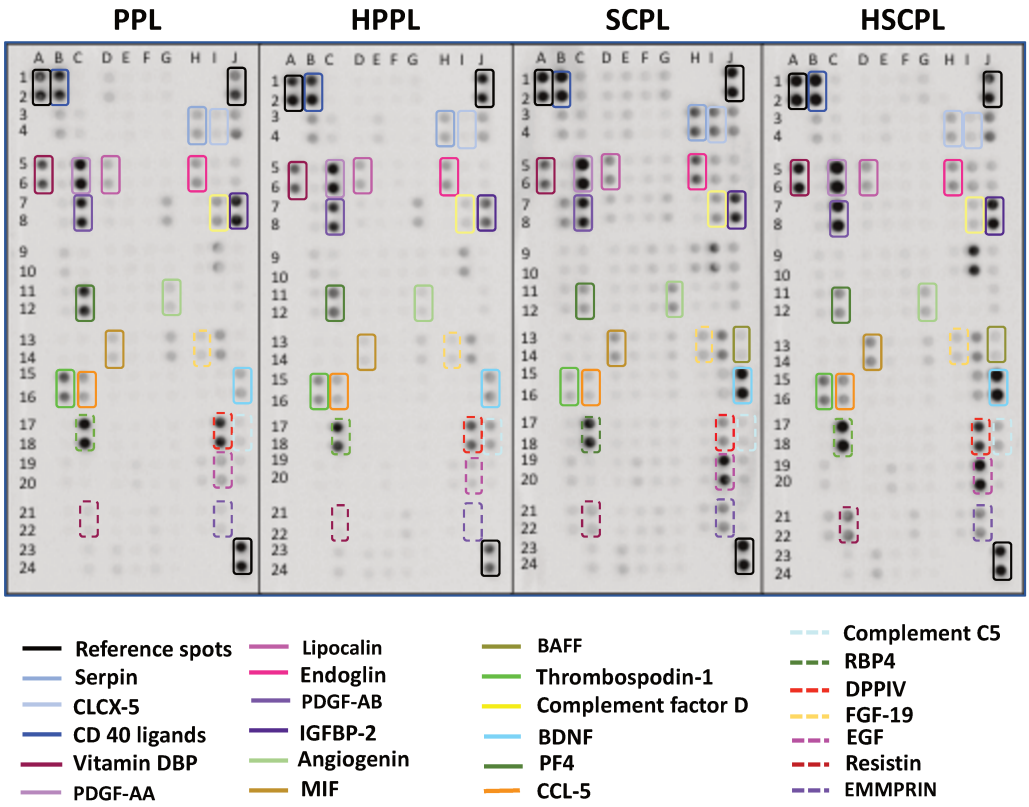

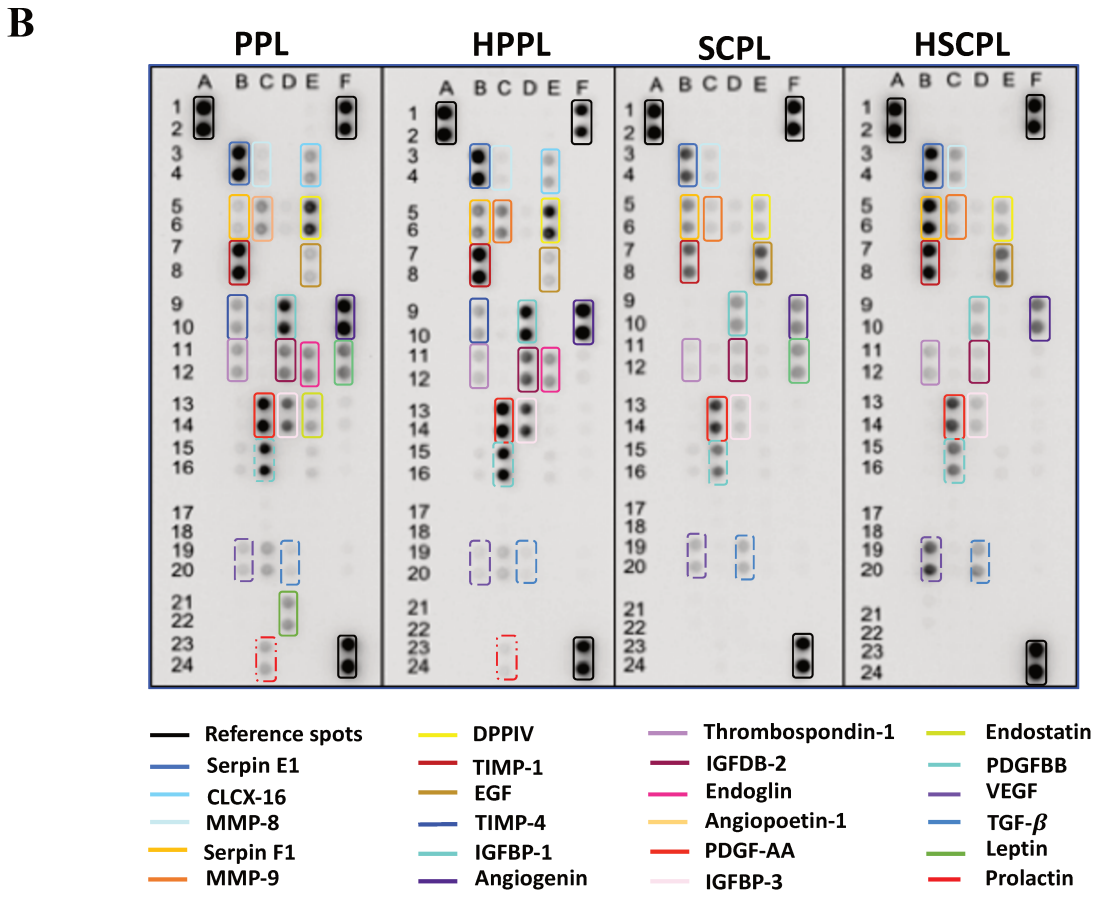

Figure 10. Proteins profiling array (a) Human cytokine array (b) Angiogenesis array. Each coordinate spots represent a positive signal generated from the protein with captured antibody. The manufacturer's list and coordinates for analytes and controls were used to identify each protein. Abbreviations: serum converted platelet lysate (HSCPL), platelet pellet lysate (PPL), heated platelet pellet lysate (HPPL).

3.1.6 Clinical chemistry and immunochemistry analysis

The biochemical composition of HPLs was determined by immunochemistry analysis, all HPLs was compared to FTPL as a reference fraction (Table 2).

The analysis demonstrated that, in general, FTPL, SCPL, and HSCPL samples suspended in plasma exhibited higher levels of albumin, glucose, IgG, and lipids (HDL and LDL) in comparison to PPL and HPPL, which were depleted of plasma. The albumin and glucose content in SCPL and HSCPL did not show a significant difference when compared to FTPL. However, they were significantly lower ($p < 0.0001$) in PPL and HPPL. There was no statistical difference among FTPL, SCPL, and HSCPL in IgG levels but it was significantly higher ($p < 0.0001$) compared to those in PPL and HPPL (< 3 mg/mL). The levels of HDL and LDL did not exhibit a statistically significant difference in SCPL and HSCPL when compared to FTPL. However, HDL and LDL were below the limit of detection (< 0.03 and 0.04 mg/mL, respectively) in both PPL and HPPL samples. Fibrinogen was detected only in FTPL at a concentration of 1.89 ± 0.46 mg/mL. However, it was below the limit of detection (< 0.4 mg/mL) in seroconverted SCPL and plasma-free PPL, as well as in their corresponding heat-treated fractions.

The chemical analysis revealed that in SCPL, HSCPL, PPL, and HPPL samples exhibited significantly higher levels of Cl ($p < 0.001$) when compared to FTPL. Moreover, the levels of Ca were found to be higher ($p < 0.001$) in SCPL and HSCPL, but lower ($p < 0.001$) in PPL and HPPL when compared to FTPL. This were likely a result of the $CaCl_2$ addition during the serum conversion process. However, the concentrations of K and P in SCPL and HSCPL were not statistically different from those in FTPL. On the other hand, K and P levels were significantly higher ($p < 0.01 \sim p < 0.001$) in PPL and HPPL when compared to FTPL. The use of PBS, which contains NaCl, KCl, Na_2HPO_4, and KH_2PO_4, to resuspend the platelet pellet to prepare PPL and HPPL could explain the higher content of Cl, K, and P in this two platelet lysate fractions.

Table 2. Clinical chemistry and immunochemistry analysis

Chemical composition	FTPL	SCPL	P value	HSCPL	P value	PPL	P value	HPPL	P value
Albumin (mg/mL)	35.67 ±1.15	38.00 ±3.46	ns	39.33 ±2.08	ns	5.67 ±0.58	***	3.33 ±0.58	***
Glucose AC (mg/mL)	2.33 ±0.67	2.38 ±0.18	ns	2.40 ±0.19	ns	0.20 ±0.20	***	0.12 ±0.16	***
Ferritin (ng/mL)	52.00 ±35.54	51.67 ±31.53	ns	52.00 ±32.00	ns	286.67 ±34.49	***	279.33 ±29.69	***
TIBC (ug/mL)	3.30 ±0.57	9.43 ±0.23	***	9.45 ±0.17	***	0.47 ±0.10	***	0.39 ±0.02	***
UIBC (ug/mL)	2.45 ±0.23	8.68 ±0.15	***	8.67 ±0.14	***	0.26 ±0.06	***	0.17 ±0.00	***
IgG (mg/mL)	11.54 ±4.11	9.20 ±5.17	ns	8.09 ±1.98	ns	<3		<3	
Triglyceride (mg/mL)	0.55 ±0.26	0.66 ±0.50	ns	0.61 ±0.40	ns	0.10 ±0.02	ns	<9	
Cholesterol (mg/mL)	1.03 ±0.67	1.47 ±0.19	**	1.48 ±0.22	**	0.17 ±0.02	***	0.06 ±0.02	***
HDL (mg/mL)	0.39 ±0.13	0.34 ±0.27	ns	0.26 ±0.10	ns	<0.03		<0.03	
LDL (mg/mL)	0.50 ±0.11	0.30 ±0.36	ns	0.35 ±0.04	ns	<0.04		<0.04	
Fibrinogen (mg/mL)	1.89 ±0.46	<0.4		<0.4		<0.4		<0.4	
Hemoglobin (g/dL)	0.10 ±0.00	0.10 ±0.00	ns	0.10 ±0.00	ns	0.27 ±0.06	ns	0.13 ±0.06	ns
Folate (ng/mL)	6.99 ±2.41	7.03 ±4.97	ns	7.57 ±5.77	ns	4.21 ±2.81	ns	4.24 ±2.61	ns
VIt B12 (pg/mL)	406.20 ±22.59	314.77 ±106.19	ns	321.00 ±108.80	ns	173.47 ±16.07	**	141.33 ±17.38	**
Cl (mEq/L)	76.00 ±2.83	123.67 ±3.79	***	123.67 ±3.06	***	126.67 ±8.39	***	127.67 ±7.51	***
Na (mEq/L)	203.33 ±72.67	158.67 ±2.08	ns	158.67 ±2.89	ns	149.67 ±5.69	ns	150.67 ±4.73	ns
K (mEq/L)	5.67 ±2.20	3.73 ±0.21	ns	3.73 ±0.21	ns	11.83 ±2.57	**	11.87 ±2.54	**
Ca (mg/dl)	8.73 ±0.40	57.73 ±0.06	***	57.50 ±0.30	***	4.93 ±1.29	***	4.77 ±1.14	***

P (mg/dL)	4.07	±0.49	3.73	±0.06	ns	3.63	±0.06	ns	31.80	±5.70	***	30.97	±5.45	***
Mg (mg/dL)	1.97	±0.12	3.70	±0.00	***	3.70	±0.00	***	1.70	±0.35	ns	1.70	±0.35	ns
Fe (ug/dL)	84.67	±33.86	75.33	±10.69	ns	78.33	±8.50	ns	20.33	±6.51	**	22.00	±2.00	**

*(** $p < 0.01$), (*** $p < 0.001$) as compared to FTPL, ns: not-significant.*

3.1.7 Functional coagulant and procoagulant activities are higher in fractions containing the plasma compartment

Thrombin generation

The data presented in Table 3 indicated significant variations in the ability to generate thrombin, as assessed by TGA, among the different HPLs. The presence of detectable thrombin generation was observed in FTPL, SCPL, HSCPL, and PPL when using both "RC-low" and "RC-high" reagents. However, thrombin generation was not detected in HPPL. “RC-low” contains a low concentration of phospholipid micelles containing recombinant human tissue factor and $CaCl_2$, whereas, in contrast, “RC-high” contains a high concentration. The data revealed that there was a significantly higher amount of thrombin generated in FTPL ($p < 0.01$) and in SCPL ($p < 0.001$) when using both "RC-low" and "RC-high" reagents, as compared to PPL. This indicates that FTPL and SCPL samples exhibited a greater capacity to generate thrombin compared to PPL under the given experimental conditions. Thrombin generated in FTPL was higher ($p < 0.01$) than that in SCPL using “RC high” but did not significantly differ using “RC low.” In the heated fraction, HSCPL, thrombin generated was significantly reduced ($p < 0.01$) compared to the unheated fraction, SCPL.

Thrombin proteolytic activity

We assessed the activity of any thrombin-like proteolytic enzyme by employing the S-2238 chromogenic substrate. For positive and negative controls, $CaCl_2$-activated plasma and normal plasma were utilized, respectively. (Figure 11A). No thrombin proteolytic activity was detected in the non-activated plasma control, as well as in the fractions FTPL and HPPL. Elevated thrombin proteolytic activities were observed in $CaCl_2$-activated plasma, SCPL, and HSCPL ($p < 0.0001$), while no significant difference was found in PPL compared to normal non-activated plasma. Proteolytic activity exhibited a significant increase in SCPL ($p < 0.0001$), but a marked decrease ($p < 0.0001$) was observed after heat treatment in HSCPL when compared to PPL and non-activated plasma. Notably, no proteolytic activity was detected in HPPL.

Phospholipid pro-coagulant activity

Results of the phospholipid pro-coagulant-dependent clotting time assays are presented in Figure 11C. Time is expressed in second (s). SCPL (30.77 ± 5.32), the clotting time was

significantly lower ($p < 0.1$), and no significant difference was observed in FTPL (17.90 ± 1.57) or HPPL (23.57 ± 3.76) compared to PPL (12.97 ± 0.40). In the heated fractions, HSCPL, a significant prolongation ($p < 0.0001$) of coagulation time (71.83 ± 11.00) was detected compared to SCPL, indicating that heat treatment reduced a functional procoagulant phospholipids.

Table 3. Determination of the thrombin generation capacity of HPL fractions using the TGA assay and RC-low (A) and RC-high (B) reagents

Sample	RC Low (A)					RC High (B)				
	Lag phase (min)	**Thrombin (nmol/L)**	**Time to peak (min)**	**Velocity Index**	**AUC**	**Lag phase (min)**	**Thrombin (nmol/L)**	**Time to peak (min)**	**Velocity Index**	**AUC**
FTPL	8.25 ± 2.87 (6-12)	99.39 ± 58.31** (35.10-148.78)	19.00 ± 4.24 (16-25)	9.71 ± 5.97 (4.10-14.88)	1390.06 ± 463.55 (853.00-1152.70)	5.00 ± 1.15 (4-6)	142.08 ± 22.51 **** ## (119.07-173.05)	11.00± 1.41 (10-13)	26.75 ± 10.13 (13.23-34.50)	2780.53 ± 330.90 (2329.76-3028.74
SCPL	3.50 ± 0.58 (3-4)	132.25 ± 15.95 *** (116.76-146.70)	24.67 ± 17.90 (4-35)	3.82 ± 0.08 (3.77-3.88)	(3761.60 ± 333.73) (3524.50-4083.20)	4.0 ± 0 (4)	113.94 ± 6.91 **** (107.38-121.07)	16.00± 14.28 (5-35)	56.97 ± 58.99 (3.91-108.70)	(3618.36 ± 167.42) (3409.33-3816.70)
HSCPL	4.00 ± 0.82 (3-5)	41.10 ± 11.55 (30.90-53.69)	46.25 ± 10.50 (34-55)	0.95 ± 0.12 (0.80-1.07)	(1042.08 ± 83.79) (980.50-1165.84)	4.0 ± 0 (4)	53.32 ± 2.86 (49.79-56.68)	52.5 ± 2.89 (50-55)	1.10 ± 0.04 (1.06-1.15)	(1302.70 ± 164.48) (1161.74-1502.86)
PPL	5.25 ± 0.50 (5-6)	6.37 ± 3.02 (3.40-9.40)	52.5 ± 7.14 (42-58)	0.14 ± 0.05 (0.10-0.19)	14.19 ± 9.46 (3.40-21.05)	6.25 ± 1.50 (5-8)	4.59 ± 5.54 (0.00-11.13)	27.00 ± 31.18 (0.00-54)	0.19 ± 0.06 (0.00-0.23)	12.13 ± 14.38 (0.00-28.28)
HPPL	14.50 ± 1.29 (13-16)	0.0 (0-0)	0.0 (0-0)	-	0.0 (0-0)	14.75 ± 1.71 (13-17)	0.0 (0-0)	0.0 (0-0)	-	0.0 (0-0)

Thrombin generation assay using RC-low (A) and RC-high (B) reagents of HPL fractions. *Data are expressed as mean ± SD (range); In the absence of thrombin formation, the velocity index is not expressed; (** $p < 0.01$), (*** $p < 0.001$), (**** $p < 0.0001$) compared to PPL, (## $p < 0.01$) compared to SCPL. Abbreviations:* ***RC Low****, low concentration of phospholipid micelles containing recombinant human tissue factor;* ***RC High****, high concentration of phospholipid micelles containing recombinant human tissue factor;* ***AUC****, area under the curve.*

3.1.8 Absolute antioxidative activity using the Zen-Bio ORAC antioxidant test assay was higher in FTPL, SCPL, and HSCPL

The antioxidative activity (Trolox equivalent) expressed as µmol/L or mmol/mg of total protein is shown in Figure 11D-E. FTPL (187%) and SCPL (176%) had a significantly higher ($p < 0.001$) µmol/L activity, but statistically lower ($p < 0.5$) and ($p < 0.01$) was found in PPL (53%) in HPPL (23%) respectively, compared to the plasma control (100%). The anti-oxidative activity, when it is normalized to the total protein content, showed no significant difference in FTPL (150%) and HSCPL (141%). However, it was significantly higher ($p < 0.01 \sim p < 0.001$) in SCPL (186%), PPL (217%), and HPPL (154%). When represented as a ratio of total proteins, PPL and HPPL, which were obtained from purified platelets, displayed antioxidative activities at a similar level to the other HPLs and were higher than the plasma control.

3.1.9 Functional characterization of platelet EVs in HPLs

The procoagulant activity was also examined by dedicated assays which determine PS-expressing and TF-expressing EVs.

PS expression

The contents of PS-expressing EVs varied among the five HPLs as shown in the Figure 11B**.** In both SCPL and FTPL, there were significantly lower levels of PS-expressing EVs ($p < 0.0001$) than in PPL. Heat treatment resulted in a significant ($p < 0.0001$) decrease in PS-expressing EVs in HPPL, compared to PPL, but no significant difference was detected in HSCPL compared to SCPL.

TF expression

TF-expressing EVs were undetectable in all HPLs**,** but they were detectable in the internal control samples (Table 4). There was no TF-bearing EVs detected in any of the HPL fractions**,** confirming the lack of TF expression by platelets of healthy blood donors [281].

Table 4. TF expression

Samples	MP-TF (pg/mL)
FTPL	≤ 0.05
PPL	≤ 0.05
HPPL	≤ 0.05
SCPL	≤ 0.05
HSCPL	≤ 0.05

Limit of detection of the assay ≤ 0.05 *pg/mL*

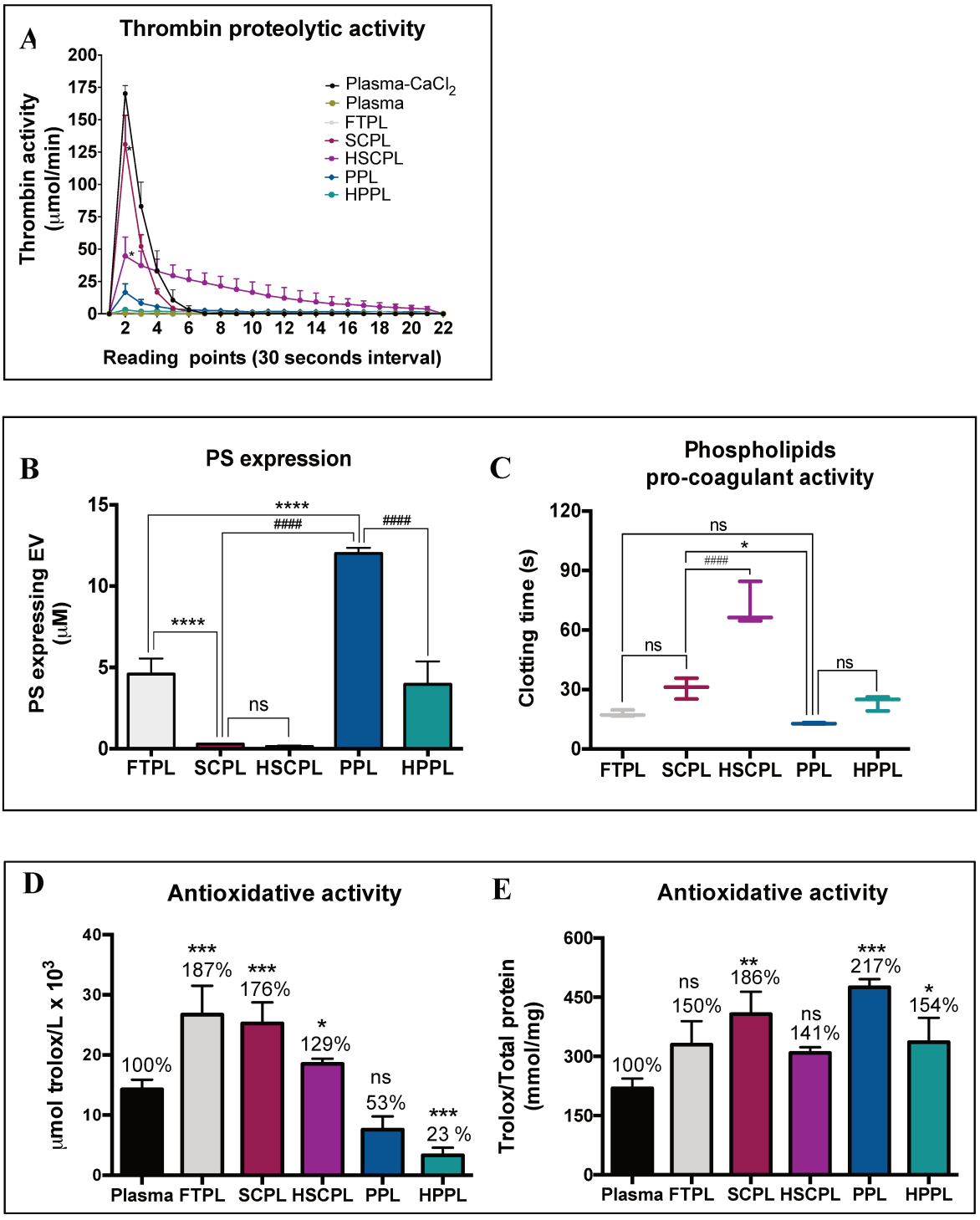

Figure 11. Functional activity of HPL fractions. (A) Thrombin proteolytic activity (B) PS expression (C) Phospholipids pro-coagulant activity (D) Antioxidative activity (E) Antioxidative activity per total protein. The data for all functional assays were obtained from at least three experiments. (A) ***Thrombin proteolytic*** *are expressed in activity (µmol/min) and shown as a mean ± SD. A normal non-activated and $CaCl_2$-activated human plasma were used as experimental controls, *p < 0.0001 as compared to non-activated plasma. (B)* ***PS expression*** *(µmol/L) shown as a mean ± SD (**** p < 0.0001), compared to FTPL, ($^{\#\#\#\#}$ p < 0.0001) compared to PPL, ns: not significant. (C)* ***Phospholipid pro-coagulant activity*** *are expressed by the clotting time (second) as a mean ± SD. (* p < 0.1) compared to PPL, ($^{\#\#\#\#}$ p < 0.0001) compared to SCPL, ns: not significant. (D)* ***Antioxidative activity*** *are expressed in µmol Trolox/L x 10^3, (E)* ***Antioxidative activity*** *are expressed in mmol Trolox per mg total protein content (mmol/mg) and shown as a mean ± SD. Plasma was used as a positive control (100%). (*** p < 0.001), (* p < 0.5), ns: not significant. Abbreviations:*

phosphatidylserine (PS), frozen-thawed platelet lysate (FTPL), serum converted platelet lysate (SCPL), heated serum converted platelet lysate (HSCPL), platelet pellet lysate (PPL), heated platelet pellet lysate (HPPL). Copyright © 2021 by Taylor & Francis Group.

3.2 The impact of nanofiltration on the composition and functional activity of HPPL

The findings of the composition and functional activity evaluations of HPLs led us to confirm the selection of HPPL as a suitable preparation for brain administration. A large-scale preparation of HPPL is needed for future clinical use and therefore to ensure batch-to-batch consistency, HPPLs is usually prepared from pooled PCs. However, pooling statistically increases the risk of viral contamination by window-phase donations, or by untested viruses. Nanofiltration has known for its robustness in removing a wide range of viruses and improving the safety manufacturers of plasma-derived products. Depending on the pore size, it entraps both enveloped and un-enveloped viruses. In this experiment we used Planova-20N filter with ±19 nm pore size (ASAHI Kasei).

Thus, we assessed the feasibility and capacity of nanofiltration as a virus removal step implemented in HPPL, in order to ensure the safety of HPPL, especially when it is used for brain treatment. We also investigated the impact of the nanofiltration on the HPPL compositions including their proteins, and EVs content as well as their functional neuroprotective and neuro-regenerative activity.

3.2.1 The feasibility of nanofiltration in HPPL and virus reduction values

HPPL made from pooled PCs made up from 50 donations following our established methods [282,283]. HPPL then was pre-filtered using 0.2- and 0.1-µm filters prior nanofiltration. The result showed that close to 20 mL of HPPL could be filtered through 0.001m^2 Planova-20N within approximately 3 hours at a constant flow-rate of 0.1 mL/minute and without reaching the maximum pressure of 0.098 MPa fixed by the supplier. Therefore, the nanofiltration of the HPPL on Planova-20N was achieved without clogging. The capacity of Planova-20N to effectively remove small viruses was assessed by spiking the MVPs into 4 mL of pre-filtered 0.2-0.1 µm HPPL, and to have an expected final concentration of 10^{10} MVPs/mL. The MVPs concentration in spiked HPPL determined by immuno-qPCR was 1.63 x 10^9 ± 8.2 x 10^8, and 1.83 x 10^9 ± 1.77 x 10^8 when frozen immediately after spiking or after being kept at room

temperature during the duration of the nanofiltration experiment, respectively. This indicated that there was no loss in detectable MVM associated to spiking into HPPL and storage at room temperature followed by freezing, demonstrating the absence of detrimental interference of the test material and the processing steps on the immune-qPCR assay. The Ct values obtained by immuno-qPCR showed a value of $3.75 \times 10^3 \pm 3.47 \times 10^3$ after nanofiltration, similar to the baseline level found for the unspiked control, therefore confirming complete removal of the MVP. This indicated that the LRVs achieved by Planova-20N nanofiltration was ≥ 5.39 log, showing a complete and extensive removal of this small model mock virus. The conditions used for HPPL nanofiltration and MVM removal data are summarized in Table 5.

Table 5. Virus removal capacity

Volume spiked	**Volume collected**	**Pressure**	**Duration**
4 mL	1.83 ± 0.11 mL	0.08 mPa	30 minutes
MPV spiked value/mL	**MVP calculated value/mL**		**Long reduction value (LRV)**
	Before filtration	**After filtration**	
1×10^{10}	(a) $1.63 \times 10^9 \pm 8.2 \times 10^8$ (b) $1.73 \times 10^9 \pm 4.97 \times 10^8$	$3.75 \times 10^3 \pm 3.47 \times 10^3$	≥ 5.39 ≥ 6.15

Immediately frozen at -80 °C after spiking (b) freeze at -80 °C after kept at the room temperature during the nanofiltration duration. N = 2 for each condition.

3.2.2 The impact of nanofiltration in HPPL compositions and functional activities

Total proteins and contents of trophic factors

We investigated the effects of nanofiltration on protein content and selected growth factors. The total protein content decreased from approximately 7 mg/mL in HPPL to around 4 mg/mL after 0.2~0.1-µm filtration and further decreased to about 3 mg/mL after Planova 20N filtration. (Figure 12). The respective content (ng/mL) in (PDGF)-AB, (EGF), and (VEGF) in HPPL, 0.2~0.1-µm-filtered HPPL, and NHPPL was: 89.2 ± 9.67, 60.86 ± 11.84, 20.54 ± 3.05 (PDGF); 6.24 ± 0.75, 4.75 ± 0.42, 5.30 ± 0.36 (EGF); and 1.17 ± 0.02, 0.97 ± 0.03, 0.7 ± 0.01 (VEGF).

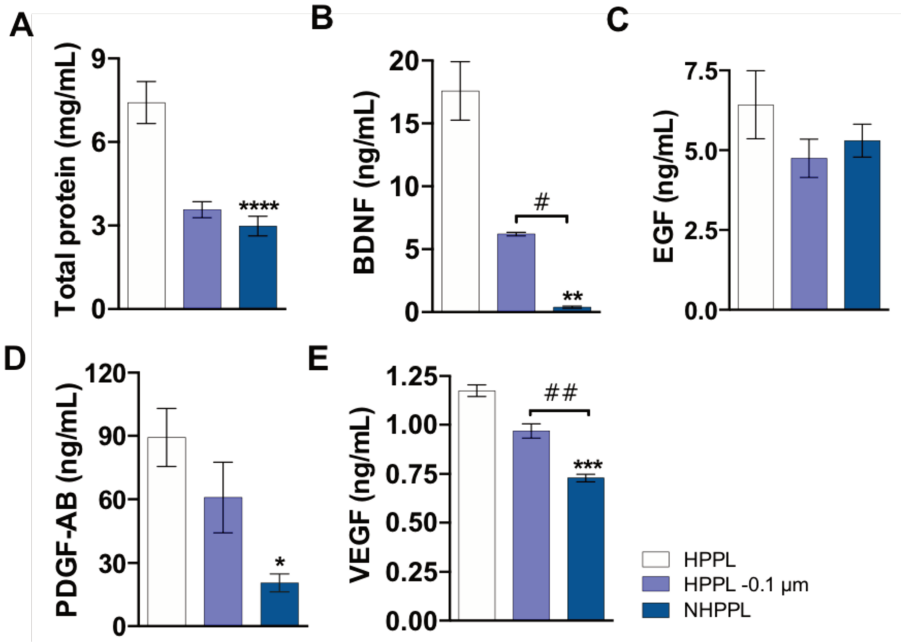

Figure 12. Total protein content and trophic factors. (A) Total protein (mg/mL) (B) BDNF (ng/mL), (C) EGF (ng/mL), (D) PDGF-AB (ng/mL), (E) VEGF (ng/mL). Results expressed as a mean ± SD (N = 3). ($p < .05$), (** $p < .01$), (*** $p < .001$), (*** $p < .0001$), as compared to HPPL, ($^{\#}p < .05$), ($^{\#\#}p < .01$) as compared to HPPL 0.1 µm. Statistical evaluation was performed by one-way ANOVA followed by Fisher's LSD test. Abbreviations: brain-derived neurotrophic factor (BDNF), platelet-derived growth factor-AB (PDGF-AB), epidermal growth factor (EGF), vascular endothelial growth factor (VEGF), heated platelet pellet lysate (HPPL), NHPPL (HPPL-P20).*

PEVs contents and related procoagulant functional activities

We investigated the size distribution and number of PEVs in HPPL before and after nanofiltration using DLS and NTA techniques. The results showed a significant reduction in the mean size distribution of PEVs, from approximately 171.5 nm to around 10.5 nm after nanofiltration (Figure 13A), as evidenced by DLS analysis. Additionally, NTA analysis revealed a substantial decrease in the concentration of PEVs, with a reduction of approximately 90%, from $6.20 \times 10^{10} \pm 3.48 \times 10^{8}$ to $6.21 \times 10^{9} \pm 3.12 \times 10^{8}$. To further evaluate the impact of PEVs on blood coagulation, we conducted the STA-procoagulant-phospholipid assay, which measures the contribution of PEVs to blood coagulation. A significant prolongation in the coagulation time by the NHPPL, with a duration of approximately 110 s, compared to the non-nanofiltered HPPL, which had a coagulation time of approximately 24 s. These results are consistent with the removal of PEVs contributing to blood coagulation, indicating the effectiveness of the nanofiltration process. We measured the content of PS-expressing EVs (Figure 13B) and found a significant reduction in NHPPL compared to the crude ($p < 0.0001$)

and the 0.2-0.1 µm-filtered HPPL ($p < 0.01$). Thus, the nanofiltration process not only resulted in a remarkable removal of EVs but also significantly decreased its procoagulant effect.

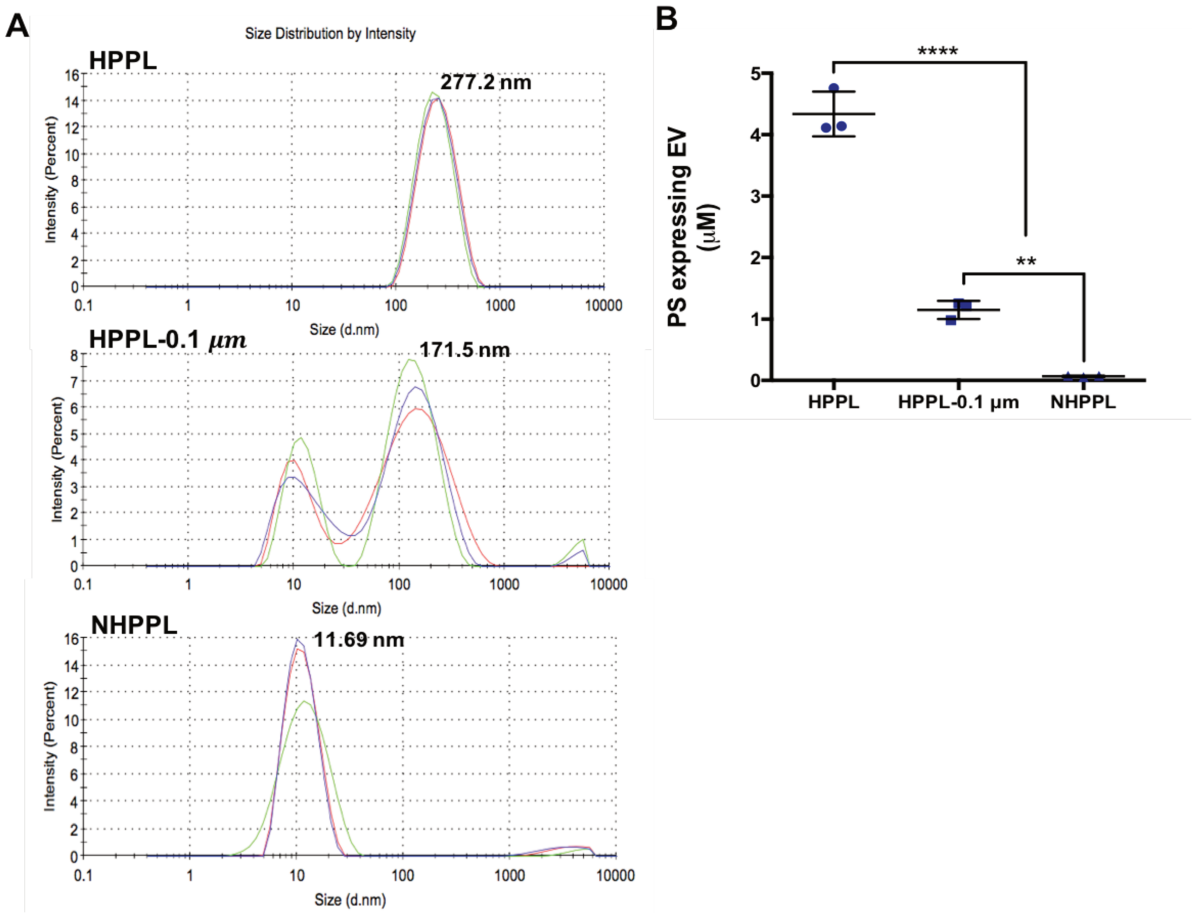

*Figure 13. PEVs content in HPPL, after 0.2-0.1 µm filtration, and in NHPPL. PEVs content in HPPL, after 0.2-0.1 µm filtration, and in NHPPL (A) PEVs size distribution analysis by DLS (B) PS expressing-PEVs. Results expressed as a mean ± SD (N = 3). (**** p < .0001), as compared to HPPL. Statistical evaluation was performed by one-way ANOVA followed by Fisher's LSD test. PEVs size measurement by DLS in HPPL, 0.2-0.1µm prefiltered HPPL (HPPL-0.1 µm), and NHPPL (HPPL-P20). The red, green and blue curves represent the first, second, and third analyses, respectively Abbreviations: phosphatidylserine (PS)*

Proteomics analysis

The proteomics analysis was done by using (LC-MS/MS). The number of proteins identified with a false discovery rate (FDR) of less than 1% at the protein level FDR were 1117, 1011, and 897 in HPPL, 0.20.1-µm-filtered HPPL, and NHPPL, respectively (as shown in Figure 14A). Among these, 813 proteins were common across all samples. Notably, antioxidants (such as superoxide dismutase, ceruloplasmin, glutathione peroxidase, gelsolin, and catalase), neurotrophic factors, and cytokines (including PDGF, VEGF, EGF, hepatocyte growth factor

(HGF), glial maturation factor beta (GMFB), PF4, and CCL5) were detected in NHPPL. Through the genes ontology (GO) analysis of the 813 common proteins, several biological processes (BPs) associated with platelet degranulation, cell-cell adhesion, the Fc-epsilon receptor signaling pathway, receptor-mediated endocytosis, the classical complement activation pathway, the Fc-gamma receptor signaling pathway involved in phagocytosis, and complement activation were identified. The cellular components (CC) analysis indicated that the top three subcategories were extracellular exosomes, cytosol, and blood microparticles. In addition, the molecular function (MF) analysis revealed that the proteins were mainly linked to cadherin binding associated with cell-cell adhesion, protein binding, antigen binding, and actin filament binding. After 0.20.1-μm filtration, 152 proteins became undetectable in HPPL, and an additional 158 proteins after Planova-20N. The GO term analysis showed that these proteins removed by both 0.2~0.1-μm filtration (as shown in Figure 14C) and then Planova-20N (as shown in Figure 14D) were associated with extracellular exosomes and cytoplasm/cytosol. These proteins act as binding proteins and have various functions in cell adhesion and signaling pathways. Moreover, the abundances of GPIb, GPV, and GVI - which are platelet EV membrane proteins expressed by non-activated platelets, and CD-62P/p-selectin expressed by activated platelets decreased after filtration.

The KEGG pathway enrichment analysis revealed that the common proteins identified in all samples were associated with complement and coagulation cascades, platelet activation, and the proteasome (Figure 15). These pathways showed decreased abundances after both 0.2~0.1-μm filtration and Planova-20N filtration. On the other hand, the KEGG pathway analysis for proteins removed by the two filtration processes showed pathways related to platelet activation, endocytosis, and chemokine signaling among HPPL proteins. However, these pathways were undetectable after 0.2~0.1-μm filtration and Planova-20N filtration. Proteins removed after 0.2~0.1-μm filtration and Planova-20N filtration were associated with pathways related to diseases such as bacterial/viral/parasitic infections (e.g., Epstein-Barr virus infection and shigellosis) and some cancers (e.g., pancreatic cancer and renal cell carcinoma). For instance, shigellosis and Chagas disease were associated with proteins removed after Planova-20N filtration (Figure 16).

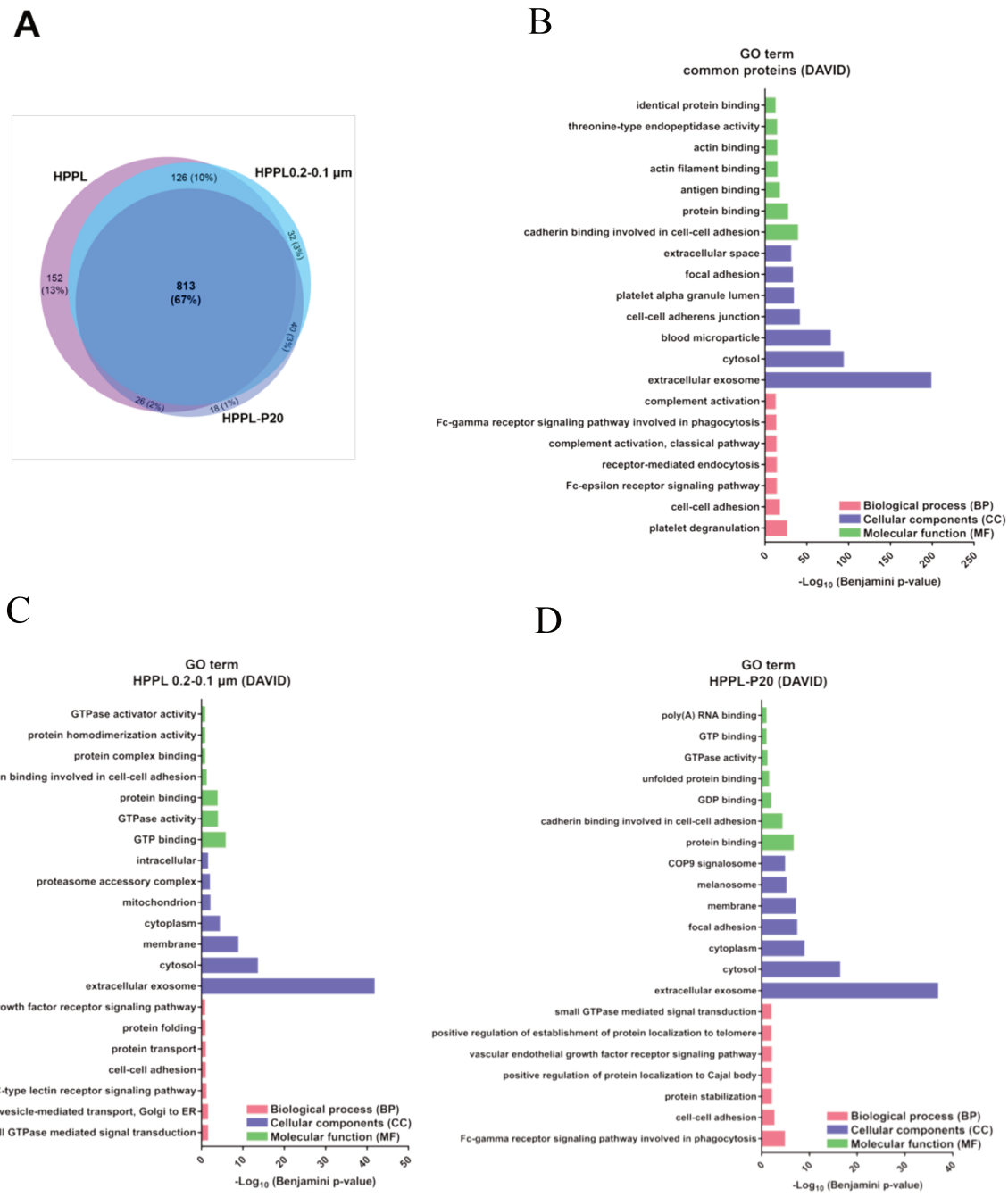

Figure 14. Venn diagram of the proteins identified in HPPL, 0.2-0.1 µm filtered HPPL (HPPL 0.2-0.1 µm) and NHPPL (HPPL-P20). (A) Venn diagram of the proteins identified in HPPL, 0.2-0.1 µm filtered HPPL (HPPL 0.2-0.1 µm) and NHPPL (HPPL-P20). (B) Gene ontology enrichment analysis of 813 proteins in common between HPPL, HPPL 0.2-0.1 µm and HPPL P-20: biological processes (BPs), molecular functions (MFs), and cellular components (CCs). (C) Gene ontology enrichment analysis of proteins that were removed from HPPL by 0.2-0.1 um filtration and (D) removed from HPPL 0.2-0.1 um filtration by Planova 20N: biological processes (BPs), molecular functions (MFs), and cellular components (CCs). The significance cut off is $p < 0.1$

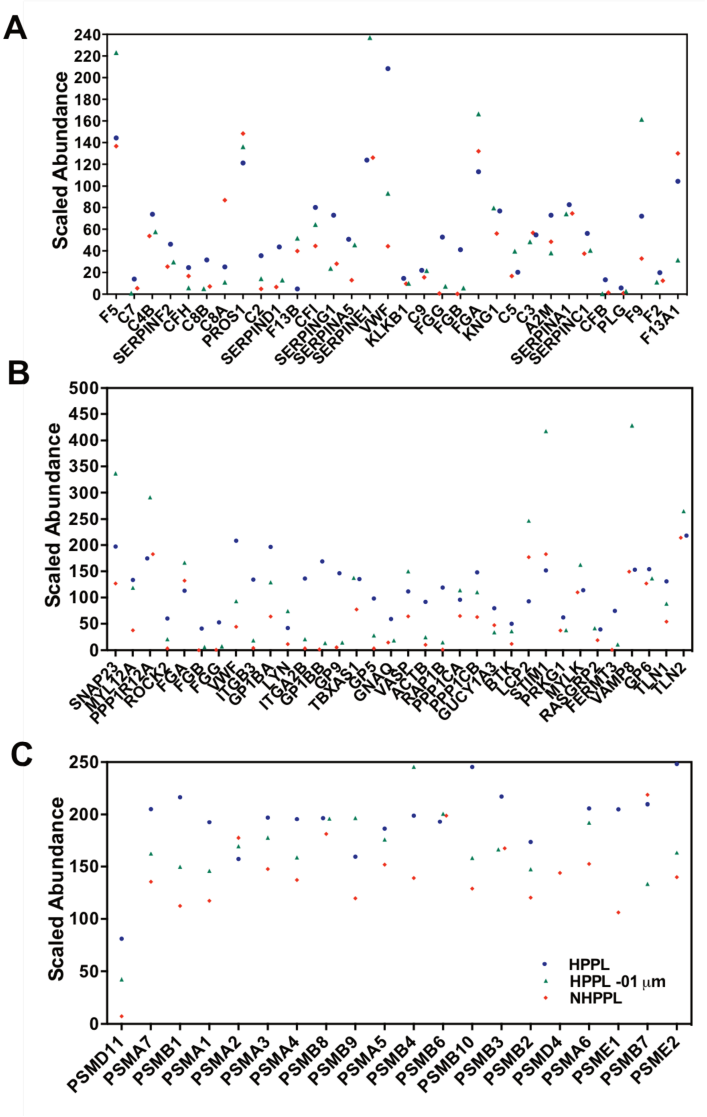

Figure 15. Relative abundance of proteins associated with KEGG pathways of complement and coagulation cascades (A), platelet activation (B) and proteasome (C) after 0.2-0.1 μm filtration and Planova-20N . ***Abbreviations:*** *coagulation factor V (F5); complement component (C7); complement C4-B (C4B); alpha-2-antiplasmin (SERPINF2); complement factor (CFH); complement component beta (C8B); complement component alpha (C8A); vitamin K-dependent protein S (PROS1); complement C2 (C2); heparin cofactor 2 (SERPIND1); coagulation factor XIII B (F13B); complement factor-I (CFI); plasma protease C1 (SERPING1); Plasma serine protease inhibitor (SERPINA5); plasminogen activator inhibitor 1 (SERPINE1) ; von willebrand factor (VWF); plasma kallikrein (KLKB1); complement component C9 (C9); fibrinogen gamma (FGG); fibrinogen beta (FGB); fibrinogen alpha chain (FGA); kininogen-1 (KNG1); complement C5 (C5); complement C3 (C3) ; alpha-2-macroglobulin (A2M); Alpha-1-antitrypsin (SERPINA1); antithrombin-III (SERPINC1); complement factor B (CFB); plasminogen (PLG); coagulation factor IX (F9); prothrombin (F2); coagulation factor XIII-A (F13A1)*

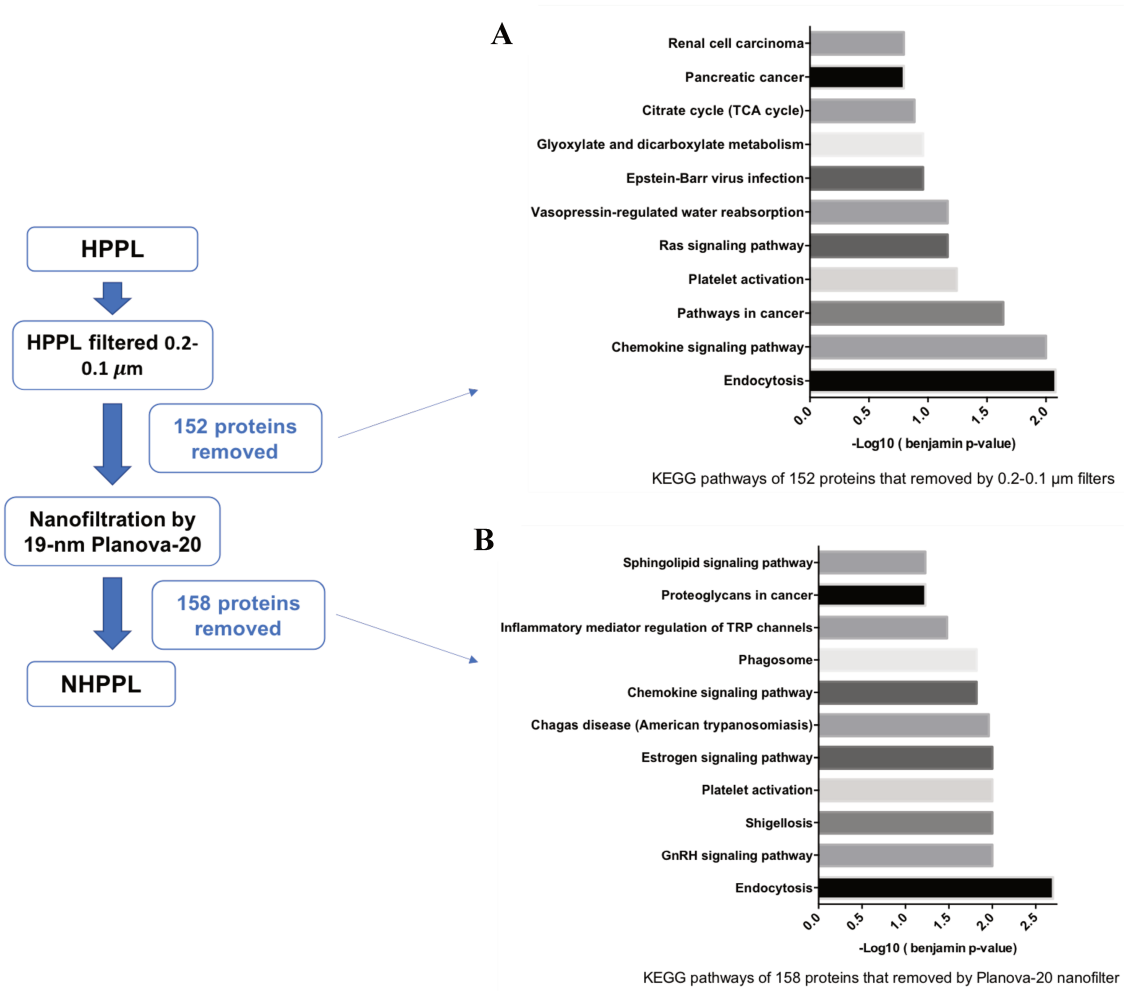

Figure 16. (A) KEGG pathways of 158 proteins that removed by 0.2-0.1 μm filters (B) KEGG pathways of 152 removed from by Planova-20N. The significance cut off is $p < 0.1$.

In vitro neuroprotective activity of NHPPL on LUHMES cells exposed to the erastin neurotoxin

Differentiated LUHMES cells were subjected to treatment with 2% (v/v) HPPL, 0.2-0.1-µm-filtered HPPL, and NHPPL for 1 hour prior to exposure to 1 µM erastin, a neurotoxic agent that induces cell death through ferroptosis. Following 24 hours of erastin exposure, cell viability was assessed using CCK-8, and the results are presented in Figure 17B. NHPPL provided a significant neuroprotective effect against erastin-induced neurotoxicity ($p < 0.0001$), similar to that achieved by HPPL and 0.2-0.1-µm-filtered HPPL ($p < 0.0001$). Microscopic observations of LUHMES cells (Figure 17A) supported these findings, showing that NHPPL treatment maintained normal cell morphology, while untreated cells exposed to erastin only displayed signs of cellular damage. These results indicate that the process of nanofiltration did not impact the neuroprotective properties of HPPL in vitro, as NHPPL was equally effective in mitigating erastin-induced neurotoxicity as the unfiltered and 0.2-0.1-µm-filtered HPPL.

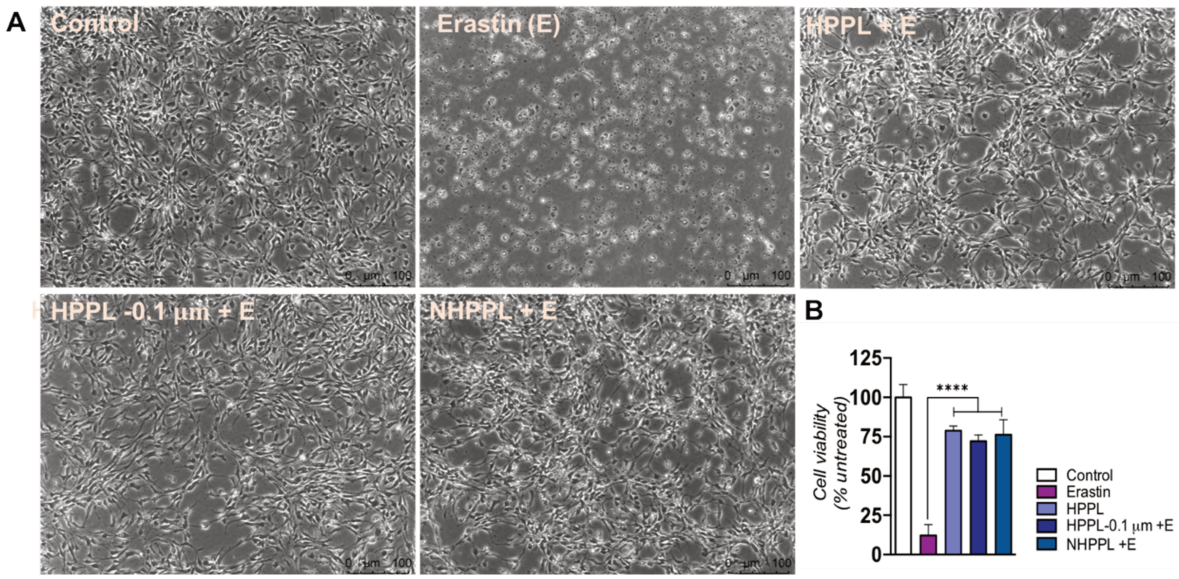

*Figure 17. Assessment of neuroprotective activity in NHPPL. LUHMES cells were pre-treated with 5% (v/v) HPPL, 0.2-0.1 µm-filtered HPPL (HPPL-0.1 µm), or NHPPL (HPPL-P20) and after 1h exposed to erastin neurotoxic. (A) Cells morphology after 24h, the scale bar is 100 µm (B) The LUHMES viability after 24h was quantified by CCK-8 assay. N=3, **** $P < 0.0001$ as compared to cells treated with erastin only. Statistical evaluation was performed by one-way ANOVA followed by by Fisher's LSD test. Abbreviations: heated platelet pellet lysate (HPPL).*

Ability of NHPPL to stimulate cell maturation in SH-SY5Y

The ability of NHPPL to induce neuronal differentiation in the absence of RA, which is a typical neuronal differentiation agent, was evaluated. Undifferentiated SH-SY5Y cells were cultured in DMEM supplemented with 10% FBS. On day 2, the medium was replaced with DMEM without FBS, and the cells were exposed to 2% (v/v) NHPPL, 2% (v/v) HPPL, or 1 μM RA (positive controls). Certain cells were maintained in a medium containing 0.5% FBS without receiving any treatment, serving as the negative control group. The culture medium was refreshed every 3 days, and on day 7, the cells were stained with the differentiation marker β-III tubulin. The findings revealed significantly higher relative fluorescence intensities of β-III tubulin in cells treated with 2% (v/v) NHPPL ($p < 0.05$), 2% (v/v) HPPL ($p < 0.01$), and RA ($p < 0.05$) compared to the negative control (Figure 18).Thus, it was concluded that HPPL nanofiltration did not compromise its capacity to induce the differentiation of SH-SY5Y cells into mature neurons..

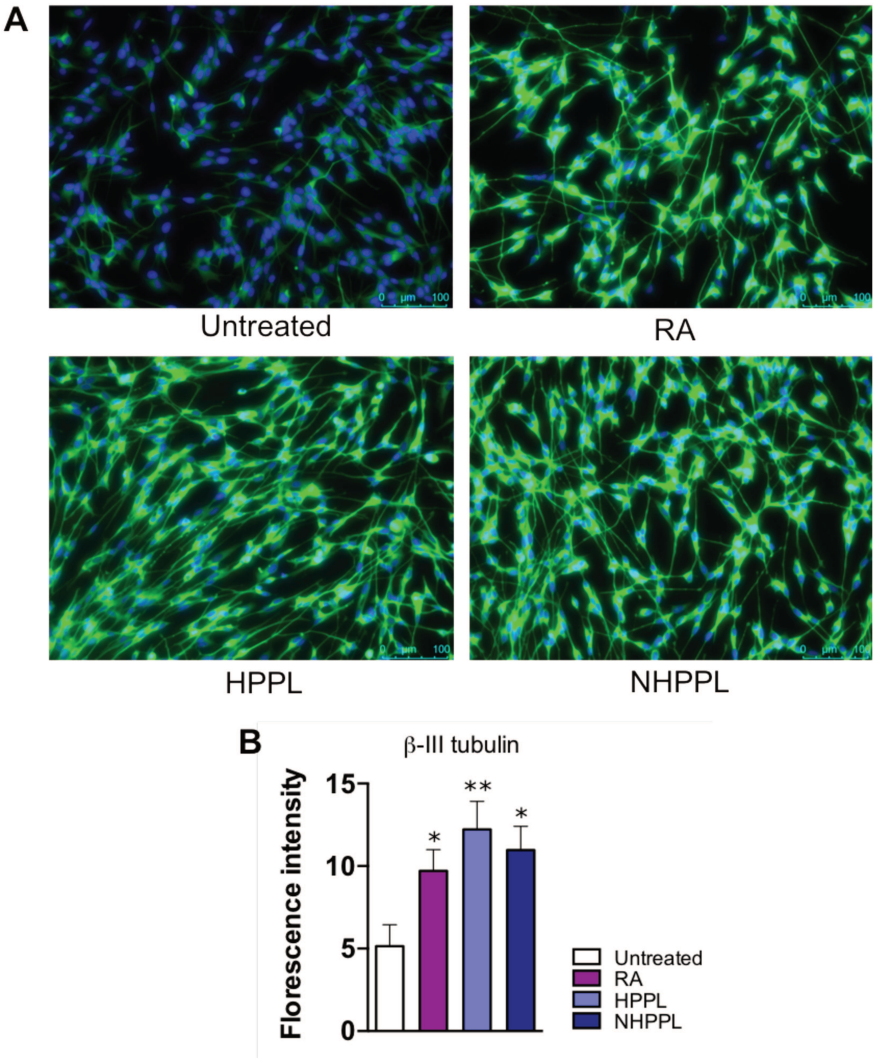

*Figure 18.. Capacity of NPPL to stimulate SH-SY5Y cells neuronal maturation. The cells were immuno-stained with β-III tubulin and counterstained with DAPI in blue. The images (A) are showing the extension of SH-SY5Y neurites under treatment with NHPPL (HPPL-P20). HPPL and retinoic acid were used as a positive control to stimulate cells differentiation. The scale bar is 100 μm (B) quantitative measurement of the fluorescence intensity using Image J. (*P < .05; **P < .01). Statistical evaluation was performed by one-way ANOVA followed by Fisher's LSD test. Abbreviations: heated-treated platelet pellet lysate (HPPL), retinoic acid (RA).*

In vivo anti-inflammatory activity in a TBI model

To induce gene expressions of several proinflammatory markers, a CCI injury was performed on the right hemisphere of mice. The mice were then treated with HPPL, NHPPL, or PBS intranasally for three consecutive days on days 0~3. No acute signs of toxicity were observed with the administration of these materials. The mice were sacrificed on day 7 post-injury, and gene expression analysis was conducted to evaluate the effects of the treatments. Compared to the sham mice, significant upregulation ($p < 0.05$) was observed in the chemokine genes Ccl3, Ccl4, Ccl5, receptor genes Tlr2 and Tlr4, astrocytic gene Gfap, and microglial marker genes Cd68 and Trem2 in the injured mice. To assess the capacity of intranasal NHPPL to mitigate the neuroinflammation triggered by the CCI, the differential gene expressions were compared to those of mice treated with PBS and HPPL administration. Figure 19 shows that HPPL treatment led to a significant downregulation ($p < 0.05$) of all tested genes compared to the PBS group, with the exception of Ccl5, which exhibited a non-significant decrease. NHPPL treatment showed a similar pattern as observed with HPPL, resulting in a significant downregulation ($p < 0.05$) of the proinflammatory genes Tlr4, Cd68, and Gfap, along with relative decreases in Ccl3, Ccl4, Ccl5, Tlr2, and Trem2. No statistically significant difference was observed in any of these markers between HPPL and NHPPL treatment. Hence, it was concluded that NHPPL retained its functional activity intact and was effective in modulating proinflammatory markers after CCI injury.

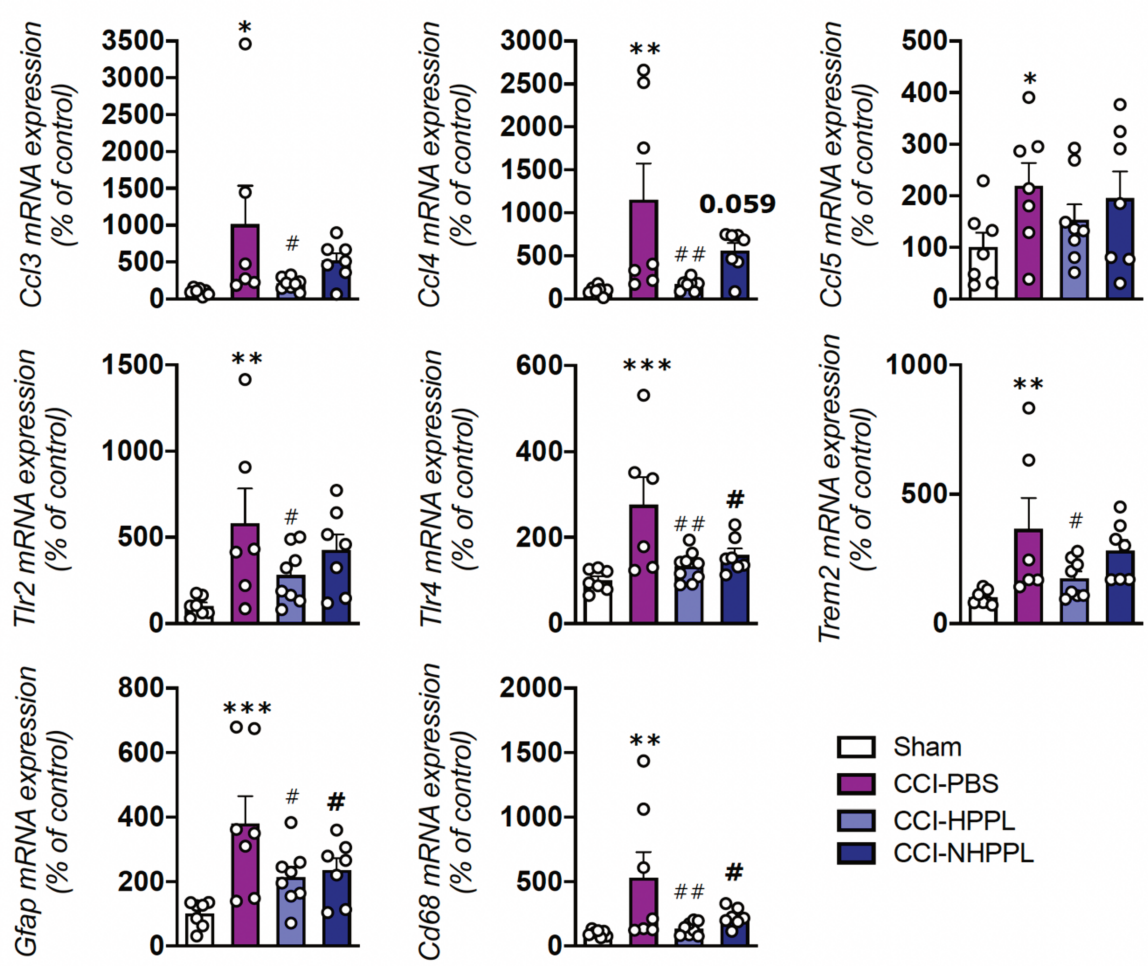

*Figure 19. Modulation of neuroinflammatory markers in the mouse model of TBI. The CCI injury was applied and mice received either 60 µL HPPL, NHPPL (HPPL-P20) or PBS, in the three consecutive days by intranasal administration. Mice were sacrificed at the day 7 post-injury, ipsilateral cortex was dissected, cytokine and glial marker mRNA levels was quantified by RT-qPCR. (n=5-7 mice per group). Data are reported as the mean ± SEM.; * $P < 0.05$, ** $P < 0.01$, *** $P < 0.001$ for CCI vs. Sham; $^{\#}P < 0.05$, $^{\#\#}P < 0.01$ for CCI-PBS vs CCI-HPPL, CCI-NHPPL by a one-way ANOVA followed by Fisher's LSD test. Abbreviations: heated-treated platelet pellet lysate (HPPL); nanofiltered HPPL (NHPPL).*

3.3 The assessment of neuroprotective and neuro-regenerative potential of PEVs

In the previous experiment we did in our lab we unveiled an abundant number of PEVs in HPLs including HPPL in the range of concentration as high as 10^{11}-10^{12} /mL by NTA. The presence of EVs in HPLs then raises a question of their respective contribution to the functional activity of HPL, in particular in their neuroprotective activity. Thus, we did an evaluation of EVs isolated from HPPL (HPPL-EVs) by SEC Izon chromatography and another type of EVs preparation obtained from the supernatant of PC (PCS-EVs) by UC at 20,000 x g for 90 minutes. Firstly, we did biophysical caharacterization to understand their number and size as well as their protein content. More importantly, we investigated their neuroprotective and neuro-regenerative activity *in vitro and in vivo.*

3.3.1 Evaluation of EVs isolated from HPPL (HPPL-EVs)

Biophysical characterization: size distribution of isolated HPPL-EVs

Size distribution of isolated HPPL-PEVs was determined by DLS have a main size distribution ~ 248 nm as shown in Figure 20.

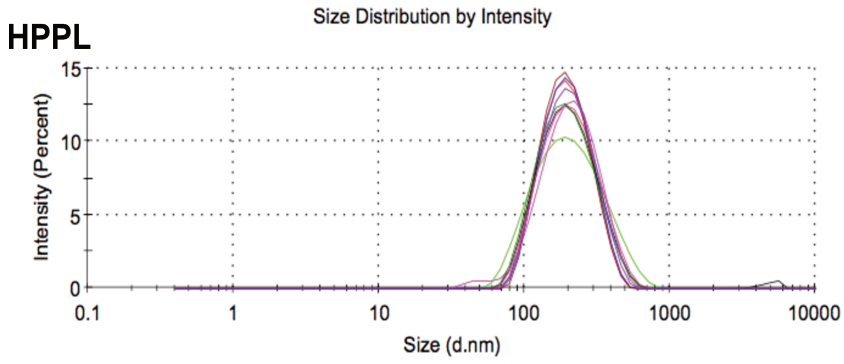

Figure 20. Population size profile, as determined by DLS, of PEVs from HPPL (HPPL-EVs). HPPL-PEVs isolated by qEV chromatography and concentrated by Amicon 50K. Abbreviations: heated platelet pellet lysate (HPPL).

Neuroprotective assessment of HPPL-EVs

In vitro study using LUHMES dopaminergic neurons was used to assess the neuroprotective activity of HPPL-EVs. Differentiated LUHMES were treated with ~4 x 10^{10}, ~1 x 10^{11} and ~2 x 10^{11} of PEVs isolated from HPPL (number was quantified by NTA). EVs in HPPL with a

number ~1 x 10^{11} were used as positive control fractions known to exert neuroprotection. After 1 hour, a dose of 1 μM erastin was added. Cell viability was assessed after 24-hours of incubation using the CCK-8 assay. Data are shown in Figure 21.

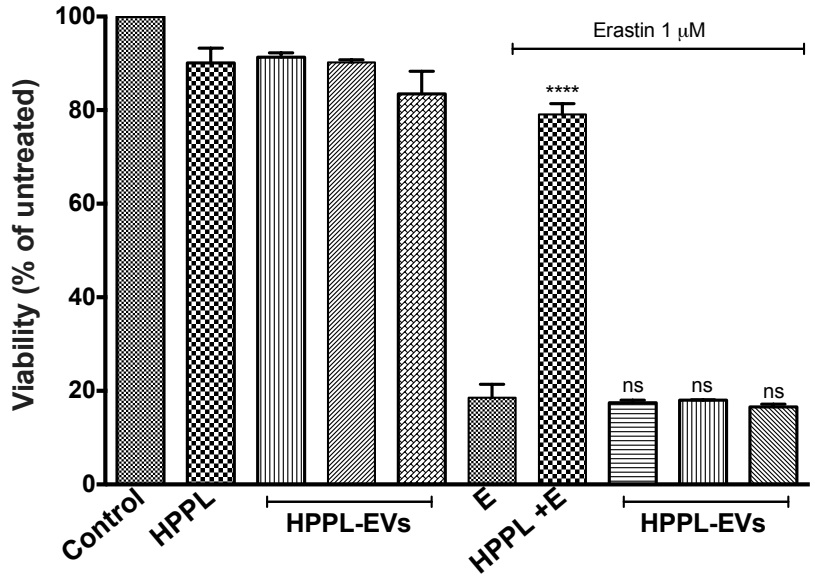

*Figure 21. The effect of HPPL-PEVs treatment on the cell viability of LUHMES cells exposed to erastin. LUHMES were treated with and without erastin. N=3, #### P<0.0001 as compared with the control without erastin. **** P<0.001*; no significant (ns) *as compared to the control with erastin. Abbreviations: Erastin (E); heated platelet pellet lysate (HPPL), Platelet extracellular vesicles (PEVs).*

Total doses of ~4 x 10^{10}, ~1 x 10^{11} and ~2 x 10^{11} PEVs isolated from purified HPPL did not show a neuroprotective effect on LUHMES cells exposed to erastin, by contrast to the neuroprotective effect observed when using ~1 x 10^{11} of PEVs which are presence in HPPL.

3.3.2 Evaluation of PEVs isolated from PC supernatant (PCS-EVs)

The results showed HPPL-EVs did not show a protective in LUHMES cell against erastin neurotoxicity. This supports our result that after HPPL-EVs and virus removal step by nanofiltration, HPPL still maintained an intact neuroprotective potential suggesting that at the dose used, HPPL-EVs were not contributing to the *in vitro* neuroprotective activity of HPPL. Different releasing mechanism of EVs might result a different functional activity. We continued to perform an examination of another EVs preparation referred to as PSC-EVs which are natural vesicles present in PC supernatant.

Biophysical characterization: size distribution of PCS-EVs

The isolated PCS-EVs consisted of a heterogeneous population from 70 to 350 nm. Their main population size is approximately 200 nm as determined by DLS, is shown in Figure 22.

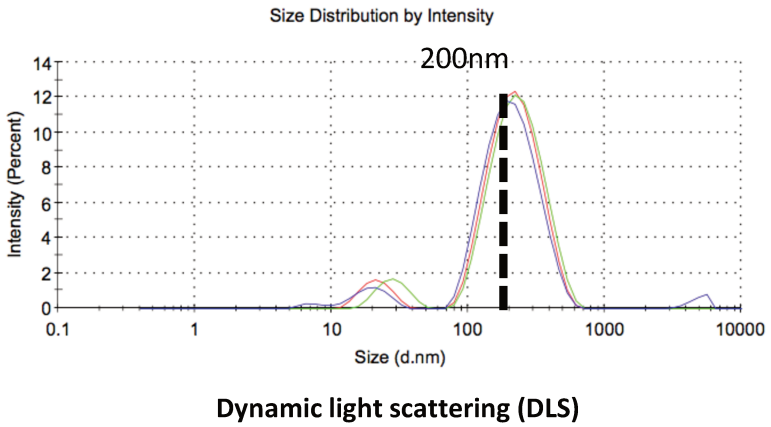

Figure 22. Particles population size profile PCS-EVs fractions determined by DLS.

The number and size distribution of PCS-EVs detected by NTA and TRPS

The PCS-EVs size and number as determined by NTA, is shown are Figure 23. NTA PCS-EVs fraction contained 10^{10}-10^{11} particles/mL with a main size distribution ranging from 100-275 nm. Particle population of PSC-EVs has a main size ranging from 150-300 nm, were detected by TRPS (Figure 24) equipped with nanopore 400 nm membrane, supported the previous NTA and DLS data.

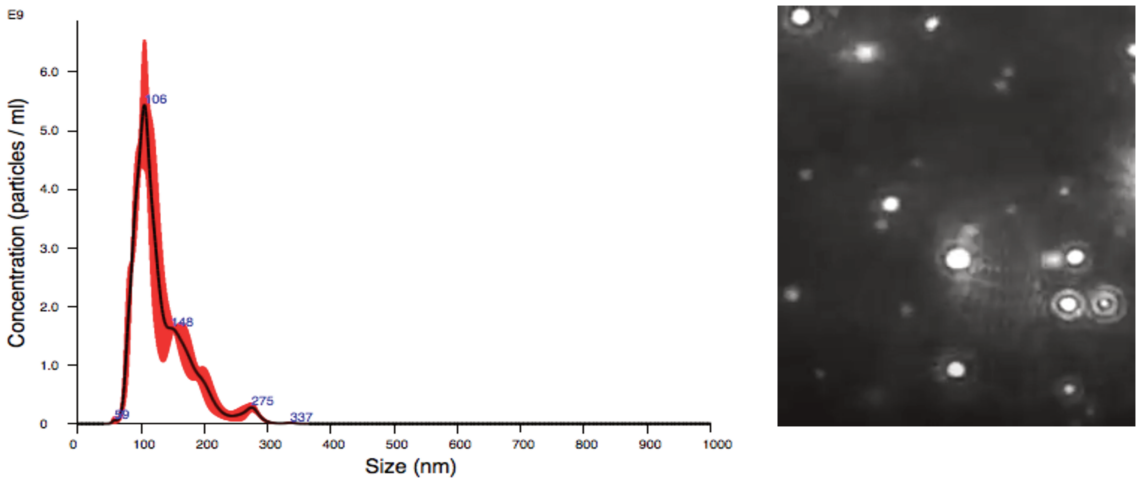

Figure 23. PCS-EVs number and size distribution determined by NTA. The sample was diluted 100-fold in 0.1 μm-filtered PBS prior to analysis.

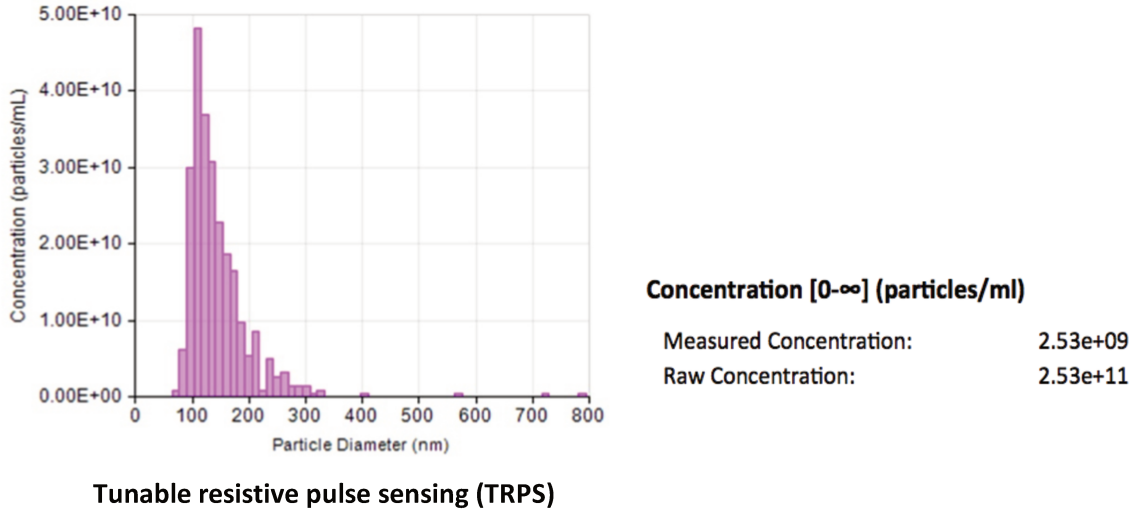

Figure 24. Concentration and size distribution of PCS-EVs determined by TRPS.

Total protein, growth factors detected in PCS-EVs

The protein quantification of PCS-EVs fraction was determined using the BCA assay. The average total protein concentration of the PCS-EVs preparation was found to be in the 3~4 mg/mL range. Selected growth factors were measured by ELISA assay. The results (N = 3) showed that PCS-EVs contained measurable amounts of BDNF, PDGF, EGF, and VEGF, expressed in ng/mL, respectively, 2.145 ± 0.921; 5.141 ± 1.858; 0.512 ± 0.082, 0.025 ± 0.021.

Proteomic profiling in PCS-EVs

Proteomic analysis was done by LC-MS/MS to have a broader understanding of the content of proteins and cytokines in PCS-EVs. The results confirmed the presence of various growth factors, antioxidants, cytokines in PCS-EVs as shown in Table 6. DAVID Bioinformatics Resources 6.8 GO enrichment analysis was performed to discover the cellular components and functional annotations of the list of proteins in PCS-EVs. We found that proteins associated with blood microparticles, platelet alpha granules, CAMP-dependent protein kinase were among the major abundant components in PCS-EVs by as shown in Figure 25. The biological processes that were involved included platelet degranulation and activation, cell-cell adhesion, immune response, and receptor-mediated endocytosis. The functional annotation analysis identified a highly enriched cluster related to serine-type endopeptidase, antigen binding, and cadherin binding involved in cell-cell adhesion (Figure 26).

Table 6. Neurotrophic, antioxidant, cytokines detected by LC-MS/MS

Examples of trophic actors in PCS-EVs		
PDGFA	catalase	Glutamate-rich protein
cAMP-dependent protein kinase	Glutathione S-transferase	VTI1A
VEGF	TGF-β1	Glutathione reductase
PDGFB	Glutathione peroxidase	IGF
HGF	SOD 1,2	Glia maturation factor

Abbreviations : Hepatocyte growth factor (HGF), Insulin-like growth factor (IGF), Platelet-derived growth factor (PDGF), Superoxide dismutase (SOD), Transforming growh factor-β1 *(TGF-* β1*), Vesicle transport through interaction with t-SNAREs 1A (VT11A),*

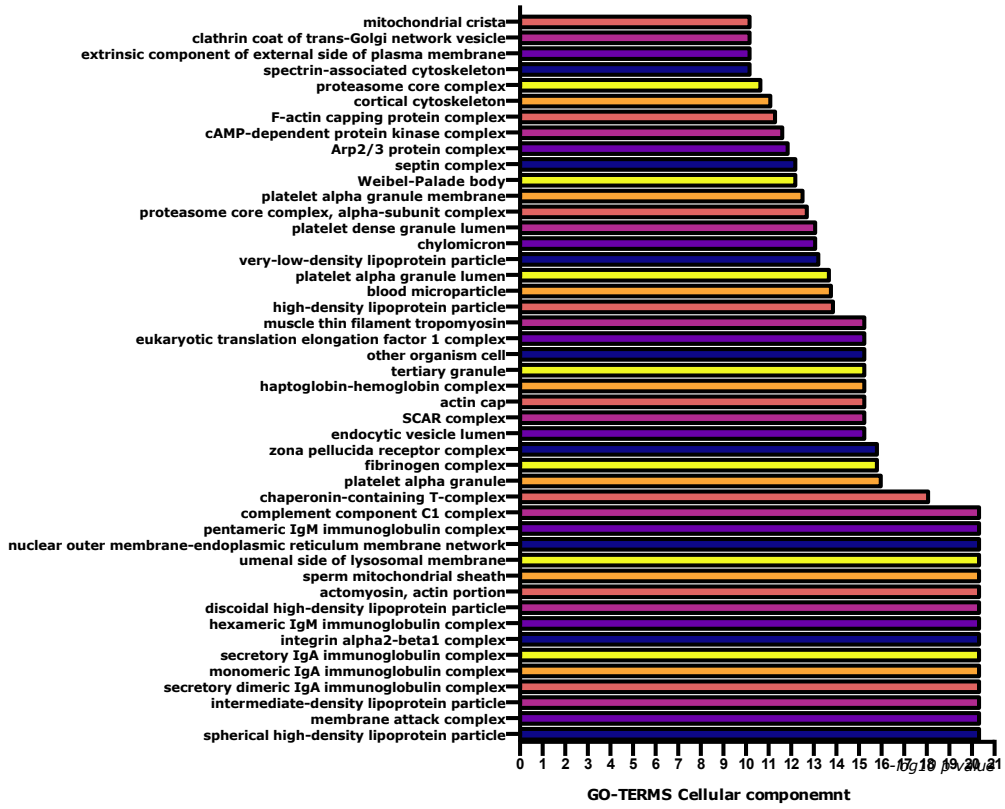

Figure 25. Gene ontology enrichment analysis of proteins in PCS-EVs using DAVID bioinformatic platform: cellular components)

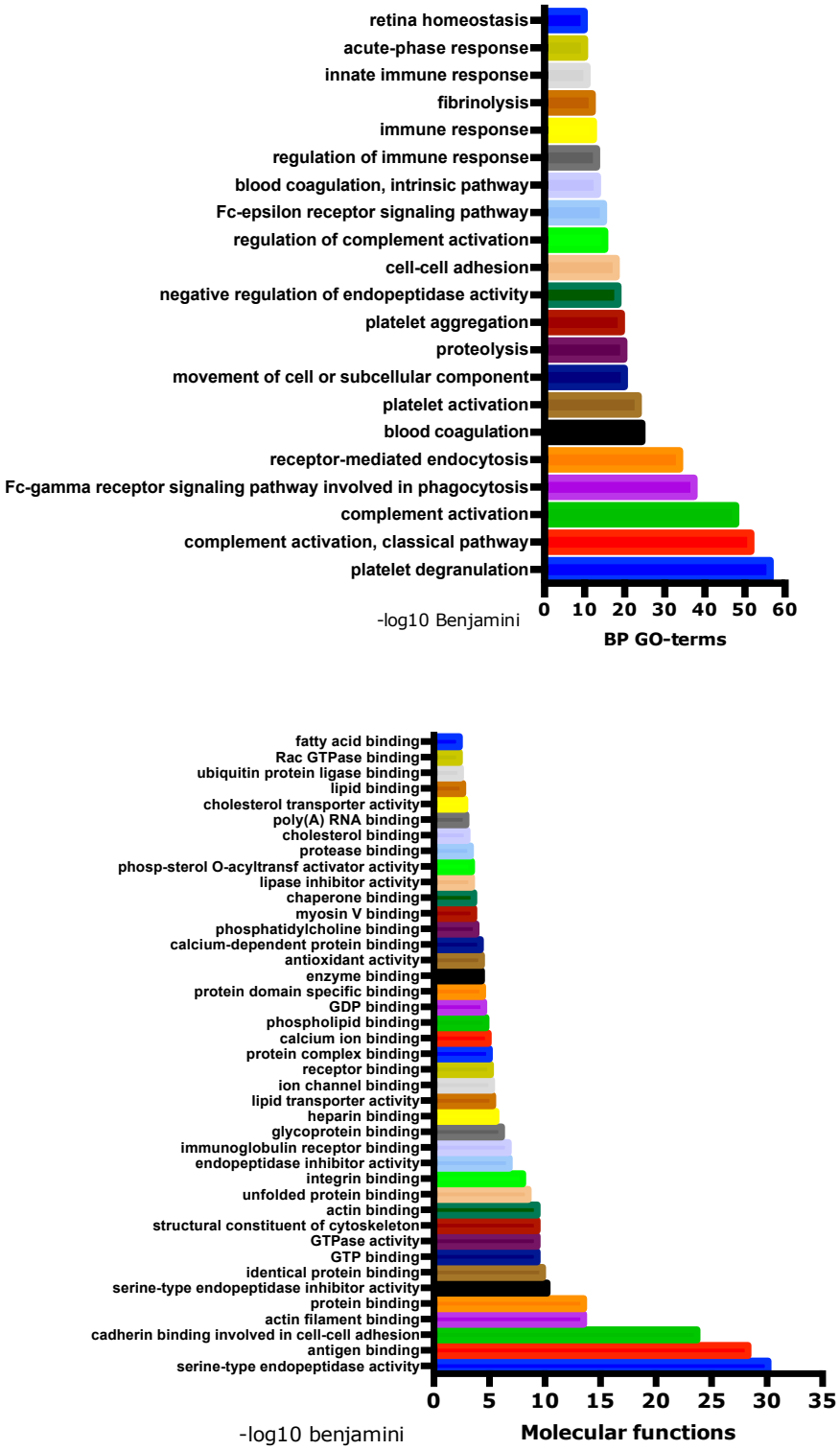

Figure 26. Gene ontology enrichment analysis of proteins in PCS-EVs using DAVID bioinformatic platform: biological process (BP), and molecular functions

The evaluation of neuroprotective potential of PCS-EVs

In vitro neuroprotective activity of PCS-EVs on LUHMES cells exposed to the erastin neurotoxin. Differentiated LUHMES cells were treated with 5% (v/v) PCS-EVs and HPPL as a positive control for 1 hour before exposure to 1 µM erastin, a neurotoxic agent that programs cell death via ferroptosis. CCK-8 cell viability results, assessed after 24 h of erastin exposure, are shown in Figure 27B. PCS-EVs treatment provided a significant neuroprotective effect against erastin neurotoxicity similar to that achieved by HPPL. PCS-EVs exert neuroprotection with 71% cell viability compared to 17% without (N=3). These data were supported by microscopic observations of LUHMES cells (Figure 27A) that evidenced a normal morphology after treatment with PCS-EVs and HPPL, in contrast to untreated cells exposed to erastin only. These results highlighted that PCS-EVs provide a strong neuroprotective effect *in vitro*.

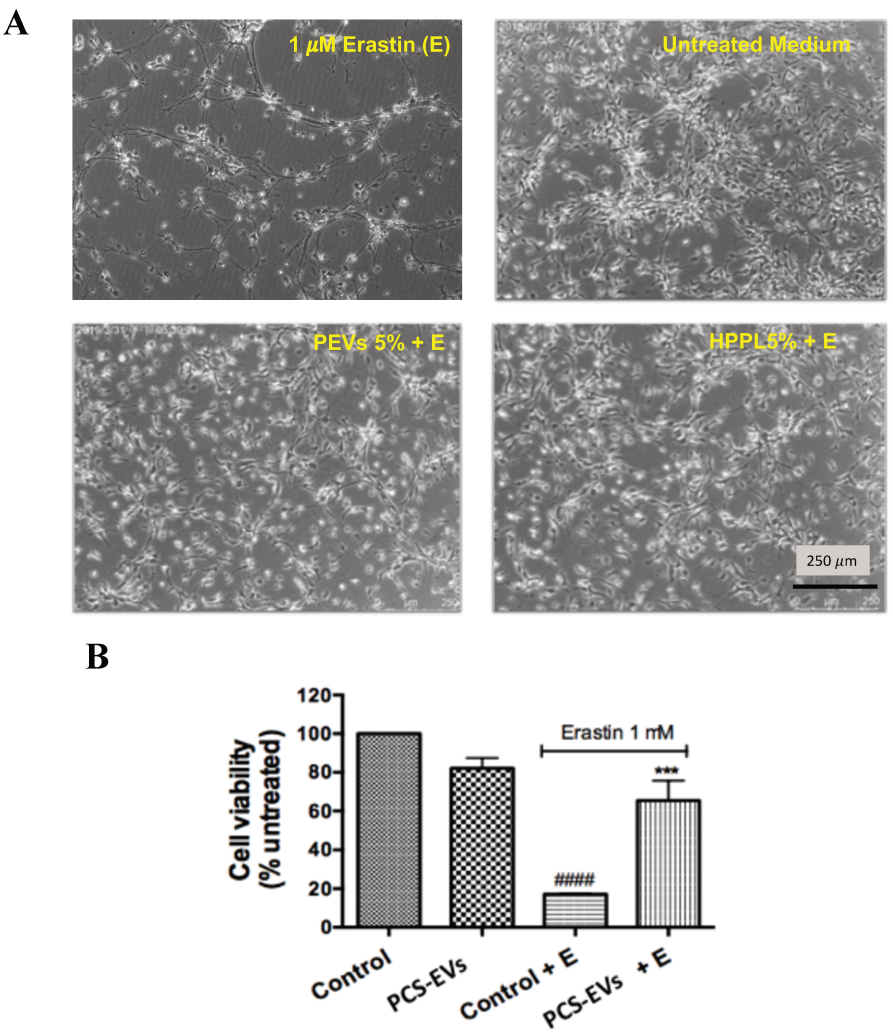

*Figure 27. The effect of PCS-EVs treatment to the cell viability of LUHMES cells exposed to erastin.. LUHMES were stimulated with and without erastin. N=3, ### P < 0.001 as compared with the control without erastin. **** P < 0.0001 as compared to the control with erastin ferroptosis. Abbreviations: Erastin*

Neurorestorative effect of PCS-EVs in vitro in scratched SH-5YSY neuroblastoma cell line

The ability of PCS-EVs to stimulate neuronal restoration on differentiated SH-SY5Y cells was performed using the scratch assay. SH-SY5Y cells were first maintained and RA was added to differentiate the cells. Furthermore, the cells monolayer was scratched using 100 uL tips and after the PCS-EVs was added. The scratch area then was monitored and observed under microscopy over 2 days (Figure 28). The result shown that PCS-EVs were able to promote neuronal reconnection and resulting in a closure of the scratched area compared to the control without PCS-EVs treatment.

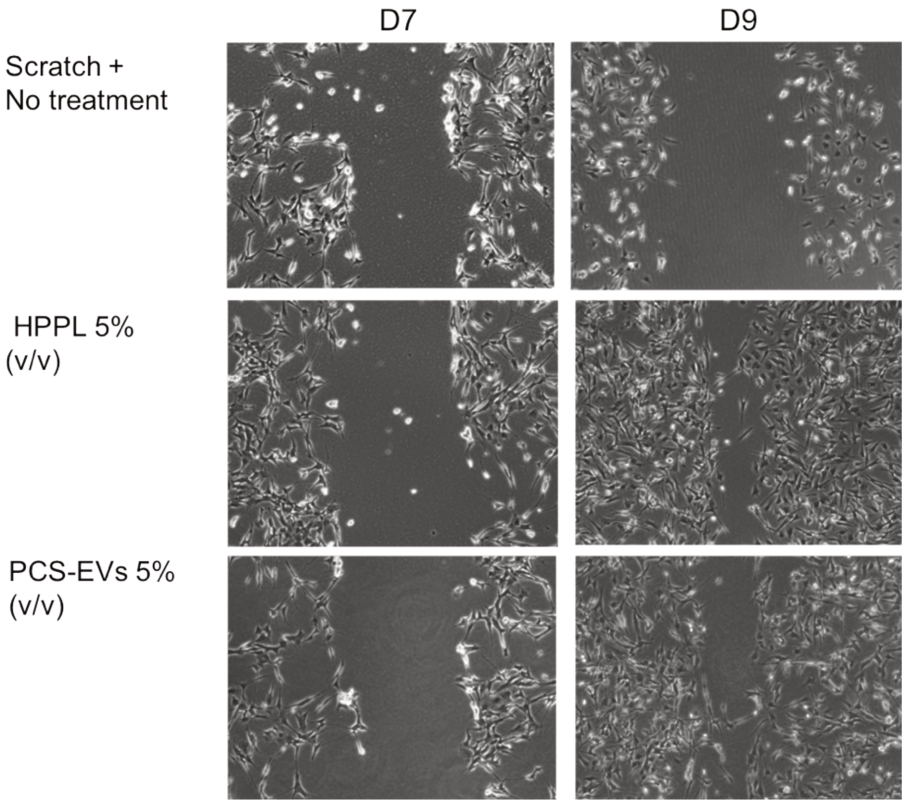

Figure 28. The neuro-restoration effect of PCS-EVs on the differentiated SH-5YSY. Scratch assay with differentiated SH-SY5Y cells. Cells without any treatment as a negative control (a) HPPL 5% (v/v) as the positive control (b), and treated with 5% (v/v) PCS-EVs (c). The neuro-restoration effect was monitored by microscopy at the indicated time-point.

PCS-EVs do not activate microglia BV-2 cells

We did test with BV-2 cells to see the treatment effect on the microglial activation. The cells were cultured and maintained to be treated with 5% of PCS-EVs (v/v) or 5 x 10^9 EVs particle, cells with 5% HPPL and without any treatment was used as negative control. These treatments

were performed without and with (100 ng/ml) LPS stimulation. We measured the pro-inflammatory marker TNF-α, that is one of major cytokines released by microglia cells upon LPS activation.

The results suggest that under normal condition (i.e. without LPS stimulation), 5% (v/v) PCS-EVs did not trigger significantly TNF-α expression compared to the control (Figure 29). This is similar with a very low level of TNF-α was detected by q-PCR when the cells were exposed to 5% (v/v) HPPL for 1 day.

PCS-EVs also successfully reduced the upregulation of TNF-α expression due to LPS pre-treatment ($p < 0.001$) compared to control and LPS treatment. After a pre-treatment with LPS, BV2 released significantly less TNF-α in the presence of PCS-EVs and HPPL ($p < 0.01$) than with LPS alone. However, when PCS-EVs were added in a higher concentration which is 10% (v/v), there was no reduction of TNF-α expression after LPS treatment. This suggests that at a higher concentration of PCS-EVs were not able to inhibit BV-2 activation due to LPS induction. A further study to understand the dose dependent effect is necessary to be done.

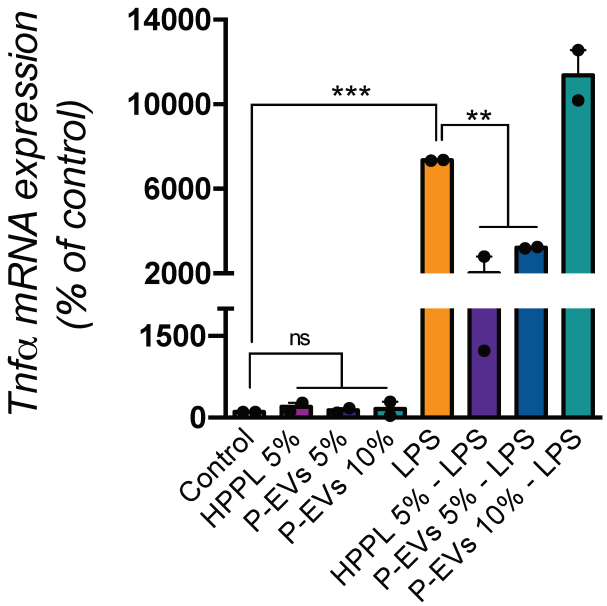

Figure 29. anti-inflammatory activity of PCS-EVs in an activated BV-2 microglia cell line. Cells were treated with 5% and 10 % (v/v) PCS-EVs for 24 h (positive control: cells treated with LPS from E. coli). TNF-α was assessed from RNA isolated from cell lysate (pooled n=3). TNF-α expression was increased in BV-2 microglia cells exposed to 100 ng/ml LPS treatment, but a lower level was found after 24 h treatment with PCS-EVs 5% (v/v). Abbreviations: Platelet concentrate supernatant-extracellular vesicles (PCS-EVs), heated platelet pellet (HPPL), Escherichia coli lipopolysaccharide (LPS).

PCS-EVs exert anti-inflammatory activity in the in vivo TBI model

We employed a CCI model of TBI to examine the anti-inflammatory activity of PCS-EVs delivered intranasally *in vivo*. This examination was done following our *in vitro* data showed that PSC-EVs able to promote neuronal-restoration and reduce the expression of inflammatory marker *TNF-α* in a scratched SH-SY5Y neuroblastoma and BV-2 microglial cell line respectively.

The CCI injury performed in the right hemisphere of mice (n = 9-10 per group) was applied to induce gene expressions of several proinflammatory markers [283]. Mice were treated with PCS-EVs at the dose 1.2 x 10^8 number of particles or PBS control intranasally for three consecutive days on days 0~3 post-injury (Figure 30).

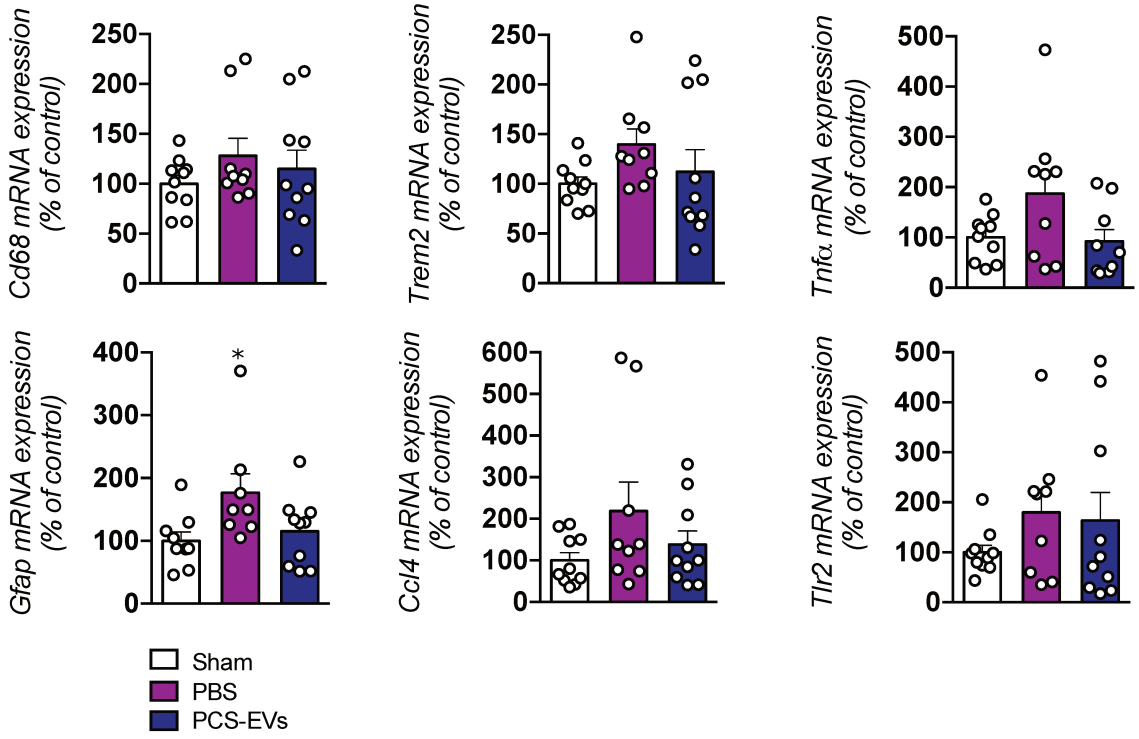

*Figure 30. Effect of PCS-EVs treatment on the expressions of inflammatory markers post injury. Changes in cytokines, chemokines, and glial markers expression in the cortex at day 7 post-injury by CCI. The inflammatory markers such as Tnf-α, GFAP, Ccl4, Tlr2, and Trem2 that initially upregulated following the injury were showing a trend of decreasing by EVs treatment. Data were presented as means ± SEM (n = 9-10 in each group). *p < 0.05 when compared to the PBS-treated group.*

Evaluation of PSC-EVs neuroprotective activity in MPTP model of PD

PCS-EVs exerted neuroprotective effect in LUHMES dopaminergic neurons against erastin neurotoxicity, a PD model *in vitro*. Indeed, this finding deserve a further evaluation on the animal level. The MPTP mice model was used as it is proved to be a reliable model for studying the degeneration of dopaminergic neurons.

One day prior to the MPTP intoxication (20 mg/kg), male C57BL/6 mice received a number of 4 x 10^{10} (dose 1) and 8 x 10^{10} PCS-EVs (dose 2) by intranasal administration. One week post treatment, mice were sacrificed and the brains were collected for IHC staining of TH positive cells, a dopaminergic neuronal marker.

Firstly, an open field behavior test using an actimetry device was performed to understand the improvement of the locomotor function of the MPTP mice after PCS-EVs treatment. The mice were allowed to navigate freely and their behavior was recorded over 10 minutes. At least 7 animals were used as a sham group (PBS only) and 17 animals per group were used for MPTP treatments, MPTP/PSC-EVs and MPTP/PBS groups. We performed the test on day 7 after MPTP/PCS-EVs treatment. The MPTP/PBS group and the experimental group did not appear to vary in any of the characteristics measured, including velocity (mean, slow, and maximum), movement (slow, rapid), and total distance (Figure 31). However, there was typically a lower resting time in this MPTP/PBS group compared to sham group. These data indicated that the MPTP treatment altered the behavior of these mice. In the group that was treated by PCS-EVs dose 1 (4 x 10^{10} EVs particles), a comparable response to the control group (PBS only) was observed in all of the animals regarding the rearing time. This data showed that PCS-EVs helped in part to rescue the locomotor deficits from MPTP treatment. This favorable effect is reinforced by an increase in the rearing number, which is known to be the most affected parameter in the MPTP model. There was a significant improvement of rearing number in the MPTP/PCS-EVs group with the dose of 4 x 10^{10} of PCS-EVs ($p < 0.05$) compared to the MPTP/PBS group. However, the treatment with 8 x 10^{10} PCS-EVs, this improvement was not detected showing that the effect depended on the dose of PCS-EVs used in this experiment.

On the other hand, our findings showed that the MPTP reduced the number of TH expression (Figure 32), demonstrating the effectiveness of our experimental paradigm in modulating

dopamine-releasing neurons in the SN. Interestingly, 4 x 10^{10} of PCS-EVs could also rescue and/or protect dopaminergic neurons in SN from the MPTP harmful effect.

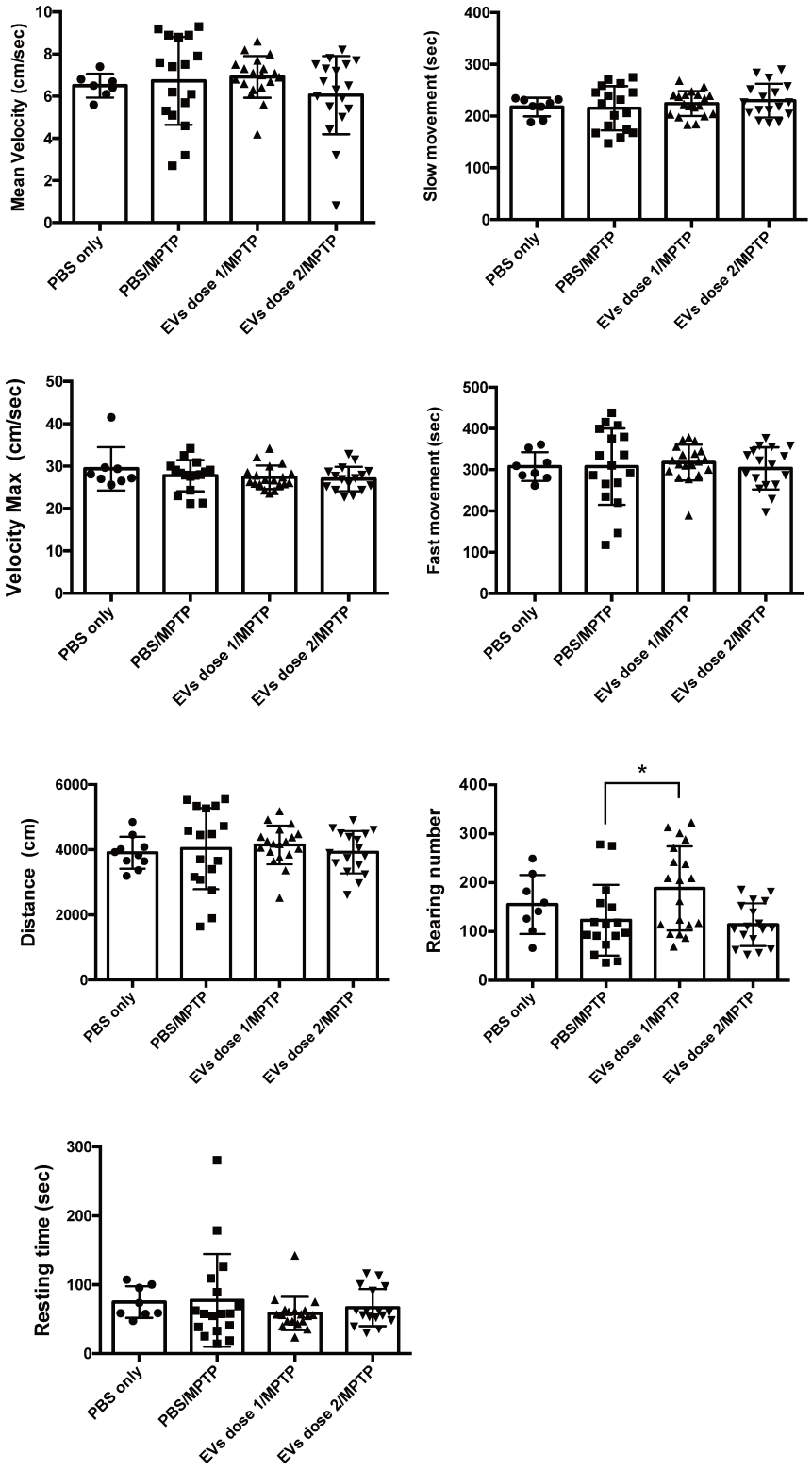

Figure 31. Impact of the PCS-EVs treatment on the behaviors of MPTP mice. Animals were left in the open field actimetry box and allowed to explore freely for 10 minutes. The test was done on day 7. Parameters

*related to their locomotor function were recorded. PCS-EVs at the dose 4 x 10^{10} (dose 1) given by i.n. delivery prior MPTP intoxication improved the rearing number compared to control MPTP group (MPTP/PBS). Data were presented as means ± SEM, n = 7 in the sham group (PBS only), and at least n=17 in the MPTP. groups *p < 0.05 compared to MPTP/PBS group.*

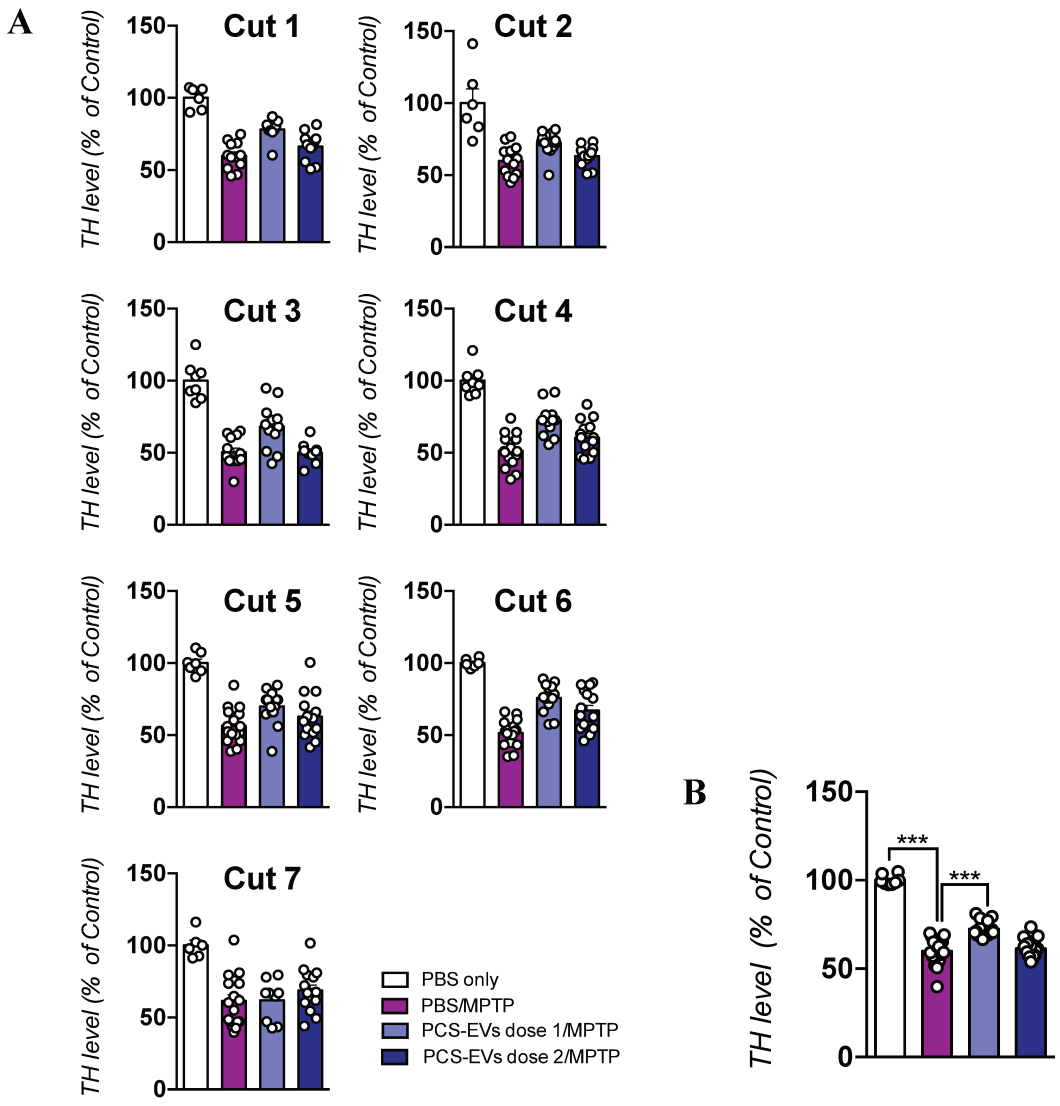

*Figure 32. The effect of PCS-EVs treatment on the TH positive cells in SN of MPTP mice. (A) TH number in the s*ubsequent area of SN (cut 1-cut 7) (B) Total TH level in all area of SN. The treatment of PSC-EVs in the concentration 4 x 10^{10} *of EVs p*articles able to protect TH expression. *Data presented as means ± SD, n = 7 in the sham group (PBS only), and at least n=17 in the MPTP. groups ***p < 0.001 compared to MPTP/PBS group. Abbreviations: substantia nigra (SN), tyrosine hydroxylase (TH)*

CHAPTER IV: DISCUSSION

4.1 Different preparation of HPLs differ in their composition and functional properties affecting their potential use for certain clinical indications

In recent years, there is a rise of interest in the use of platelet-derived biomaterials rich in growth and healing factors in the fields of regenerative medicine, cell therapy, and tissue engineering [284,285]. Platelet biomaterials are being applied in a various fields of regenerative medicine such as for wound healing, cartilage repair, bone regeneration, treatment of ulcers burns, osteoarthritis, and dry eyes [148-150]. HPLs also have been used as a xeno-free growth medium supplement for a variety of human cells propagation [139,141]. Potential use for HPLs abundant in numerous neurotrophins factors is also being investigated for the treatment of neurological disorders, including stroke [174], PD [155,161,177], AD [176], ALS [179,286] and TBI [161,287]. There are several methods frequently used to prepare HPLs such as by freeze/thaw cycles, sonication or chemical treatment, and thrombin activation. These procedures were implemented in order to stimulate the release of platelet factors. Furthermore, the lysate produced is then centrifuged to eliminate cellular debris, and the supernatant is recovered as HPLs [19,288].

However, even though the number of scientifically validated HPL therapeutic applications is growing, the manufacturing processes for HPL vary widely, and little is known about their composition and functional properties to develop dedicated preparations best suited for specific clinical indications. It is obvious that customized platelet material preparations are clinically recommended to optimally fit each tissue healing mechanism while eliminating undesired blood components. For instance, the presence of fibrin are beneficial in the wound healing process of skin ulcers. However, for the treatment of eye disease, fibrin deposition may cause clogging in retinal vascular endothelial [289,290]. Moreover, its presence in clinical applications to the central nervous system may cause toxicity due to fibrin deposition, disruption of the blood brain barrier, potentially leading to neuroinflammation and neurodegeneration [291,292] . It is critical to control the total protein content in HPL when it is intended for brain administration. The removal of unnecessary proteins are required in order to avoid overloading in the cerebrospinal fluid. Furthermore, HPL manufacturing methods may also affect the content in

EVs [174], which are functional messengers for tissue healing that are believed to influence the regenerative and cell growth-stimulating potential of HPLs [293-296].

In order to extensively characterize different formulations of HPLs, we prepared 5 different types of HPLs, including by freeze/thaw methods and thrombin activation. All HPLs were prepared from clinical-grade of apheresis PCs collected from healthy blood donors. The PCs were collected in the presence of anti-coagulant, not subjected to leukofiltration, and were suspended in 100% plasma, as is done with most applications in regenerative medicine [150].

FTPL was prepared by subjecting the PC to three cycles of freeze-and-thaw steps in order to release platelet contents [271]. This treatment is used to produce HPL for human cell propagation [296] and preparations similar to FTPL are administered for joint healing and bone regeneration [297-299]. SCPL is serum-converted HPL prepared by the addition of calcium salt ($CaCl_2$) in the presence of glass beads, induces the activation of endogenous thrombin, lead to fibrin formation and platelet degranulation, thus the growth factors released remained in the supernatant [300]. The serum forming from this seroconversion is also used for serum eye drops to treat dry-eye syndrome, as fibrinogen depletion appears preferable [301,302]. Fibrinogen-depleted HPL was evaluated to relieve dry eye-induced graft-versus-host disease [303]. Seroconversion HPL has also been studied for culture growth supplementation, with the advantage of not requiring the use of an anticoagulant [304]. HSCPL was evaluated since that heat-treatment step at 56 °C for 30~60 minutes is found to inactivate immunological components and enhances expansion of the corneal epithelium and endothelium cells growth, implying clinical benefits in treating ocular diseases [160,302,305]. PPL was prepared from isolated platelets after a removal of plasma and is therefore depleted of the plasma protein compartment. Such preparations were evaluated for treating brain stroke in animal models [174]. Finally, heated fraction HPPL, as a purified platelet lysate was also evaluated for brain administration [306]. The heat treatment at 56 °C for 30 minutes was used to further deplete fibrinogen, inactivate proteolytic enzyme activity, and thereby enhance neuroprotective activity compared to the fraction without heating [155,161,287]. Moreover, we did extensive characterization to understand their compositions and functional activity, which are believed to be relevant HPLs functionals in cell therapy and regenerative medicine [147,150,181,307,308]. This was accomplished by conducting several selected analyses. These assessments are including to understand their content in proteins, growth and trophic factors, albumin, IgG, fibrinogen, complement components, and the cytokines and angiogenesis-related protein profiling studies. This assessment was done to

reveal the existence of plasma proteins in comparison to platelet proteomes, as well as the presence of growth factors, cytokines, or other molecules thought to be crucial for HPL activity.

Our findings unveiled significant major differences in the compositions and functional properties of these HPLs. PPL and HPPL, derived from isolated platelets exhibited higher levels of growth factors, particularly in BDNF, PDGF-AB, EGF, VEGF, and TGF-β, compared to other HPLs. This enrichment was also evident when comparing these growth factors to total protein concentrations, indicating the impact of plasma removal during preparation. On the other hand, HPLs obtained from platelets diluted in normal plasma, FTPL and or seroconverted SCPL, respectively, contained higher amounts of IGF-1, as expected, due to its presence in the plasma compartment [181], along with measurable levels of other growth factors. While HPPL had lower content of BDNF, PDGF-AB, and EGF compared to PPL, the VEGF/protein ratio remained consistent, and TGF-β was enriched despite the heat-treatment.

The antigenic contents of C3 and C4, major proteins in the complement pathways and immune system [309] were found to be equivalent to those in normal plasma (C3: 80~170 mg/dL; C4: 13~44 mg/dL) in FTPL, SCPL, and HSCPL, indicating no significant removal of these proteins during the preparation of these HPLs. Conversely, PPL and HPPL showed low levels of C3 and C4, in line with the fact that these proteins are predominantly present in the plasma compartment [310], while platelets have relatively low content [311]. Recent studies have suggested that overexpression of C3 and C4 can exacerbate inflammation, leading to neuronal loss in conditions like AD and other neurological disorders [312,313]. Therefore, the use of HPLs depleted of C3 and C4, as seen in PPL and HPPL, might be preferable for brain administration to mitigate potential inflammatory responses.

A proteome profiling array was used to identify proteins present in platelets, and it successfully detected various proteins in all HPLs, including BDNF, CCL5 (RANTES), CXCL-5, complement component C5, complement factor D, EGF, FGF-19, lipocalin-2, MIF, MMP-9, PF4, PDGF-AA, PDGF-AB, serpin, thrombospondin-1, TIMP-1, and VEGF. These proteins are well-known constituents of platelets and were found to be present consistently across all HPLs. However, notable differences in cytokine and angiogenesis-related protein profiles were observed among the HPLs. Specifically, the levels of BAFF, prolactin, and TIMP-4 varied among the different HPLs. The detection of a protein profile in HPLs requires further characterization such as by using a complementary proteomic study such as by mass

spectrometry and followed by a further quantification assay. The presence of neuro-trophic factors, anti-angiogenesis related protein or protein involved in tissue regeneration, as well as other cytokines known to have a function in particular physiological and pathological conditions, are important to know for a better indication of HPL use.

The biochemical analysis was carried out with a specific emphasis on identifying the presence of salts or ions that could indicate the use of anticoagulants or additive solutions during platelet collection, as well as any serum-conversion and platelet degranulation stages triggered by calcium salts. The results revealed that FTPL, SCPL, and HSCPL contained higher concentrations of albumin, glucose, IgG, and lipids (HDL and LDL) compared to PPL and HPPL, which aligns with the reduced presence of plasma in the latter two fractions. Fibrinogen was detected only in FTPL, suggesting the absence of a clotting factor-removal step. It was undetectable (< 0.4 mg/mL) in seroconverted SCPL, plasma-free PPL, and their respective heat-treated fractions. The elevated levels of Cl and Ca observed in SCPL and HSCPL likely resulted from the addition of $CaCl_2$ during serum conversion. Furthermore, the increased levels of Cl, K, and P in PPL and HPPL can be attributed to the suspension of the platelet pellet in PBS, which contains NaCl, KCl, Na_2HPO4, and KH_2PO4. While understanding the composition of HPL remains essential, it is also interesting to explore its potential influence on promoting coagulation or whether it lacks such an effect altogether.

Additionally, it is crucial to evaluate thrombin activity in HPLs to unveil the pro-coagulant proteolytic activity of thrombin. To measure thrombin generation over time, TGA assay was used, which allows the assessment of thrombin formation resulting from the presence of pro-coagulant factors like pro-coagulant EVs [278] or activated Factor XIa. TGA assay has become a mandatory requirement for commercial release of plasma-derived immunoglobulins as a release criteria to decrease the risks of thrombo-embolic events in patients. [314,315] However use of the TGA assay has not been described previously for assessing the procoagulant activity of platelet lysates for clinical use. Thrombin activity present in the HPLs, and capacity to trigger immediate fibrin formation of relevance for wound healing [316], was assessed using a chromogenic assay using S-2238 substrate [317]. The presence of active pro-coagulant phospholipids, including those associated with EVs, was determined by measuring the shortening of clotting time [318].

Our results showed that there are significant variations in the ability of HPLs to produce thrombin, as determined by TGA. Using both "low" and "high" concentrations of phospholipid micelles containing recombinant human tissue factor and $CaCl_2$, larger thrombin quantities were formed with time in FTPL, SCPL, and HSCPL, but much less in PPL, while thrombin generation was undetectable in HPPL. Moreover, the chromogenic assay showed that due to the lack of an activation step, no proteolytic activity was detected in FTPL. In contrast, compared to PPL and non-activated plasma, proteolytic activity was significantly higher in SCPL ($p < 0.0001$) but significantly ($p < 0.0001$) decreased after heat treatment in HSCPL. The proteolytic activity was found to be absent in HPPL. In SCPL and HSCPL, the addition of $CaCl_2$ triggered the activation of coagulation factor zymogens, converting them into proteolytic enzymes, ultimately resulting in thrombin formation and fibrin generation. This activation occurred because the material used to generate SCPL and HSCPL contained the complete range of coagulation factors present in plasma. On the other hand, PPL, which lacks most of the plasma components, exhibited significantly lower levels of thrombin. Additionally, when heat treatment was applied to produce HPPL, thrombin either precipitated or became inactivated, as thrombin is sensitive to heat [306,319].

Finally, the assessment of pro-coagulant EVs expressing PS and TF, which can be influenced by the HPL manufacturing method, was assessed using bio-immuno assays involving specific EV capture, followed by quantifying thrombin or Factor Xa generation, respectively [320]. All HPL fractions, particularly PPL, contained PS-expressing EVs. Higher PS contents in PPL are consistent with its preparation from isolated platelets, the cellular origin of these EVs. Furthermore, during the preparation of SCPL and HSCPL, the process of serum conversion and fibrin formation may result in the "consumption" and entrapment of PS-expressing EVs within fibrin clots [321]. The application of heat treatment to both SCPL and PPL resulted in a reduction of procoagulant activity and the quantity of PS-expressing EVs. This result is supported by the STA-procoagulant-PPL assay, which demonstrated that SCPL and FTPL exhibited shorter clotting times in comparison to PPL. Additionally, both heat-treated fractions showed a prolongation of the clotting time, further supporting the decreased procoagulant activity observed after heat treatment. TF-bearing EVs were not detectable in any of the HPL fractions, providing evidence that platelets from healthy blood donors do not express TF [281].

The antioxidative capacity of HPLs was determined as a means of detecting the presence of compounds with preserved antioxidant activity [322]. This capacity may contribute in sustaining

a conditions with significant oxidative stress in some clinical states, some molecules such as hydroxyl, peroxyl, or free radicals and the tissue-damaging actions of these reactive oxygen species [323]. Antioxidants can counterbalance a harsh environment characterized by high oxidative stress, which is often observed in certain pathological conditions like neurodegenerative disorders [324], osteoarthritis [325], and ocular diseases [101]. FTPL, SCPL, and HSCPL exhibited the highest absolute antioxidative capacity, which can be attributed to their plasma contents containing antioxidative proteins like albumin, as well as ascorbic acid and uric acid. These components likely contribute to their enhanced antioxidative properties [326-328]. PPL and HPPL, derived from purified platelets, also demonstrated antioxidative activities, showing comparable levels to the other HPLs and even surpassing the plasma control when expressed as a ratio of total proteins. This indicates that PPL and HPPL possess significant antioxidative capabilities despite being prepared from purified platelets.

In conclusion, the first section of our thesis revealed substantial variations among the five HPL preparations in terms of protein contents, protein profile components, chemical compositions, and functional activities, all of which were influenced by the specific mode of preparation employed.. Indeed, these observed differences in HPL preparations could have significant biological implications, and it is essential to take them into careful consideration when designing and choosing HPLs for specific clinical applications. Further research is warranted to precisely determine which HPL variants are most suitable for particular therapeutic uses. This will enable us to optimize and tailor HPL treatments to achieve the best possible clinical outcomes.

The findings from our study also provide support for choosing HPPL as the preferred platelet lysate treatment for brain administration. Moreover, HPPL may be considered preferable for the repair of delicate tissues, such as corneal endothelium, where the presence of neurotrophins could be of significant value in enhancing cell functionality [329], but proteolytic activity and fibrin deposition could be harmful to the cornea [330]. In contrast, the presence of prothrombin or thrombin in FTPL, SCPL, and HSCPL can have a beneficial effect by inducing the formation of a 3D-fibrin scaffold, which is highly useful for healing skin ulcers and burns [277,331,332].

4.2 The implementation of nanofiltration to develop a virus safe HPPL and the removal of EVs

The outcomes of our first work to analyze the characterize the composition and functional activity of HPLs, led us to confirm the selection of HPPL as a suitable preparation for the brain administration. HPPL was purposefully prepared from a concentrated platelet fraction after the removal of plasma compartment; consequently, this fraction is loaded with platelet trophic factors and active molecules, which are known to contribute to the HPPL neuroprotective activity. Heat treatment was also implemented to remove the bulk of proteins. This step is critical to minimize CSF proteins overload such as neurotoxic fibrinogen, prothrombotic factors, and thrombin proteolytic enzymes, and thus to assure the safety for brain administration [282].

Indeed, earlier preclinical studies have shown that our tailor-HPPL is highly neuroprotective in an MPTP mice model of PD [282]. In mouse models of mild and moderate/severe TBI, HPPL was also found to modulate immune responses, promote wound healing, and improve cognitive function [283]. These *in vivo* models confirmed the *in vitro* neuroprotective and neuro-regenerative activities of HPPLs in primary neuronal cells and neuronal cell cultures [161,286]. These data imply that HPPL could be a promising therapeutic option, particularly for the treatment of neurological disorders.

A large-scale preparation of HPPL is needed for future clinical use. Thus, to ensure batch-to-batch consistency, HPPL is usually prepared from pooling of multiple allogeneic PCs. However, as it is derived from blood donation, pooling statistically increases the risk of viral contamination. Strategies include a rigorous screening of potential blood donors and virus testing of individual donations such as using serological and nucleic acid assays are conducted to prevent the transmission. However, there is still a risk of possible pathogen infection, which might occur during the donation window period, or untested viruses [140,141]. As a result, virus elimination step will be critical to reducing the risk of transfusion-transmitted viral infections, especially, a robust virus inactivation that does not compromise the therapeutic safety and efficacy of the product will be required. In addition, a method that can also be applied for a pooled platelet biomaterials is necessary to ensure optimal viral safety, particularly for HPPL, which is intended to be used for brain administration.

Moreover, our previous study showed that HPLs fractions contain abundant population of EVs, as high as 10^{11}-10^{12}/mL including in HPPL. They might be released as a result of the activation process or shear stress given during the lysate preparation [106,107]. EVs released from platelet (PEVs) could act as signaling particles between platelets and other cells, containing platelet-derived biological substances including growth factors and cytokines from the α-granules, and they may significantly contribute to the intracellular communication of platelet response and function [116]. Thus, suggest that P-EVs may support platelet functional role for regenerative therapy. The such a high number of PEVs particularly in HPPL, raises a question of what can be the contribution of these EVs to their neuroprotective activity. The presence of PEVs in may contribute to the beneficial action of HPPL, however, should the PEVs be eventually identified as being detrimental, their removal from HPPL is considered.

Nanofiltration has known for its robustness in removing a wide range of viruses and improving the safety manufacturers of plasma-derived products. Depending on the pore size, it entraps both enveloped and un-enveloped viruses [191,270]. In this experiment, we used Planova-20N filter (ASAHI Kasei, Japan) consist of hollow cellulose fibers, with $\pm$19 nm pore size. It is small enough to hold viruses and still considered as an adequately large to allow proteins to flow pass the nanosized membranes. On the other hand, this filter could potentially remove other particles including EVs.

Therefore, in the second part of our work, we evaluated the feasibility and efficacy of nanofiltration implemented to ensure the virus safety of HPPL. We therefore also investigated its impact of on the HPPL compositions including in their proteins and EVs content as well as more importantly their functional neuroprotective and neuro-regenerative activity. Furthermore, while the EVs were eliminated throughout the filtrations process, it is prompting us to determine the role of neuroprotective of these EVs alone by conducting an experiment to isolate and assess their activity separately.

The feasibility of the nanofiltration and virus reduction value

Our results showed that HPPL could be subjected to a dedicated nanofiltration process using 19-nm pore-size cartridges. Over 20 mL of HPPL could be filtered through the 0.001-m^2 Planova-20N system in approximately 3.5 hours at a constant flow-rate of 0.1 mL/minute and low pressure, corresponding to over 20 L of industrial-scale HPPL using a commercial 1-m^2 Planova-20N cartridge and an amount of over 80 L HPPL could be filtered using a commercial

4-m^2 Planova-20N illustration the feasibility for a larger scale preparation. Virus-removal experiment measured by immuno-qPCR analysis using MVP (parvovirus model) spiking was higher than 5 log units showed the effective at removing even small viruses. In the biological product industry particularly blood plasma-derived products, nanofiltration has been demonstrated to be a reliable method of virus reduction [191,333] and the average pore size of the filters used generally ranges from 35, 19, or 15 nm [192,333]. To prevent filter clogging, the properties of the proteins to be filtered, particularly their size are taken into consideration when choosing the nanofilter cut-off. Blood protein sizes range from 3 to 15 nm [192]. It has been reported that Planova 20N nanofilter with a mean pore size of 19 ± 2 nm has the ability to eliminate all described viruses transmitted through blood, such as the small non-enveloped parvovirus B19 (B19V, 18-26 nm), the hepatitis A virus (26-29 nm), hepatitis E virus (27-34 nm)[174] from a variety of manufacturing fractionated plasma products [191,334]. The potential of these filter was also confirmed by examining the nanofilter at a microscopic level [335]. As a result, in our experiment, Planova 20N should eliminate all known blood-borne viruses, giving the nonfiltered HPPL (NHPPL) a significant margin of safety.

The impact of nanofiltration on the HPPL content: depletion of proteins compositions and EVs

Total protein and selected growth factors, including neurotrophic PDGF-AB and VEGF, showed decreases in protein quantification data and ELISA assessments. The decrease could be attributable to non-specific adsorption on the Planova-20N hollow-fiber membranes or dilution during nanofiltration. Since the VEGF, PDGF, and EGF molecules have molecular masses of 40 kDa, 30 kDa, and 6 kDa, respectively, and that the HPPL trophic factors have similar molecular masses, this parameter is relevant for assessing viral reduction methods based on size-exclusion. On the other hand, the growth factors removed may be linked with EVs and other lipid vesicles seen in HPPL and eliminated during the filtration sequences. DLS analysis showed that the particle primary size distribution was reduced from roughly 280 nm in the HPPL to around 12 nm in the NHPPL, and NTA suggested that the filtration techniques reduced EV numbers by more than 99% (2 logs). The value may be underestimated due to the existence of proteins in the 5~12-nm range that are not eliminated by nanofiltration and are reactive by DLS and NTA. Furthermore, the MP-PS functional assay, a capture assay that quantifies functional PS-expressing EVs, was employed to assess the influence of nanofiltration on these specific EVs. We found that the number of EVs containing PS in NHPPL was substantially lower than in HPPL. The STA-procoagulant-PPL assay showed that

procoagulant PEVs were removed, as evidenced by a significantly prolonged in coagulation time from the NHPPL compared to the HPPL. The reduction in PS-expressing EVs due to nanofiltration should further lower the risks of coagulation and therefore increase the safety of NHPPL for brain delivery.

Moreover, proteomics analysis showed that the majority of the proteins eliminated were linked to extracellular exosomes. This support the DLS, NTA, and functional prothrombotic and procoagulant EV which all was demonstrated EV elimination. EVs are categorized as "small", "medium", or "large" based on their size [336]. In platelet lysates, EVs range in size approximately from 50 to 300 nm [337]. Proteins related to EVs that remain detectable after nanofiltration could indicate that they are present in a soluble form or that the EVs were fragmented into smaller entities during the nanofiltration process. Proteomics analysis also revealed that the number of detected proteins decreased after nanofiltration, but more than 80% of them were in common. Proteins that contribute to HPPL functional role for brain administration, such as antioxidants, cytokines, and neurotrophic factors, were well preserved in NHPPL, with a high similarity in the biological processes involved. The KEGG database study revealed that the filtration/nanofiltration sequence nanofiltration eliminated more proteins linked with disease-related pathways. Bacterial/viral/parasitic infection-related pathways and proteins associated with cancers were among them. The decrease in abundance could be due to the removal of PEVs. Indeed, PEVs are associated with biological responses during infections and the development of cancer [338]. Additionally, platelets in the bloodstream are known to contribute to defensive mechanisms against many infections and may encounter activation that triggers multiple signaling pathways via its secretome products and immune cell recruitment [339,340]. Furthermore, the KEGG pathway analysis revealed that the abundances of several proteins involved in coagulation were decreasing. This finding suggests that nanofiltration improve the safety of HPPL, and when delivered to the brain, it should have a reduced risk of thrombogenicity.

The impact of nanofiltration on the neuroprotective and neuro-regenerative potentials of HPPL

An *in vitro* study was performed using LUHMES cells as a PD model to unveil any impact of nanofiltration on the neuroprotective activity of HPPL. NHPPL at a dose of 5% (v/v) maintained its ability to protect cells from the erastin neurotoxic drug. Cells remained viable 24 h post-treatment, similar to that achieved with the HPPL in our previous studies [276,282].

We also looked at NHPPL potential for promoting cell maturation, as we had done with HPPL previously [161,276]. The SH-SY5Y neuroblastoma cell line was used in our study, and seven days of post-stimulation with 2% NHPPL, cells significantly expressed the β-III tubulin maturation marker, as found in HPPL and RA used as positive controls. As a result, NHPPL retained its ability to induce cell differentiation, essential to counteract increasing neuronal degeneration.

We performed CCI, an *in vivo* model of mild TBI [341], to assess the capacity of the NHPPL to modulate proinflammatory genes after an injury, as previously described HPPL non subjected to nanofiltration [283]. HPPL and NHPPL were delivered through intranasal route over three consecutive days and their anti-inflammatory actions in ipsilateral cortical tissues were evaluated seven days after injury. HPPL and NHPPL were given at a dose of sixty microliters daily for a total dose of one hundred eighty microliters over three days. This daily dosing was selected based on our previous *in vivo* studies using HPPL in PD [282] and TBI [283] mouse models. Furthermore, the *in vitro* functional activity of the HPPL and NHHPL batches used here was consistent with that observed with HPPL in our previous studies [161,282,342]. The expression of proinflammatory markers revealed that the upregulation of inflammatory markers in non-treated TBI mice were considerably reduced in mice treated with both the HPPL and NHPPL This finding suggests that the HPPL preserved its anti-inflammatory activity in TBI models following nanofiltration. Also, when compared to our earlier study, which included both topical and intranasal treatments [283]. The present results show that i.n. treatment of the NHPPL alone was effective in this TBI mouse model. This is clinically important in the treatment of TBI when there is no brain access and intranasal administration would be the only feasible delivery route.

Overall our findings showed that nanofiltration implemented in HPPL to ensure the virus safety for brain administration is feasible. It is robust to lower the viral, prothrombotic, and procoagulant risks but preserves the neuroprotective and anti-inflammatory properties in neuronal pre-clinical PD and TBI. The fact that nanofiltered HPPL maintained their functional activities regardless of the EVs depletion, revealed that EVs in HPPL did not exert a neuroprotective effect.

4.3 The assessment of neuroprotective and neuro-regenerative potentials of PEVs

In order to further confirm the functional activity of EVs in HPPL (HPPL-EVs), we first analyzed them separately. These EVs were isolated by SEC-Izon chromatography, and their concentration was determined using NTA.

An assessment using *in vitro* LUHMES cell model exposed to erastin was performed. A total number of ~4 x 10^{10}, ~1 x 10^{11} and ~2 x 10^{11} HPPL-derived EVs did not significantly affect the cell viability after 24 hours showing a lack of toxicity. However, they were not able to protect the LUHMES cells from erastin neurotoxicity. This validates our finding that after removal of HPPL-EVs and viruses using nanofiltration, HPPL still retained its neuroprotective potential. However, interestingly another preparation of PEVs isolated from platelet concentrate supernatant (PCS-EVs) were tested in the same time and was able to exert neuroprotective activity. This is demonstrating that various EV preparations could have distinct functional effects. It is likely due to the triggering factors, HPPL-EVs were produced by freeze-thaw steps and therefore expressed higher pro-coagulant PS [343], and also as previously noted, the removal of EVs in HPPL after nanofiltration was accompanied by a decrease in PS, reflect their functional activity. In fact, PCS-EVs are naturally occurring vesicles found in plasma supernatant. It is being demonstrated that EVs isolated from plasma without any stimulation showing no conjugation with Annexin – showing no or less PS [112], thus suggest that this EVs preparation have less of pro-coagulant activity and more suitable for the brain administration. We then did further characterization of PCS-EVs on their biophysical profile and functional activities.

Our analysis showed that isolated PCS-EVs have a size distribution profile that are consistent with previous studies of EVs in human plasma or serum [344,345]. Determined by DLS, our PCS-EVs had a heterogeneous population with a major population size of roughly 200 nm and a range in size from 70 to 350 nm. NTA and TRPS measurements revealed that the concentration of EVs in this preparation was in a range of 10^{10}–11^{11} particles/mL. The protein profile of PCS-EVs was characterized by ELISA and proteomic analysis. The data showed that PCS-EVs contain an substantial amount of BDNF, PDGF, EGF, and VEGF determined by ELISA. PDGF, BDNF, EGF, and VEGF are growth factors particularly highly present in platelets, and therefore their relative abundance in PEVs is expected [155,346]. Proteomic analysis also confirmed the presence of these factors and revealed some others including platelet cytokines

and antioxidants, in the list as follow: PDGF-A, PDGF-B, VEGF, HGF, TGF-β1, IGF, cAMP-dependent protein kinase, catalase, Glutathione S-transferase, Glutathione peroxidases, SOD 1,2, Glutamate-rich protein, VTI1A, Glutathione reductase, Glia maturation factor. DAVID Bioinformatics Resources 6.8 GO enrichment analysis showed that platelet degranulation and activation, cell-cell adhesion, immune response, receptor mediated endocytosis were among the biological processes involved by proteins component in PCS-EVs. The highly enriched cluster found in the functional annotation analysis found to be related mostly to serine-type endopeptidase and its inhibitor, proteins integrin and antigen binding, cadherin binding involved cell-cell adhesion. Proteins associated with blood microparticles (MVs), platelet alpha granules, CAMP-dependent protein kinase were confirmed among the major abundant components in PCS-EVs.

In vitro functional outcomes of PCS-EVs treatment

Our initial work was to confirm the neuroprotective activity of PCS-EVs using LUHMES cells, The results have shown that a number of ~1 x 10^{10} PCS-EVs given to the cells were able to exert a significant neuroprotective activity against erastin neurotoxic. PCS-EVs were showed to exert neuroprotection with 65% cell viability compared to 17% without. The PCS-EVs derived from platelets themselves are known for carrying a functional plethora of molecules that was originally from dense and α-granules, explaining their protective activity. In addition, the antioxidant molecules found in PCS-EVs such as glutathione peroxidases, SOD1, and SOD2, possibly involve to eliminate the increasing of harmful lipid reactive oxygen species induced-ferroptosis after erastin treatment [207,347,348].

Moreover, considering the growth factors content that regulate numerous processes in cellular and wound healing, the ability of PCS-EVs to promote neuronal cell growth and repair *in vitro* was then evaluated. Human neuroblastoma cells SH-SY5Y were used together with an established scratch wound assay. We revealed that PCS-EVs significantly increased the capacity for neuronal repair by promoting the neuronal reconnection. This is consistent with the finding that a variety of growth factors including PDGF, BDNF, IGF-1, able to stimulate differentiation and increased cellular survival of SH- SY5Y [348-350].

We did test with BV-2 cells to see the treatment effect on the microglial activation. Pro-inflammatory marker TNF-α, that is one of major cytokines released by microglia cells upon LPS activation was measured [351,352]. Our results demonstrated that PCS-EVs, in the dose used,

exert favorable anti-inflammatory and restorative activities in BV-2 triggered by LPS. However, at a double concentration applied, there was an increasing of TNF-α expression, indicating that higher PCS-EVs dose was ineffective at inhibiting BV-2 activation caused by LPS induction. The elevation of TNF-α is possibly due to greater dose eventually increase the protein accumulation and lead to over-reactive response of BV-2 caused by LPS. In the normal condition (i.e. without LPS stimulation), PCS-EVs in both doses used did not trigger significantly TNF-α expression compared to the control, showed that they did not induce BV-2 microglia activation confirming the safety of PSC-EVs treatment.

***In vivo* anti-inflammatory and neuro-protective effect of PCS-EVs**

In the present study, we examined for the first time the efficacy of PCS-EVs delivered through intranasal routes to modulate inflammatory actions following TBI in mice. The well-established CCI model was used to stimulate mild TBI resulting from head impactor given with a controlled parameter. The PCS-EVs given for three consecutive days post-injury was found contribute to exert anti-inflammatory effect following the injury. The inflammatory markers such assessed such as CD68, Tnf-α, Gfap, Ccl4, Tlr2, and Trem2 that initially upregulated following the injury were showing a trend of decreasing by EVs treatment.

Furthermore, in our experiments with PD model, MPTP mice were subjected to PCS-EVs i.n. administration. MPTP is a validated a reliable animal model of PD used to target specifically dopaminergic neurons. In this study we used a classical acute MPTP mouse model where 4 doses were used over one day. PCS-EVs delivered intranasally a day before the intoxication. Our results showed that PCS-EVs treatment improved the locomotor function after deterioration in MPTP mice. This is showed especially by the increasing of rearing number in the mice treated by the PCS-EVs in certain dose (4×10^{10} EVs particles). Following our behavioral findings, IHC analysis confirmed our earlier *in-vitro* result using LUHMES. PCS-EVs therapy enhanced the number of TH positive cells after MPTP, demonstrating a protective impact on the dopaminergic neurons. However, using a higher, we did not observe a similar impact, indicating that a further study is needed to determine the most effective dose for an optimum therapeutic outcome**.**

Taken together, their neuroprotective, neuro-regenerative and anti-inflammatory activity demonstrated *in vitro* and *in vivo* in our study appear to be regulated by multiple of growth

factors, antioxidant compounds, and cytokines found in our PCS-EVs. As shown in a previous study, PEVs containing a combination of several growth factors were able to enhance NSC proliferation and differentiation, as well as supports angiogenesis, survival and neurogenesis *in vivo* in ischemic rats [123,124]. Their study showed that an inhibition of FGF2, VEGF, or PDGF found in their PEVs fraction significantly reduced its functional activities. However, blocking each individual growth factor did not entirely prevent their effects, supporting an additive effect. In our PSC-EVs, the presence of some growth factors was proven beneficial to protect dopaminergic neurons, promote neuronal survival and growth, and modulate inflammation post injury. For instance, BDNF together with PDGF-BB promoted newly generated cells in the *substantia nigra* and *striatum* in PD rat model [26]. BDNF in a response to neuronal damage aids neuronal restoration, which is known to be regulated via a complex network of signaling pathways linked to cell survival, inhibition of cell death, anti-inflammation, and synaptic plasticity [20,29]. PDGF-BB protects dopaminergic neurons associated to Akt/ERK/CREB pathways in MPTP mice [47]. IGF-1 protects dopaminergic neurons and increases the overall survival of human neural progenitor cells *in vitro* and after grafting in a rat model of PD [72]. IGF-1 help suppressed the degeneration of neurons and improved a motor activity after brain injury [69]. Treatment with VEGF rescued the dopaminergic neuronal fibers from 6-OHDA toxicities and preserved the number of TH-positive neurons in striatum and SN in rats PD model [84-86]. TGF-β1 exert anti-apoptotic and anti-inflammation, prevent the degeneration of hippocampal neurons in ischemic rats. It has also been demonstrated that TGF-βs able to protect dopaminergic cells against MPTP and 6-ODHA in *in vivo* model of PD [92,93]. The depletion of these growth factors are also often associated with an increasing of vulnerability due to oxidative stress as a result of injury [49,353]. Pretreatment with PDGF-AA or PDGF-BB reduced oxidative stress was associated with the increasing activity of antioxidants such catalase, glutathione peroxidase, and SOD [50]. Antioxidant act as anti-inflammatory properties and help reduce inflammation in the brain [354,355], which likely explaining the activity of PCS-EVs to regulate inflammation after TBI. The activation of catalase, SOD, and glutathione suppress the amount of free radicals in cells, prevent intracellular Ca^{++} release, and stop the afterward apoptotic signaling, eventually protect the loss of dopaminergic neurons in MPTP animal model [356,357].

The nanoscale size of EVs might elucidate their capacity to reach the brain and thus delivering their therapeutic factors. Indeed, one of the advantages of using EVs as a carrier is that they are able to overcome tissue barriers, including BBB [125,126]. A study showed that specifically

platelet EVs can be internalized by human brain endothelial cells by endocytosis supporting this hypothesis [127].

Finally, we conclude that EVs isolated from the supernatant of human platelet concentrates abbreviated as PCS-EVs abundant in neurotrophic factors, cytokines, and anti-oxidant, were found to have a robust neuroprotective effect in an established *in vitro model* of PD, neuro-restoration on differentiated neuroblastoma cells (TBI model) and does not induce the activation of microglial cells, confirming their safety. Our *in vivo* study confirmed the anti-inflammatory effect in CCI-TBI mice. PCS-EVs exerted neuroprotective activity on the dopaminergic neurons and able to improve locomotor deficits in MPTP animal model of PD. This finding opens an intriguing perspective in the development of neuroprotective EV-based biotherapies.

We elaborated that biochemical and functional properties of HPL preparations greatly vary depending upon their mode of production, with potential impacts on the safety and efficacy. Further research is needed to define which HPLs are most suitable for specific clinical applications. Additionally, characterization of the HPL protein profile for instance by proteomic analysis and quantification of individual components are required to development of suitable *in vitro* and *in vivo* preclinical models.

The first part of our work also led us to confirm the selection of HPPL as a suitable preparation for the brain administration HPPL, prepared from isolated platelets were enriched in growth factors, depleted of plasma proteins, and low of generated thrombin and pro-thrombogenic activity. Nanofiltration technology can be readily implemented to manufacture clinical-grade virus safe HPPLs to increase viral safety and tolerance, even more reduce prothrombotic and procoagulant risks, and without affecting the neuroprotective and anti-inflammatory functions. The finding that nanofiltered HPPL maintained their functional activities regardless of the EVs depletion, revealed that EVs in HPPL did not exert a neuroprotective effect. However, our assessment showed that EVs isolated from the supernatant of human PCs are not toxic at the concentration used and were found to have a robust neuroprotective effect in an established *in vitro* and *in vivo* model of PD and TBI when delivered intranasally. This opens up a valuable perspective for the development of neuroprotective EV-based biotherapies that can contain neurotrophic factors, anti-oxidant and anti-inflammatory cytokines to support neuronal growth and survival.

Indeed, our findings confirmed that both NHPPL and PCS-EVs biomaterials exhibit potential benefits for brain administration. Moreover, for their future clinical utilization, several critical factors, including safety, efficacy, and scalability, must be carefully evaluated. In terms of safety and efficacy, prior studies have extensively investigated both NHPPL and PCS-EVs and have demonstrated their promising safety profiles for treating brain pathology at selected doses. Nevertheless, further investigations are necessary to assess their long-term safety and potential adverse effects.

EVs however hold a unique properties that make them a promising carrier for delivering therapeutic agents to the brain. EVs as small membrane-bound vesicles and have been shown able to cross the BBB, especially PCS-EVs which are derived from platelet notably can be used

as a natural carrier. Thus, for future application of PCS-EVs they can be engineered to carry specific biomolecules, such as drugs or nucleic acids, and delivered to target cells in the brain, as this have previous study done with another type of EVs. Although, there is also no doubt that the NHPPL proteome are able to reach the brain and thus exert their neuroprotective functions, as accumulating studies have shown, for instance when they are delivered by intranasal delivery. Consequently, the selection of the optimal biomaterials is also depends upon the specific therapeutic objectives.

Moreover, regarding the scalability for clinical applications, large-scale preparation of NHPPL is considered to be easier than PCS-EVs. NHPPL yields a higher volume per unit of platelet concentrate, producing approximately ~12 mL of purified lysate following isolation methods and sequence filtrations, including virus removal steps. On the other hand, PCS-EVs production generates only ~2.3 mL from one single platelet donation. However, as NHPPL are prepared from the isolated platelets, thus the supernatant from the same PC can be employed to extract PCS-EVs. As a result, a single platelet concentrate bag can yield both NHPPL and PCS-EVs, potentially reducing the amount of starting material needed and making optimal use of platelet donations.

REFERENCES

1. Machlus KR, Italiano Jr. The incredible journey: From megakaryocyte development to platelet formation. 2013;201(6):785-796.
2. White JG, Michelson A. Platelet structure. 2007;2:45-71.
3. Broos K, De Meyer SF, Feys HB, et al. Blood platelet biochemistry. 2012;129(3):245-249.
4. Aslan JE, Itakura A, Gertz JM, et al. Platelet shape change and spreading. *Platelets and Megakaryocytes*. Springer; 2012:91-100.
5. Cines DB, Blanchette VS. Immune thrombocytopenic purpura. 2002;346(13):995-1008.
6. Schafer AI. Thrombocytosis. 2004;350(12):1211-1219.
7. Rowley JW, Schwertz H, Weyrich AS. Platelet mRNA: the meaning behind the message. 2012;19(5):385.
8. Jenne C, Urrutia R, Kubes P. Platelets: bridging hemostasis, inflammation, and immunity. 2013;35(3):254-261.
9. Duerschmied D, Suidan GL, Demers M, et al. Platelet serotonin promotes the recruitment of neutrophils to sites of acute inflammation in mice. 2013;121(6):1008-1015.
10. King SM, Reed GL. Development of platelet secretory granules. Elsevier; 2002:293-302.
11. Blair P, Flaumenhaft RJBr. Platelet α-granules: Basic biology and clinical correlates. 2009;23(4):177-189.
12. Nurden AT. Platelets, inflammation and tissue regeneration. 2011;105(S 06):S13-S33.
13. Li JL, Zarbock A, Hidalgo AJJoEM. Platelets as autonomous drones for hemostatic and immune surveillance. 2017;214(8):2193-2204.
14. Bosch G, van Schie HT, de Groot MW, et al. Effects of platelet-rich plasma on the quality of repair of mechanically induced core lesions in equine superficial digital flexor tendons: a placebo-controlled experimental study. 2010;28(2):211-217.
15. Joo S-J. Mechanisms of platelet activation and integrin αIIβ3. 2012;42(5):295-301.
16. Ni H, Freedman J. Platelets in hemostasis and thrombosis: role of integrins and their ligands. 2003;28(3):257-264.
17. McNicol A, Israels SJ. Platelet dense granules: structure, function and implications for haemostasis. 1999;95(1):1-18.
18. Heijnen H, Van Der Sluijs P. Platelet secretory behaviour: as diverse as the granules… or not? 2015;13(12):2141-2151.
19. Burnouf T, Strunk D, Koh MB, Schallmoser K. Human platelet lysate: replacing fetal bovine serum as a gold standard for human cell propagation? 2016;76:371-387.
20. Habtemariam S. The brain-derived neurotrophic factor in neuronal plasticity and neuroregeneration: new pharmacological concepts for old and new drugs. 2018;13(6):983.
21. Zhao H, Alam A, San C-Y, et al. Molecular mechanisms of brain-derived neurotrophic factor in neuro-protection: recent developments. 2017;1665:1-21.
22. Wei Z, Liao J, Qi F, Meng Z, Pan S. Evidence for the contribution of BDNF-TrkB signal strength in neurogenesis: An organotypic study. 2015;606:48-52.
23. Kubo T, Nonomura T, Enokido Y, et al . Brain-derived neurotrophic factor (BDNF) can prevent apoptosis of rat cerebellar granule neurons in culture. 1995;85(2):249-258.
24. Kowiański P, Lietzau G, Czuba E, et al. BDNF: a key factor with multipotent impact on brain signaling and synaptic plasticity. 2018;38:579-593.
25. Hosomi S, Yamashita T, Aoki M, et al. The p75 receptor is required for BDNF-induced differentiation of neural precursor cells. 2003;301(4):1011-1015.

26. Mohapel P, Frielingsdorf H, Häggblad J, et al. Platelet-derived growth factor (PDGF-BB) and brain-derived neurotrophic factor (BDNF) induce striatal neurogenesis in adult rats with 6-hydroxydopamine lesions. 2005;132(3):767-776.
27. Fumagalli F, Racagni G, Riva M. Shedding light into the role of BDNF in the pharmacotherapy of Parkinson's disease. 2006;6(2):95-104.
28. Numakawa T, Suzuki S, Kumamaru E, et al. BDNF function and intracellular signaling in neurons. 2010;
29. Chen A, Xiong L-J, Tong Y, Mao M. The neuroprotective roles of BDNF in hypoxic ischemic brain injury. 2013;1(2):167-176.
30. Weishaupt N, Blesch A, Fouad K. BDNF: the career of a multifaceted neurotrophin in spinal cord injury. 2012;238(2):254-264.
31. Kaplan DR, Miller FD. Neurotrophin signal transduction in the nervous system. 2000;10(3):381-391.
32. Almeida R, Manadas B, Melo C, et al. Neuroprotection by BDNF against glutamate-induced apoptotic cell death is mediated by ERK and PI3-kinase pathways. 2005;12(10):1329-1343.
33. Jiang Y, Wei N, Lu T, et al. Intranasal brain-derived neurotrophic factor protects brain from ischemic insult via modulating local inflammation in rats. 2011;172:398-405.
34. Valerio A, Dossena M, Bertolotti P, et al. Leptin is induced in the ischemic cerebral cortex and exerts neuroprotection through NF-κB/c-Rel–dependent transcription. 2009;40(2):610-617.
35. Kajiya M, Shiba H, Fujita T, et al. Brain-derived neurotrophic factor protects cementoblasts from serum starvation-induced cell death. 2009;221(3):696-706.
36. Fredriksson L, Li H, Eriksson U. The PDGF family: four gene products form five dimeric isoforms. 2004;15(4):197-204.
37. Fretto L, Snape A, Tomlinson J, et al. Mechanism of platelet-derived growth factor (PDGF) AA, AB, and BB binding to alpha and beta PDGF receptor. 1993;268(5):3625-3631.
38. Sjölund M, Hedin U, Sejersen T, et al. Arterial smooth muscle cells express platelet-derived growth factor (PDGF) A chain mRNA, secrete a PDGF-like mitogen, and bind exogenous PDGF in a phenotype-and growth state-dependent manner. 1988;106(2):403-413.
39. Raines EW, Dower SK, Ross R. Interleukin-1 mitogenic activity for fibroblasts and smooth muscle cells is due to PDGF-AA. 1989;243(4889):393-396.
40. Sil S, Periyasamy P, Thangaraj A, et al. PDGF/PDGFR axis in the neural systems. 2018;62:63-74.
41. Fruttiger M, Karlsson L, Hall AC, et al. Defective oligodendrocyte development and severe hypomyelination in PDGF-A knockout mice. 1999;126(3):457-467.
42. Zhou L, Shao C-Y, Xie Y-J, et al. Gab1 mediates PDGF signaling and is essential to oligodendrocyte differentiation and CNS myelination. 2020;9:e52056.
43. Hart CE, Forstrom JW, Kelly JD, et al. Two Classes of PDGF Receptor Eecognize Different Isoforms of PDGF. 1988;240(4858):1529-1531.
44. Peng F, Yao H, Bai X, et al. Platelet-derived growth factor-mediated induction of the synaptic plasticity gene Arc/Arg3. 1. 2010;285(28):21615-21624.
45. Satoh T, Nakatsuka D, Watanabe Y, et al. Neuroprotection by MAPK/ERK kinase inhibition with U0126 against oxidative stress in a mouse neuronal cell line and rat primary cultured cortical neurons. 2000;288(2):163-166.
46. Funa K, Sasahara M. The roles of PDGF in development and during neurogenesis in the normal and diseased nervous system. 2014;9:168-181.
47. Chen H, Teng Y, Chen X, et al. Platelet-derived growth factor (PDGF)-BB protects dopaminergic neurons via activation of Akt/ERK/CREB pathways to upregulate tyrosine hydroxylase. 2021;27(11):1300-1312.

48. Peng F, Dhillon N, Callen S, et al. Platelet-derived growth factor protects neurons against gp120-mediated toxicity. 2008;14(1):62-72.
49. Zheng L, Ishii Y, Tokunaga A, et al. Neuroprotective effects of PDGF against oxidative stress and the signaling pathway involved. 2010;88(6):1273-1284.
50. Cheng B, Mattson MP. PDGFs protect hippocampal neurons against energy deprivation and oxidative injury: evidence for induction of antioxidant pathways. 1995;15(11):7095-7104.
51. Cox WG, Hemmati-Brivanlou A. Caudalization of neural fate by tissue recombination and bFGF. 1995;121(12):4349-4358.
52. Ghosh A, Greenberg ME. Distinct roles for bFGF and NT-3 in the regulation of cortical neurogenesis. 1995;15(1):89-103.
53. Ferrari G, Minozzi M-C, Toffano G, et al. Basic fibroblast growth factor promotes the survival and development of mesencephalic neurons in culture. 1989;133(1):140-147.
54. Liu W-G, Wang Z-Y, Huang Z-S. Bone marrow-derived mesenchymal stem cells expressing the bFGF transgene promote axon regeneration and functional recovery after spinal cord injury in rats. 2011;33(7):686-694.
55. Vescovi AL, Reynolds BA, Fraser DD, et al. bFGF regulates the proliferative fate of unipotent (neuronal) and bipotent (neuronal/astroglial) EGF-generated CNS progenitor cells. 1993;11(5):951-966.
56. Aoyagi A, Nishikawa K, Saito H, et al. Characterization of basic fibroblast growth factor-mediated acceleration of axonal branching in cultured rat hippocampal neurons. 1994;661(1-2):117-126.
57. Cheng Y, Tao Y, Black IB, et al. A single peripheral injection of basic fibroblast growth factor (bFGF) stimulates granule cell production and increases cerebellar growth in newborn rats. 2001;46(3):220-229.
58. Cheng Y, Black IB, DiCicco-Bloom E. Hippocampal granule neuron production and population size are regulated by levels of bFGF. 2002;15(1):3-12.
59. Fujii H, Matsubara K, Sakai K, et al. Dopaminergic differentiation of stem cells from human deciduous teeth and their therapeutic benefits for Parkinsonian rats. 2015;1613:59-72.
60. Lin Q, Wong HL, Tian F-R, et al. Enhanced neuroprotection with decellularized brain extracellular matrix containing bFGF after intracerebral transplantation in Parkinson's disease rat model. 2017;517(1-2):383-394.
61. Cai P, Ye J, Zhu J, et al. Inhibition of endoplasmic reticulum stress is involved in the neuroprotective effect of bFGF in the 6-OHDA-induced Parkinson's disease model. 2016;7(4):336.
62. Chen P, Tang H, Zhang Q, et al. Basic fibroblast growth factor (bFGF) protects the blood–brain barrier by binding of FGFR1 and activating the ERK signaling pathway after intra-abdominal hypertension and traumatic brain injury. 2020;26:e922009-1.
63. Sun D, Bullock MR, McGinn MJ, et al. Basic fibroblast growth factor-enhanced neurogenesis contributes to cognitive recovery in rats following traumatic brain injury. 2009;216(1):56-65.
64. Anderson MF, Åberg MA, Nilsson M, et al. Insulin-like growth factor-I and neurogenesis in the adult mammalian brain. 2002;134(1-2):115-122.
65. Le Roith D, Scavo L, Butler A, Metabolism. What is the role of circulating IGF-I? 2001;12(2):48-52.
66. Kavran JM, McCabe JM, Byrne PO, et al. How IGF-1 activates its receptor. 2014;3:e03772.
67. Dyer AH, Vahdatpour C, Sanfeliu A, Tropea D. The role of Insulin-Like Growth Factor 1 (IGF-1) in brain development, maturation and neuroplasticity. 2016;325:89-99.
68. Costales J, Kolevzon A. The therapeutic potential of insulin-like growth factor-1 in central nervous system disorders. 2016;63:207-222.

69. Hayes CA, Valcarcel-Ares MN, Ashpole NM. Preclinical and clinical evidence of IGF-1 as a prognostic marker and acute intervention with ischemic stroke. 2021;41(10):2475-2491.
70. Ge L, Liu S, Rubin L, Lazarovici P, et al. Research Progress on Neuroprotection of Insulin-like Growth Factor-1 towards Glutamate-Induced Neurotoxicity. 2022;11(4):666.
71. Kazanis I, Bozas E, Philippidis H, et al. Neuroprotective effects of insulin-like growth factor-I (IGF-I) following a penetrating brain injury in rats. 2003;991(1-2):34-45.
72. Ebert AD, Beres AJ, Barber AE, et al. Human neural progenitor cells over-expressing IGF-1 protect dopamine neurons and restore function in a rat model of Parkinson's disease. 2008;209(1):213-223.
73. Takahashi H, Shibuya M. The vascular endothelial growth factor (VEGF)/VEGF receptor system and its role under physiological and pathological conditions. 2005;109(3):227-241.
74. Lambrechts D, Carmeliet P. VEGF at the neurovascular interface: therapeutic implications for motor neuron disease. 2006;1762(11-12):1109-1121.
75. Bautch VL, James JM, migration. Neurovascular development: The beginning of a beautiful friendship. 2009;3(2):199-204.
76. Devos D, Moreau C, Lassalle P, et al. Low levels of the vascular endothelial growth factor in CSF from early ALS patients. 2004;62(11):2127-2129.
77. Moreau C, Gosset P, Kluza J, et al. Deregulation of the hypoxia inducible factor-1α pathway in monocytes from sporadic amyotrophic lateral sclerosis patients. 2011;172:110-117.
78. Just N, Moreau C, Lassalle P, et al. High erythropoietin and low vascular endothelial growth factor levels in cerebrospinal fluid from hypoxemic ALS patients suggest an abnormal response to hypoxia. 2007;17(2):169-173.
79. Moreau C, Devos D, Brunaud-Danel V, et al. Paradoxical response of VEGF expression to hypoxia in CSF of patients with ALS. 2006;77(2):255-257.
80. Azzouz M, Ralph GS, Storkebaum E, et al. VEGF delivery with retrogradely transported lentivector prolongs survival in a mouse ALS model. 2004;429(6990):413-417.
81. Sun Y, Jin K, Xie L, et al. VEGF-induced neuroprotection, neurogenesis, and angiogenesis after focal cerebral ischemia. 2003;111(12):1843-1851.
82. Jin K, Mao X, Batteur S, McEachron E, et al. Caspase-3 and the regulation of hypoxic neuronal death by vascular endothelial growth factor. 2001;108(2):351-358.
83. Jin KL, Mao XO, Greenberg DA. Vascular endothelial growth factor: direct neuroprotective effect in in vitro ischemia. 2000;97(18):10242-10247.
84. Yasuhara T, Shingo T, Muraoka K, et al. Neurorescue effects of VEGF on a rat model of Parkinson's disease. 2005;1053(1-2):10-18.
85. Tian Y-y, Tang C-J, Wang J-n, et al. Favorable effects of VEGF gene transfer on a rat model of Parkinson disease using adeno-associated viral vectors. 2007;421(3):239-244.
86. Yasuhara T, Shingo T, Kobayashi K, et al. Neuroprotective effects of vascular endothelial growth factor (VEGF) upon dopaminergic neurons in a rat model of Parkinson's disease. 2004;19(6):1494-1504.
87. Cao L, Jiao X, Zuzga DS, et al. VEGF links hippocampal activity with neurogenesis, learning and memory. 2004;36(8):827-835.
88. Clark DA, Coker R. Transforming growth factor-beta (TGF-beta). 1998;30(3):293-298.
89. Letterio JJ, Roberts AB. REGULATION OF IMMUNE RESPONSES BY TGF-β. 1998;16(1):137-161. doi:10.1146/annurev.immunol.16.1.137
90. Gomes FCA, de Oliveira Sousa V, Romão L. Emerging roles for TGF-β1 in nervous system development. 2005;23(5):413-424.
91. Henrich-Noack P, Prehn J, Krieglstein J. TGF-β1 protects hippocampal neurons against degeneration caused by transient global ischemia: dose-response relationship and potential neuroprotective mechanisms. 1996;27(9):1609-1615.

92. Tesseur I, Nguyen A, Chang B, et al. Deficiency in neuronal TGF-β signaling leads to nigrostriatal degeneration and activation of TGF-β signaling protects against MPTP neurotoxicity in mice. 2017;37(17):4584-4592.
93. Dobolyi A, Vincze C, Pál G, et al. The neuroprotective functions of transforming growth factor beta proteins. 2012;13(7):8219-8258.
94. Théry C, Witwer KW, Aikawa E, et al. Minimal information for studies of extracellular vesicles 2018 (MISEV2018): a position statement of the International Society for Extracellular Vesicles and update of the MISEV2014 guidelines. 2018;7(1):1535750.
95. Tricarico C, Clancy J, D'Souza-Schorey C. Biology and biogenesis of shed microvesicles. 2017;8(4):220-232.
96. Abels ER, Breakefield XO. Introduction to extracellular vesicles: biogenesis, RNA cargo selection, content, release, and uptake. 2016;36:301-312.
97. Oggero S, Austin-Williams S, Norling LV. The contrasting role of extracellular vesicles in vascular inflammation and tissue repair. 2019;10:1479.
98. Todorova D, Simoncini S, Lacroix R, et al. Extracellular vesicles in angiogenesis. 2017;120(10):1658-1673.
99. Żmigrodzka M, Witkowska-Piłaszewicz O, Winnicka AJIjoms. Platelets extracellular vesicles as regulators of cancer progression—an updated perspective. 2020;21(15):5195.
100. Van Niel G, d'Angelo G, Raposo G. Shedding light on the cell biology of extracellular vesicles. 2018;19(4):213-228.
101. Ung L, Pattamatta U, Carnt N, Wilkinson-Berka JL, et al. Oxidative stress and reactive oxygen species: a review of their role in ocular disease. *Clinical Science*. 2017;131(24):2865-2883.
102. Johnstone RM, Adam M, Hammond J, et al. Vesicle formation during reticulocyte maturation. Association of plasma membrane activities with released vesicles (exosomes). 1987;262(19):9412-9420.
103. György B, Szabó TG, Pásztói M, et al. Membrane vesicles, current state-of-the-art: emerging role of extracellular vesicles. *Cellular and Molecular Life Sciences*. 2011/08/01 2011;68(16):2667-2688. doi:10.1007/s00018-011-0689-3
104. Raposo G, Stahl PD. Extracellular vesicles: a new communication paradigm? 2019;20(9):509-510.
105. Wolf P. The nature and significance of platelet products in human plasma. 1967;13(3):269-288.
106. Antwi-Baffour S, Adjei J, Aryeh C, et al. Understanding the biosynthesis of platelets-derived extracellular vesicles. 2015;3(3):133-140.
107. Gasecka A, Nieuwland R, Siljander PR-M. Platelet-derived extracellular vesicles. *Platelets*. Elsevier; 2019:401-416.
108. Morel O, Morel N, Freyssinet J-M, et al. Platelet microparticles and vascular cells interactions: a checkpoint between the haemostatic and thrombotic responses. 2008;19(1):9-23.
109. Owens III AP, Mackman N. Microparticles in hemostasis and thrombosis. 2011;108(10):1284-1297.
110. Ferreira P, Bozbas E, Tannetta S, et al. Mode of induction of platelet-derived extracellular vesicles is a critical determinant of their phenotype and function. 2020;10(1):1-8.
111. Puhm F, Boilard E, Machlus KR. Platelet extracellular vesicles: beyond the blood. 2021;41(1):87-96.
112. Connor DE, Exner T, Ma DDF, et al. The majority of circulating platelet-derived microparticles fail to bind annexin V, lack phospholipid-dependent procoagulant activity and demonstrate greater expression of glycoprotein Ib. 2010;103(05):1044-1052.

113. Blair TA, Frelinger III. Platelet surface marker analysis by mass cytometry. 2020;31(5):633-640.
114. Brisson AR, Tan S, Linares R, Gounou C, et al. Extracellular vesicles from activated platelets: a semiquantitative cryo-electron microscopy and immuno-gold labeling study. 2017;28(3):263-271.
115. Toth B, Liebhardt S, Steinig K, et al. Platelet-derived microparticles and coagulation activation in breast cancer patients. 2008;100(10):663-669.
116. Melki I, Tessandier N, Zufferey A, et al. Platelet microvesicles in health and disease. 2017;28(3):214-221.
117. Widyaningrum R, Wu Y-W, Delila L, et al. In vitro evaluation of platelet extracellular vesicles (PEVs) for corneal endothelial regeneration. 2022;33(8):1237-1250.
118. Guo S-C, Tao S-C, Yin W-J, et al. Exosomes derived from platelet-rich plasma promote the re-epithelization of chronic cutaneous wounds via activation of YAP in a diabetic rat model. 2017;7(1):81.
119. Tao S-C, Guo S-C, Zhang C-Q. Platelet-derived extracellular vesicles: an emerging therapeutic approach. 2017;13(7):828.
120. Nebie O, Buée L, Blum D, et al. Can the administration of platelet lysates to the brain help treat neurological disorders? 2022;79(7):379.
121. Antich-Rosselló M, Forteza-Genestra MA, Monjo M, et al. Platelet-derived extracellular vesicles for regenerative medicine. 2021;22(16):8580.
122. Sadallah S, Eken C, Martin PJ, Schifferli JA. Microparticles (ectosomes) shed by stored human platelets downregulate macrophages and modify the development of dendritic cells. 2011;186(11):6543-6552.
123. Hayon Y, Dashevsky O, Shai E, et al. Platelet microparticles induce angiogenesis and neurogenesis after cerebral ischemia. 2012;9(3):185-192.
124. Hayon Y, Dashevsky O, Shai E, et al. Platelet microparticles promote neural stem cell proliferation, survival and differentiation. 2012;47:659-665.
125. Saint-Pol J, Gosselet F, Duban-Deweer S, et al. Targeting and crossing the blood-brain barrier with extracellular vesicles. 2020;9(4):851.
126. Zhang Y, Chopp M, Meng Y, et al. Effect of exosomes derived from multipluripotent mesenchymal stromal cells on functional recovery and neurovascular plasticity in rats after traumatic brain injury. 2015;122(4):856-867.
127. Faille D, El-Assaad F, Mitchell AJ, et al. Endocytosis and intracellular processing of platelet microparticles by brain endothelial cells. 2012;16(8):1731-1738.
128. Qu M, Lin Q, Huang L, et al. Dopamine-loaded blood exosomes targeted to brain for better treatment of Parkinson's disease. 2018;287:156-166.
129. Zaldivia MT, McFadyen JD, Lim B, et al. Platelet-derived microvesicles in cardiovascular diseases. 2017;4:74.
130. Heal JM, Blumberg N. Optimizing platelet transfusion therapy. 2004;18(3):149-165.
131. Ballem PJ, Segal GM, Stratton JR, Gernsheimer T, Adamson JW, Slichter S. Mechanisms of thrombocytopenia in chronic autoimmune thrombocytopenic purpura. Evidence of both impaired platelet production and increased platelet clearance. 1987;80(1):33-40.
132. Khan AI, Anwer F. Platelet Transfusion. *StatPearls [Internet]*. StatPearls Publishing; 2022.
133. Schrezenmeier H, Seifried E. Buffy-coat-derived pooled platelet concentrates and apheresis platelet concentrates: which product type should be preferred? 2010;99(1):1-15.
134. van der Meer PF. Platelet concentrates, from whole blood or collected by apheresis? 2013;48(2):129-131.

135. Tynngård N. Preparation, storage and quality control of platelet concentrates. 2009;41(2):97-104.
136. Shrivastava M. The platelet storage lesion. 2009;41(2):105-113.
137. Van der Meer P. PAS or plasma for storage of platelets? A concise review. 2016;26(5):339-342.
138. Burnouf T. Modern plasma fractionation. 2007;21(2):101-117.
139. Farrugia A, Robert P. Plasma protein therapies: current and future perspectives. 2006;19(1):243-258.
140. Vermeulen M, Dickens C, Lelie N, et al. Hepatitis B virus transmission by blood transfusion during 4 years of individual-donation nucleic acid testing in South Africa: estimated and observed window period risk. 2012;52(4):880-892.
141. Cho HJ, Koo JW, Roh SK, et al. COVID-19 transmission and blood transfusion: A case report. *Journal of infection and public health*. 2020;13(11):1678-1679. doi:10.1016/j.jiph.2020.05.001
142. Goodrich RP, Edrich RA, Li J, Seghatchian J. The Mirasol™ PRT system for pathogen reduction of platelets and plasma: an overview of current status and future trends. 2006;35(1):5-17.
143. Lu W, Fung M. Platelets treated with pathogen reduction technology: current status and future direction. 2020;9
144. Marschner S, Goodrich R. Pathogen reduction technology treatment of platelets, plasma and whole blood using riboflavin and UV light. 2011;38(1):8-18.
145. Oeller M, Laner-Plamberger S, Krisch L, et al. Human platelet lysate for good manufacturing practice-compliant cell production. 2021;22(10):5178.
146. Schallmoser K, Strunk D. Preparation of pooled human platelet lysate (pHPL) as an efficient supplement for animal serum-free human stem cell cultures. 2009;(32)
147. Nurden AT. Platelets, inflammation and tissue regeneration. *Thromb Haemost*. May 2011;105 Suppl 1:S13-33. doi:10.1160/THS10-11-0720
148. Zamani M, Yaghoubi Y, Movassaghpour A, et al. Novel therapeutic approaches in utilizing platelet lysate in regenerative medicine: Are we ready for clinical use? *J Cell Physiol*. Aug 2019;234(10):17172-17186. doi:10.1002/jcp.28496
149. Le AD, Enweze L, DeBaun MR, Dragoo JL. Current clinical recommendations for use of platelet-rich plasma. *Current reviews in musculoskeletal medicine*. 2018;11(4):624-634.
150. Burnouf T, Goubran HA, Chen TM, et al. Blood-derived biomaterials and platelet growth factors in regenerative medicine. *Blood Rev*. Mar 2013;27(2):77-89. doi:10.1016/j.blre.2013.02.001
151. Harrison P. The use of platelets in regenerative medicine and proposal for a new classification system: guidance from the SSC of the ISTH. *J Thromb Haemost*. Sep 2018;16(9):1895-1900. doi:10.1111/jth.14223
152. Harrison P, Alsousou J. Studies on platelet rich plasma - new editorial policy for "Platelets". *Platelets*. 2020;31(3):281-282. doi:10.1080/09537104.2020.1729013
153. Ahmed TA, Dare EV, Hincke M. Fibrin: a versatile scaffold for tissue engineering applications. *Tissue Engineering Part B: Reviews*. 2008;14(2):199-215.
154. Linnes MP, Ratner BD, Giachelli CM. A fibrinogen-based precision microporous scaffold for tissue engineering. *Biomaterials*. 2007;28(35):5298-5306.
155. Chou ML, Wu JW, Gouel F, et al. Tailor-made purified human platelet lysate concentrated in neurotrophins for treatment of Parkinson's disease. *Biomaterials*. Oct 2017;142:77-89. doi:10.1016/j.biomaterials.2017.07.018
156. Piers TM, East E, Villegas-Llerena C, et al. Soluble fibrinogen triggers non-cell autonomous ER stress-mediated microglial-induced neurotoxicity. *Frontiers in Cellular Neuroscience*. 2018;12:404.

157. Sulimai N, Lominadze D. Fibrinogen and Neuroinflammation During Traumatic Brain Injury. *Mol Neurobiol*. Aug 10 2020;doi:10.1007/s12035-020-02012-2
158. Geremicca W, Fonte C, Vecchio S. Blood components for topical use in tissue regeneration: evaluation of corneal lesions treated with platelet lysate and considerations on repair mechanisms. *Blood Transfusion*. 2010;8(2):107.
159. Thery C, Witwer KW, Aikawa E, et al. Minimal information for studies of extracellular vesicles 2018 (MISEV2018): a position statement of the International Society for Extracellular Vesicles and update of the MISEV2014 guidelines. *Journal of extracellular vesicles*. 2018;7(1):1535750. doi:10.1080/20013078.2018.1535750
160. Anitua E, Muruzabal F, De la Fuente M, et al. Effects of heat-treatment on plasma rich in growth factors-derived autologous eye drop. *Exp Eye Res*. Feb 2014;119:27-34. doi:10.1016/j.exer.2013.12.005
161. Nebie O, Devos D, Vingtdeux V, et al. The neuroprotective activity of heat-treated human platelet lysate biomaterials manufactured from outdated pathogen-reduced (amotosalen/UVA) platelet concentrates. *J Biomed Sci*. Oct 31 2019;26(1):89. doi:10.1186/s12929-019-0579-9
162. Budzynski AZ. Chromogenic substrates in coagulation and fibrinolytic assays. 2001;32(7):365-368.
163. Lövgren A, Deinum J, Rosén S, et al. Characterization of thrombin derived from human recombinant prothrombin. 2015;26(5):545.
164. Germishuizen W, Gyure D, Stubbings D, et al. Quantifying the thrombogenic potential of human plasma-derived immunoglobulin products. 2014;42(5):260-270.
165. Marchetti M, Tartari CJ, Russo L, et al. Phospholipid-dependent procoagulant activity is highly expressed by circulating microparticles in patients with essential thrombocythemia. 2014;89(1):68-73.
166. Prior RL Plasma antioxidant measurements. 2004;134(11):3184S-3185S.
167. Castellano JM, Mosher KI, Abbey RJ, et al. Human umbilical cord plasma proteins revitalize hippocampal function in aged mice. 2017;544(7651):488-492.
168. Abbruzzese TA, Guzman RJ, Martin RL, et al. Matrix metalloproteinase inhibition limits arterial enlargement in a rodent arteriovenous fistula model. 1998;124(2):328-335.
169. Petrov D, Mansfield C, Moussy A, Hermine O. ALS Clinical Trials Review: 20 Years of Failure. Are We Any Closer to Registering a New Treatment? Review. *Front Aging Neurosci*. 2017;9(68)doi:10.3389/fnagi.2017.00068
170. Prasad EM, Hung S-Y. Current Therapies in Clinical Trials of Parkinson's Disease: A 2021 Update. *Pharmaceuticals (Basel)*. 2021;14(8):717.
171. Huang L-K, Chao S-P, Hu C-J. Clinical trials of new drugs for Alzheimer disease. *Journal of Biomedical Science*. 2020/01/06 2020;27(1):18. doi:10.1186/s12929-019-0609-7
172. Nebie O, Carvalho K, Barro L, et al. Human platelet lysate biotherapy for traumatic brain injury: preclinical assessment. *Brain*. 2021;doi:10.1093/brain/awab205
173. Gouel F, Do Van B, Chou ML, et al. The protective effect of human platelet lysate in models of neurodegenerative disease: involvement of the Akt and MEK pathways. 2017;11(11):3236-3240.
174. Hayon Y, Dashevsky O, Shai E, et al. Platelet lysates stimulate angiogenesis, neurogenesis and neuroprotection after stroke. *Thromb Haemost*. Aug 2013;110(2):323-30. doi:10.1160/TH12-11-0875
175. Anitua E, Pascual C, Antequera D, et al. Plasma rich in growth factors (PRGF-Endoret) reduces neuropathologic hallmarks and improves cognitive functions in an Alzheimer's disease mouse model. *Neurobiol Aging*. Jul 2014;35(7):1582-95. doi:10.1016/j.neurobiolaging.2014.01.009

176. Anitua E, Pascual C, Perez-Gonzalez R, et al. Intranasal delivery of plasma and platelet growth factors using PRGF-Endoret system enhances neurogenesis in a mouse model of Alzheimer's disease. *PLoS One*. 2013;8(9):e73118. doi:10.1371/journal.pone.0073118
177. Anitua E, Pascual C, Perez-Gonzalez R, et al. Intranasal PRGF-Endoret enhances neuronal survival and attenuates NF-kappaB-dependent inflammation process in a mouse model of Parkinson's disease. *J Control Release*. Apr 10 2015;203:170-80. doi:10.1016/j.jconrel.2015.02.030
178. Gouel F, Timmerman K, Gosset P, et al. Whole and fractionated human platelet lysate biomaterials-based biotherapy induces strong neuroprotection in experimental models of amyotrophic lateral sclerosis. *Biomaterials*. 2022;doi:10.1016/j.biomaterials.2021.121311
179. Gouel F, Rolland AS, Devedjian JC, et al. Past and Future of Neurotrophic Growth Factors Therapies in ALS: From Single Neurotrophic Growth Factor to Stem Cells and Human Platelet Lysates. *Front Neurol*. 2019;10:835. doi:10.3389/fneur.2019.00835
180. Nebie O, Barro L, Wu Y-W, et al. Heat-treated human platelet pellet lysate modulates microglia activation, favors wound healing and promotes neuronal differentiation in vitro. *Platelets*. 2021;32(2):226-237.
181. Burnouf T, Strunk D, Koh MB, et al. Human platelet lysate: Replacing fetal bovine serum as a gold standard for human cell propagation? *Biomaterials*. Jan 2016;76:371-87. doi:10.1016/j.biomaterials.2015.10.065
182. Blumel J, Schwantes A, Baylis SA, et al. Strategies toward virus and prion safe human platelet lysates. *Transfusion*. 2020;60(1):219-220. doi:10.1111/trf.15581
183. Burnouf T, Barro L, Nebie O, et al. Viral safety of human platelet lysate for cell therapy and regenerative medicine: Moving forward, yes, but without forgetting the past. *Transfus Apher Sci*. 2019;58(6):102674. doi:10.1016/j.transci.2019.102674
184. Busch MP, Bloch EM, Kleinman S. Prevention of transfusion-transmitted infections. *Blood*. 2019;133(17):1854-1864.
185. Burnouf T, Radosevich M. Reducing the risk of infection from plasma products: specific preventative strategies. *Blood Rev*. 2000;14(2):94-110. doi:10.1054/blre.2000.0129
186. Gehrie EA, Rutter SJ, Snyder EL. Pathogen Reduction: The State of the Science in 2019. *Hematol Oncol Clin North Am*. 2019;33(5):749-766. doi:10.1016/j.hoc.2019.05.001
187. Seltsam A, Müller TH. UVC irradiation for pathogen reduction of platelet concentrates and plasma. 2011;38(1):43-54.
188. Perez-Pujol S, Tonda R, Lozano M, et al. Effects of a new pathogen-reduction technology (Mirasol PRT) on functional aspects of platelet concentrates. 2005;45(6):911-919.
189. Magron A, Laugier J, Provost P, et al. Pathogen reduction technologies: the pros and cons for platelet transfusion. 2018;29(1):2-8.
190. Ware A, Jacquot C, Tobian A, et al. Pathogen reduction and blood transfusion safety in Africa: strengths, limitations and challenges of implementation in low-resource settings. 2018;113(1):3-12.
191. Roth NJ, Dichtelmüller HO, Fabbrizzi F, et al. Nanofiltration as a robust method contributing to viral safety of plasma-derived therapeutics: 20 years' experience of the plasma protein manufacturers. *Transfusion*. 2020;60(11):2661-2674.
192. Burnouf T, Radosevich M. Nanofiltration of plasma-derived biopharmaceutical products. *Haemophilia*. 2003;9(1):24-37. doi:10.1046/j.1365-2516.2003.00701.x
193. Gitler AD, Dhillon P, Shorter J. Neurodegenerative disease: models, mechanisms, and a new hope. 2017;10(5):499-502.
194. Dugger BN, Dickson DW. Pathology of neurodegenerative diseases. 2017;9(7):a028035.
195. Brettschneider J, Tredici KD, Lee VM-Y, et al. Spreading of pathology in neurodegenerative diseases: a focus on human studies. 2015;16(2):109-120.

196. Stephenson J, Nutma E, van der Valk P, et al. Inflammation in CNS neurodegenerative diseases. 2018;154(2):204-219.
197. Reynolds A, Laurie C, Mosley RL, et al. Oxidative stress and the pathogenesis of neurodegenerative disorders. 2007;82:297-325.
198. De Lau LM, Breteler MM. Epidemiology of Parkinson's disease. 2006;5(6):525-535.
199. Eriksen N, Stark AK, Pakkenberg BJB, et al. Age and Parkinson's disease-related neuronal death in the substantia nigra pars compacta. 2009:203-213.
200. Matsui H, Takahashi RJB, Shinpo NSKn. Pathological mechanisms of Parkinson's disease. 2009;61(4):441-446.
201. Massano J, Bhatia KP. Clinical approach to Parkinson's disease: features, diagnosis, and principles of management. 2012;2(6):a008870.
202. Goldman SM. Environmental toxins and Parkinson's disease. 2014;54:141-164.
203. Holmqvist S, Chutna O, Bousset L, et al. Direct evidence of Parkinson pathology spread from the gastrointestinal tract to the brain in rats. 2014;128(6):805-820.
204. Lücking CB, Brice A. Alpha-synuclein and Parkinson's disease. 2000;57(13):1894-1908.
205. Al-Hilaly YK, Biasetti L, Blakeman BJ, et al. The involvement of dityrosine crosslinking in α-synuclein assembly and deposition in Lewy Bodies in Parkinson's disease. 2016;6(1):1-13.
206. Butkovich LM, Houser MC, Tansey MG. α-synuclein and noradrenergic modulation of immune cells in Parkinson's disease pathogenesis. 2018;12:626.
207. Mahoney-Sánchez L, Bouchaoui H, Ayton S, et al. Ferroptosis and its potential role in the physiopathology of Parkinson's Disease. 2021;196:101890.
208. Devos D, Hirsch E, Wyse R. Seven solutions for neuroprotection in Parkinson's disease. 2021;36(2):306-316.
209. Mahoney-Sanchez L, Bouchaoui H, Boussaad I, et al. Alpha synuclein determines ferroptosis sensitivity in dopaminergic neurons via modulation of ether-phospholipid membrane composition. 2022;40(8):111231.
210. Laloux C, Gouel F, Lachaud C, et al. Continuous cerebroventricular administration of dopamine: A new treatment for severe dyskinesia in Parkinson's disease? 2017;103:24-31.
211. Allert N, Cheeran B, Deuschl G, et al. Postoperative rehabilitation after deep brain stimulation surgery for movement disorders. 2018;129(3):592-601.
212. Politis M, Lindvall O. Clinical application of stem cell therapy in Parkinson's disease. 2012;10(1):1-7.
213. Yasuhara T, Kameda M, Agari T, Date I. Regenerative medicine for Parkinson's disease. 2015;55(2):113-123.
214. Razgado-Hernandez LF, Espadas-Alvarez AJ, Reyna-Velazquez P, et al. The transfection of BDNF to dopamine neurons potentiates the effect of dopamine D3 receptor agonist recovering the striatal innervation, dendritic spines and motor behavior in an aged rat model of Parkinson's disease. 2015;10(2):e0117391.
215. Sleeman IJ, Boshoff EL, Duty S. Fibroblast growth factor-20 protects against dopamine neuron loss in vitro and provides functional protection in the 6-hydroxydopamine-lesioned rat model of Parkinson's disease. 2012;63(7):1268-1277.
216. Gouel F, Rolland A-S, Devedjian J-C, et al. Past and future of neurotrophic growth factors therapies in ALS: from single neurotrophic growth factor to stem cells and human platelet lysates. 2019;10:835.
217. Parikh S, Koch M, Narayan RK. Traumatic Brain Injury. 2007;45(3):119-135. doi:10.1097/AIA.0b013e318078cfe7
218. Rutland-Brown W, Langlois JA, Thomas KE, Xi YL. Incidence of Traumatic Brain Injury in the United States, 2003. 2006;21(6):544-548.

219. Greve MW, Zink BJ. Pathophysiology of traumatic brain injury. 2009;76(2):97-104. doi:https://doi.org/10.1002/msj.20104
220. Ekmark-Lewén S, Lewén A, Israelsson C, et al. Vimentin and GFAP responses in astrocytes after contusion trauma to the murine brain. 2010;28(3):311-321.
221. Li D-R, Zhang F, Wang Y, et al. Quantitative analysis of GFAP-and S100 protein-immunopositive astrocytes to investigate the severity of traumatic brain injury. 2012;14(2):84-92.
222. VandeVord PJ, Leung LY, Hardy W, et al.. Up-regulation of reactivity and survival genes in astrocytes after exposure to short duration overpressure. 2008;434(3):247-252.
223. Chiu C-C, Liao Y-E, Yang L-Y, et al. Neuroinflammation in animal models of traumatic brain injury. 2016;272:38-49.
224. Lotharius J, Barg S, Wiekop P, et al. Effect of mutant α-synuclein on dopamine homeostasis in a new human mesencephalic cell line. 2002;277(41):38884-38894.
225. Pierce SE, Tyson T, Booms A, et al. Parkinson's disease genetic risk in a midbrain neuronal cell line. 2018;114:53-64.
226. Zhang X-m, Yin M, Zhang M-h. Cell-based assays for Parkinson's disease using differentiated human LUHMES cells. 2014;35(7):945-956.
227. Scholz D, Pöltl D, Genewsky A, et al. Rapid, complete and large-scale generation of post-mitotic neurons from the human LUHMES cell line. 2011;119(5):957-971.
228. Sherer TB, Betarbet R, Testa CM, et al. Mechanism of toxicity in rotenone models of Parkinson's disease. 2003;23(34):10756-10764.
229. Xiong N, Long X, Xiong J, et al. Mitochondrial complex I inhibitor rotenone-induced toxicity and its potential mechanisms in Parkinson's disease models. 2012;42(7):613-632.
230. Risiglione P, Leggio L, Cubisino SA, et al. High-resolution respirometry reveals MPP+ Mitochondrial toxicity mechanism in a cellular model of Parkinson's Disease. 2020;21(21):7809.
231. Oshiro N, Yoshino Ki, Hidayat S, et al. Dissociation of raptor from mTOR is a mechanism of rapamycin-induced inhibition of mTOR function. 2004;9(4):359-366.
232. Do Van B, Gouel F, Jonneaux A, et al. Ferroptosis, a newly characterized form of cell death in Parkinson's disease that is regulated by PKC. 2016;94:169-178.
233. Guiney SJ, Adlard PA, Bush AI, et al. Ferroptosis and cell death mechanisms in Parkinson's disease. 2017;104:34-48.
234. Wang L, Liu Y, Du T, et al. ATF3 promotes erastin-induced ferroptosis by suppressing system Xc–. 2020;27(2):662-675.
235. Meredith GE, Rademacher DJ. MPTP mouse models of Parkinson's disease: an update. 2011;1(1):19-33.
236. Mustapha M, Taib CNM. MPTP-induced mouse model of Parkinson's disease: A promising direction for therapeutic strategies. 2021;21(4):422.
237. Huang D, Xu J, Wang J, et al. Dynamic changes in the nigrostriatal pathway in the MPTP mouse model of Parkinson's disease. 2017;2017
238. Bjugstad KB, Redmond Jr DE, Teng YD, et al. Neural stem cells implanted into MPTP-treated monkeys increase the size of endogenous tyrosine hydroxylase-positive cells found in the striatum: a return to control measures. 2005;14(4):183-192.
239. Chotibut T, Davis RW, Arnold JC, et al. Ceftriaxone increases glutamate uptake and reduces striatal tyrosine hydroxylase loss in 6-OHDA Parkinson's model. 2014;49(3):1282-1292.
240. Devos D, Moreau C, Devedjian JC, et al. Targeting chelatable iron as a therapeutic modality in Parkinson's disease. 2014;21(2):195-210.
241. Sanchez B, Relova JL, Gallego R, et al. Dihydroxyvitamin D3 administration to 6-hydroxydopamine-lesioned rats increases glial cell line-derived neurotrophic factor and

partially restores tyrosine hydroxylase expression in substantia nigra and striatum. 2009;87(3):723-732.
242. Iravani MM, Syed E, Jackson MJ, et al. A modified MPTP treatment regime produces reproducible partial nigrostriatal lesions in common marmosets. 2005;21(4):841-854.
243. Shipley MM, Mangold CA, Szpara ML. Differentiation of the SH-SY5Y human neuroblastoma cell line. 2016;(108):e53193.
244. Kovalevich J, Langford D. Considerations for the use of SH-SY5Y neuroblastoma cells in neurobiology. 2013:9-21.
245. Lopez-Suarez L, Al Awabdh S, Coumoul X, et al. The SH-SY5Y human neuroblastoma cell line, a relevant in vitro cell model for investigating neurotoxicology in human: focus on organic pollutants. 2022;
246. Lopes FM, Schröder R, da Frota Júnior MLC, et al. Comparison between proliferative and neuron-like SH-SY5Y cells as an in vitro model for Parkinson disease studies. 2010;1337:85-94.
247. Nebie O, Barro L, Wu Y-W, et al. Heat-treated human platelet pellet lysate modulates microglia activation, favors wound healing and promotes neuronal differentiation in vitro. 2021;32(2):226-237.
248. Kong L, Yao Y, Xia Y, et al. Osthole alleviates inflammation by down-regulating NF-κB signaling pathway in traumatic brain injury. 2019;41(2):349-360.
249. Xiao B, Chai Y, Lv S, et al. Endothelial cell-derived exosomes protect SH-SY5Y nerve cells against ischemia/reperfusion injury. 2017;40(4):1201-1209.
250. Blasi E, Barluzzi R, Bocchini V, et al. Immortalization of murine microglial cells by a v-raf/v-myc carrying retrovirus. 1990;27(2-3):229-237.
251. Orihuela R, McPherson CA, Harry G. Microglial M1/M2 polarization and metabolic states. 2016;173(4):649-665.
252. Oh YT, Lee JY, Yoon H, et al. Lipopolysaccharide induces hypoxia-inducible factor-1 alpha mRNA expression and activation via NADPH oxidase and Sp1-dependent pathway in BV2 murine microglial cells. 2008;431(2):155-160.
253. Woo J, Han D, Wang JI, Park J, et al. Quantitative proteomics reveals temporal proteomic changes in signaling pathways during BV2 mouse microglial cell activation. 2017;16(9):3419-3432.
254. Hwang KY, Oh YT, Yoon H, et al. Baicalein suppresses hypoxia-induced HIF-1α protein accumulation and activation through inhibition of reactive oxygen species and PI 3-kinase/Akt pathway in BV2 murine microglial cells. 2008;444(3):264-269.
255. Kalish BT, Whalen MJ. Weight drop models in traumatic brain injury. 2016:193-209.
256. Tweedie D, Rachmany L, Rubovitch V, et al. Exendin-4, a glucagon-like peptide-1 receptor agonist prevents mTBI-induced changes in hippocampus gene expression and memory deficits in mice. 2013;239:170-182.
257. Sullivan HG, Martinez J, Becker DP, et al. Fluid-percussion model of mechanical brain injury in the cat. 1976;45(5):520-534.
258. Lyeth BG. Historical review of the fluid-percussion TBI model. 2016;7:217.
259. Garman RH, Jenkins LW, Switzer III RC, et al. Blast exposure in rats with body shielding is characterized primarily by diffuse axonal injury. 2011;28(6):947-959.
260. Säljö A, Bao F, Haglid KG, Hansson H-A. Blast exposure causes redistribution of phosphorylated neurofilament subunits in neurons of the adult rat brain. 2000;17(8):719-726.
261. Chauhan NB, Gatto R, Chauhan MB. Neuroanatomical correlation of behavioral deficits in the CCI model of TBI. 2010;190(1):1-9.
262. Chen Y, Mao H, Yang KH, et al. A modified controlled cortical impact technique to model mild traumatic brain injury mechanics in mice. 2014;5:100.

263. LIGHTHALL JW, GOSHGARIAN HG, PINDERSKI CR. Characterization of axonal injury produced by controlled cortical impact. 1990;7(2):65-76.
264. Zweckberger K, Erös C, Zimmermann R, et al. Effect of early and delayed decompressive craniectomy on secondary brain damage after controlled cortical impact in mice. 2006;23(7):1083-1093.
265. Jin X, Ishii H, Bai Z, Itokazu T, et al. Temporal changes in cell marker expression and cellular infiltration in a controlled cortical impact model in adult male C57BL/6 mice. 2012;7(7):e41892.
266. Carlson SW, Madathil SK, Sama DM, et al. Conditional overexpression of insulin-like growth factor-1 enhances hippocampal neurogenesis and restores immature neuron dendritic processes after traumatic brain injury. 2014;73(8):734-746.
267. Santi A, Genis L, Torres Aleman I. A coordinated action of blood-borne and brain insulin-like growth factor I in the response to traumatic brain injury. 2018;28(6):2007-2014.
268. Yan HQ, Yu J, Kline AE, et al. Evaluation of combined fibroblast growth factor-2 and moderate hypothermia therapy in traumatically brain injured rats. 2000;887(1):134-143.
269. Nebie O, Carvalho K, Barro L, et al. Human platelet lysate biotherapy for traumatic brain injury: preclinical assessment. 2021;144(10):3142-3158.
270. Burnouf T, Radosevich M. Nanofiltration of plasma-derived biopharmaceutical products. *J Haemophilia*. 2003;9(1):24-37.
271. Strandberg G, Sellberg F, Sommar P, et al. Standardizing the freeze-thaw preparation of growth factors from platelet lysate. *Transfusion*. Apr 2017;57(4):1058-1065. doi:10.1111/trf.13998
272. Burnouf T, Tseng YH, Kuo YP, et al. Solvent/detergent treatment of platelet concentrates enhances the release of growth factors. 2008;48(6):1090-1098.
273. Chen MS, Wang TJ, Lin HC, et al. Four types of human platelet lysate, including one virally inactivated by solvent-detergent, can be used to propagate Wharton jelly mesenchymal stromal cells. *N Biotechnol*. Mar 25 2019;49:151-160. doi:10.1016/j.nbt.2018.11.003
274. Vermeulen M, Dickens C, Lelie N, et al. Hepatitis B virus transmission by blood transfusion during 4 years of individual-donation nucleic acid testing in South Africa: estimated and observed window period risk. *Transfusion*. 2012;52(4):880-892.
275. Barro L, Su YT, Nebie O, et al. A double-virally-inactivated (Intercept-solvent/detergent) human platelet lysate for in vitro expansion of human mesenchymal stromal cells. *Transfusion*. Jun 2019;59(6):2061-2073. doi:10.1111/trf.15251
276. Barro L, Delila L, Nebie O, et al. Removal of minute virus of mice-mock virus particles by nanofiltration of culture growth media supplemented with 10% human platelet lysate. *Cytotherapy*. 2021;23(5):S176. doi:10.1016/S146532492100579X
277. Kljenak A, Tominac Trcin M, Bujić M, et al. Fibrin gel as a scaffold for skin substitute–production and clinical experience. 2016;55(2.):279-288.
278. Chou ML, Lin LT, Devos D, et al. Nanofiltration to remove microparticles and decrease the thrombogenicity of plasma: in vitro feasibility assessment. *Transfusion*. Oct 2015;55(10):2433-44. doi:10.1111/trf.13162
279. Delila L, Wu YW, Nebie O, et al. Extensive characterization of the composition and functional activities of five preparations of human platelet lysates for dedicated clinical uses. *Platelets*. 2021;32(2):259-272. doi:10.1080/09537104.2020.1849603
280. Widyaningrum R, Burnouf T, Nebie O, et al. A purified human platelet pellet lysate rich in neurotrophic factors and antioxidants repairs and protects corneal endothelial cells from oxidative stress. *Biomed Pharmacother*. Oct 2021;142:112046. doi:10.1016/j.biopha.2021.112046
281. Mann K, Brummel K, Butenas S. What is all that thrombin for? 2003;1(7):1504-1514.

282. Chou M-L, Wu J-W, Gouel F, et al. Tailor-made purified human platelet lysate concentrated in neurotrophins for treatment of Parkinson's disease. *Biomaterials*. 2017;142:77-89.
283. Nebie O, Carvalho K, Barro L, et al. Human platelet lysate biotherapy for traumatic brain injury: preclinical assessment. *Brain*. Nov 29 2021;144(10):3142-3158. doi:10.1093/brain/awab205
284. Burnouf T, Goubran HA. Regenerative effect of expired platelet concentrate in human therapy: An update. 2022:103363.
285. Cecerska-Heryć E, Goszka M, Serwin N, et al. Applications of the regenerative capacity of platelets in modern medicine. 2022;64:84-94.
286. Gouel F, Do Van B, Chou ML, et al. The protective effect of human platelet lysate in models of neurodegenerative disease: involvement of the Akt and MEK pathways. *J Tissue Eng Regen Med*. Nov 2017;11(11):3236-3240. doi:10.1002/term.2222
287. Nebie O, Barro L, Wu YW, et al. Heat-treated human platelet pellet lysate modulates microglia activation, favors wound healing and promotes neuronal differentiation in vitro. *Platelets*. Feb 27 2020:1-12. doi:10.1080/09537104.2020.1732324
288. Strandberg G, Sellberg F, Sommar P, et al. Standardizing the freeze-thaw preparation of growth factors from platelet lysate. 2017;57(4):1058-1065.
289. Ramsby M, Kreutzer D. Fibrin induction of thrombospondin in corneal endothelial cells in vitro. 1993;34(1):165-174.
290. Ramsby ML, Kreutzer DL. Fibrin induction of thrombospondin in corneal endothelial cells in vitro. *Invest Ophthalmol Vis Sci*. Jan 1993;34(1):165-74.
291. Cortes-Canteli M, Mattei L, Richards AT, Norris EH, Strickland S. Fibrin deposited in the Alzheimer's disease brain promotes neuronal degeneration. *Neurobiol Aging*. Feb 2015;36(2):608-17. doi:10.1016/j.neurobiolaging.2014.10.030
292. Sweeney MD, Sagare AP, Zlokovic BV. Blood-brain barrier breakdown in Alzheimer disease and other neurodegenerative disorders. *Nat Rev Neurol*. Mar 2018;14(3):133-150. doi:10.1038/nrneurol.2017.188
293. van der Pol E, Harrison P. From platelet dust to gold dust: physiological importance and detection of platelet microvesicles. *Platelets*. May 2017;28(3):211-213. doi:10.1080/09537104.2017.1282781
294. Goubran HA, Burnouf T, Stakiw J, et al. Platelet microparticle: a sensitive physiological "fine tuning" balancing factor in health and disease. *Transfus Apher Sci*. Feb 2015;52(1):12-8. doi:10.1016/j.transci.2014.12.015
295. Torreggiani E, Perut F, Roncuzzi L, et al. Exosomes: novel effectors of human platelet lysate activity. *Eur Cell Mater*. Sep 22 2014;28:137-51; discussion 151. doi:10.22203/ecm.v028a11
296. Schallmoser K, Henschler R, Gabriel C, et al. Production and Quality Requirements of Human Platelet Lysate: A Position Statement from the Working Party on Cellular Therapies of the International Society of Blood Transfusion. *Trends Biotechnol*. Jan 2020;38(1):13-23. doi:10.1016/j.tibtech.2019.06.002
297. Perut F, Filardo G, Mariani E, et al. Preparation method and growth factor content of platelet concentrate influence the osteogenic differentiation of bone marrow stromal cells. *Cytotherapy*. Jul 2013;15(7):830-9. doi:10.1016/j.jcyt.2013.01.220
298. Roffi A, Filardo G, Assirelli E, et al. Does platelet-rich plasma freeze-thawing influence growth factor release and their effects on chondrocytes and synoviocytes? *BioMed research international*. 2014;2014
299. Altaie A, Owston H, Jones E. Use of platelet lysate for bone regeneration-are we ready for clinical translation? 2016;8(2):47.

300. Huber SC, Cunha Junior JL, Montalvao S, et al. In vitro study of the role of thrombin in platelet rich plasma (PRP) preparation: utility for gel formation and impact in growth factors release. *J Stem Cells Regen Med*. 2016;12(1):2-9.
301. Drew VJ, Tseng CL, Seghatchian J, et al. Reflections on Dry Eye Syndrome Treatment: Therapeutic Role of Blood Products. *Front Med (Lausanne)*. 2018;5:33. doi:10.3389/fmed.2018.00033
302. Giannaccare G, Versura P, Buzzi M, et al. Blood derived eye drops for the treatment of cornea and ocular surface diseases. *Transfus Apher Sci*. Aug 2017;56(4):595-604. doi:10.1016/j.transci.2017.07.023
303. Giannaccare G, Pellegrini M, Bernabei F, et al. Ocular surface system alterations in ocular graft-versus-host disease: All the pieces of the complex puzzle. 2019:1-11.
304. Mojica-Henshaw MP, Morris J, Kelley L, et al. Serum-converted platelet lysate can substitute for fetal bovine serum in human mesenchymal stromal cell cultures. 2013;15(12):1458-1468.
305. Chou ML, Burnouf T, Wang TJ. Ex vivo expansion of bovine corneal endothelial cells in xeno-free medium supplemented with platelet releasate. *PLoS One*. 2014;9(6):e99145. doi:10.1371/journal.pone.0099145
306. Le Borgne S, Graber M. Amidase activity and thermal stability of human thrombin. 1994;48(2):125-135.
307. Alsousou J, Ali A, Willett K, et al. The role of platelet-rich plasma in tissue regeneration. *Platelets*. 2013;24(3):173-82. doi:10.3109/09537104.2012.684730
308. De Pascale MR, Sommese L, Casamassimi A, et al. Platelet derivatives in regenerative medicine: an update. *Transfus Med Rev*. Jan 2015;29(1):52-61. doi:10.1016/j.tmrv.2014.11.001
309. Dunkelberger JR, Song W-C. Complement and its role in innate and adaptive immune responses. *Cell Research*. 2010/01/01 2010;20(1):34-50. doi:10.1038/cr.2009.139
310. Middleton O, Wheadon H, Michie A. Classical complement pathway. 2016;
311. Kayser W, Mueller-Eckhardt C, Bhakdi S, Ebert K. Platelet-associated complement C3 in thrombocytopenic states. 1983;54(3):353-363.
312. Alexander JJ, Anderson AJ, Barnum SR, et al. The complement cascade: Yin-Yang in neuroinflammation--neuro-protection and -degeneration. *Journal of neurochemistry*. Dec 2008;107(5):1169-87. doi:10.1111/j.1471-4159.2008.05668.x
313. Shi Q, Chowdhury S, Ma R, et al. Complement C3 deficiency protects against neurodegeneration in aged plaque-rich APP/PS1 mice. 2017;9(392)
314. Etscheid M, Breitner-Ruddock S, Gross S, et al. Identification of kallikrein and FXIa as impurities in therapeutic immunoglobulins: implications for the safety and control of intravenous blood products. *Vox sanguinis*. 2012;102(1):40-46.
315. Germishuizen WA, Gyure DC, Stubbings D, et al. Quantifying the thrombogenic potential of human plasma-derived immunoglobulin products. *Biologicals*. Sep 2014;42(5):260-70. doi:10.1016/j.biologicals.2014.04.002
316. Opneja A, Kapoor S, Stavrou EX. Contribution of platelets, the coagulation and fibrinolytic systems to cutaneous wound healing. *Thromb Res*. Jul 2019;179:56-63. doi:10.1016/j.thromres.2019.05.001
317. Mattler L, Bang N. Serine protease specificity for peptide chromogenic substrates. *Thrombosis and haemostasis*. 1977;38(08):0776-0792.
318. Laroche M, Dunois C, Vissac AM, et al. Update on functional and genetic laboratory assays for the detection of platelet microvesicles. *Platelets*. 2017;28(3):235-241.
319. Machovich R, Arányi PJT, haemostasis. Effect of calcium ion on the interaction between thrombin and heparin. Thermal denaturation. 1977;38(07):0677-0684.

320. Amiral J, Seghatchian J. The diagnostic usefulness of capture assays for measuring global/specific extracellular micro-particles in plasma. *Transfus Apher Sci*. Oct 2015;53(2):127-36. doi:10.1016/j.transci.2015.10.009
321. Arakelyan A, Fitzgerald W, Vagida M, et al. Addition of thrombin reduces the recovery of extracellular vesicles from blood plasma. *J Circ Biomark*. Jan-Dec 2016;5:1849454416663648. doi:10.1177/1849454416663648
322. Plantier JL, Duretz V, Devos V, et al. Comparison of antioxidant properties of different therapeutic albumin preparations. *Biologicals*. Jul 2016;44(4):226-233. doi:10.1016/j.biologicals.2016.04.002
323. Bergamini CM, Gambetti S, Dondi A, Cervellati C. Oxygen, reactive oxygen species and tissue damage. *Current pharmaceutical design*. 2004;10(14):1611-1626.
324. Barnham KJ, Masters CL, Bush AI. Neurodegenerative diseases and oxidative stress. *Nature reviews Drug discovery*. 2004;3(3):205-214.
325. Lepetsos P, Papavassiliou AG. ROS/oxidative stress signaling in osteoarthritis. *Biochimica et Biophysica Acta (BBA)-Molecular Basis of Disease*. 2016;1862(4):576-591.
326. Roche M, Rondeau P, Singh NR, et al. The antioxidant properties of serum albumin. 2008;582(13):1783-1787.
327. Turell L, Radi R, Alvarez B. The thiol pool in human plasma: the central contribution of albumin to redox processes. 2013;65:244-253.
328. Polidori MC, Stahl W, Eichler O, et al. Profiles of antioxidants in human plasma. 2001;30(5):456-462.
329. Lambiase A, Manni L, Bonini S, et al. Nerve growth factor promotes corneal healing: structural, biochemical, and molecular analyses of rat and human corneas. *Invest Ophthalmol Vis Sci*. Apr 2000;41(5):1063-9.
330. Kao WW, Kao CW, Kaufman AH, et al. Healing of corneal epithelial defects in plasminogen- and fibrinogen-deficient mice. *Invest Ophthalmol Vis Sci*. Mar 1998;39(3):502-8.
331. Chen TM, TSAI JC, Burnouf T. A novel technique combining platelet gel, skin graft, and fibrin glue for healing recalcitrant lower extremity ulcers. 2010;36(4):453-460.
332. Somani A, Rai R. Comparison of efficacy of autologous platelet-rich fibrin versus saline dressing in chronic venous leg ulcers: A randomised controlled trial. 2017;10(1):8.
333. Inouye M, Burnouf T. The role of nanofiltration in the pathogen safety of biologicals: an update. *Current Nanoscience*. 2020;16(3):413-424.
334. Farcet MR, Lackner C, Antoine G, et al. Hepatitis E virus and the safety of plasma products: investigations into the reduction capacity of manufacturing processes. *Transfusion*. Feb 2016;56(2):383-91. doi:10.1111/trf.13343
335. Adan-Kubo J, Tsujikawa M, Takahashi K, et al. Microscopic visualization of virus removal by dedicated filters used in biopharmaceutical processing: Impact of membrane structure and localization of captured virus particles. *Biotechnology progress*. 2019;35(6):e2875.
336. Théry C, Witwer KW, Aikawa E, et al. Minimal information for studies of extracellular vesicles 2018 (MISEV2018): a position statement of the International Society for Extracellular Vesicles and update of the MISEV2014 guidelines. *JExtracellVesicles*. 2018;7(1):1535750. doi:10.1080/20013078.2018.1535750
337. Nyam-Erdene A, Nebie N, Delila L, et al. Characterization and Chromatographic Isolation of Platelet Extracellular Vesicles from Human Platelet Lysates for Applications in Neuroregenerative Medicine. *ACS, Biomaterials Science & Engineering*. 2021;7(12):5823-5835. doi:10.1021/acsbiomaterials.1c01226
338. Melki I, Tessandier N, Zufferey A, et al. Platelet microvesicles in health and disease. *Platelets*. May 2017;28(3):214-221. doi:10.1080/09537104.2016.1265924

339. Yeaman MR. Platelets in defense against bacterial pathogens. *Cell Mol Life Sci*. 2010;67(4):525-44. doi:10.1007/s00018-009-0210-4
340. Jenne CN, Urrutia R, Kubes P. Platelets: bridging hemostasis, inflammation, and immunity. *Int J Lab Hematol*. Jun 2013;35(3):254-61. doi:10.1111/ijlh.12084
341. Dixon CE, Clifton GL, Lighthall JW, et al. A controlled cortical impact model of traumatic brain injury in the rat. *Journal of neuroscience methods*. 1991;39(3):253-262.
342. Nebie O, Barro L, Wu YW, et al. Heat-treated human platelet pellet lysate modulates microglia activation, favors wound healing and promotes neuronal differentiation in vitro. *Platelets*. Feb 17 2021;32(2):226-237. doi:10.1080/09537104.2020.1732324
343. Yuana Y, Böing AN, Grootemaat AE, et al. Handling and storage of human body fluids for analysis of extracellular vesicles. 2015;4(1):29260.
344. Brennan K, Martin K, FitzGerald S, et al. A comparison of methods for the isolation and separation of extracellular vesicles from protein and lipid particles in human serum. 2020;10(1):1039.
345. Nyam-Erdene A, Nebie O, Delila L, et al. Characterization and chromatographic isolation of platelet extracellular vesicles from human platelet lysates for applications in neuroregenerative medicine. 2021;7(12):5823-5835.
346. Burnouf T, Goubran HA, Chou M-L, et al. Platelet microparticles: Detection and assessment of their paradoxical functional roles in disease and regenerative medicine. *Blood Reviews*. 2014/07/01/ 2014;28(4):155-166. doi:https://doi.org/10.1016/j.blre.2014.04.002
347. Lu J, Yang J, Zheng Y, Chen X, et al. Extracellular vesicles from endothelial progenitor cells prevent steroid-induced osteoporosis by suppressing the ferroptotic pathway in mouse osteoblasts based on bioinformatics evidence. 2019;9(1):16130.
348. Lavenius E, Parrow V, Nånberg E, et al. Basic FGF and IGF-I promote differentiation of human SH-SY5Y neuroblastoma cells in culture. 1994;10(1):29-39.
349. Goldie BJ, Barnett MM, Cairns M. BDNF and the maturation of posttranscriptional regulatory networks in human SH-SY5Y neuroblast differentiation. 2014;8:325.
350. Zhu X, Yao H, Peng F, Callen S, Buch S. PDGF-mediated protection of SH-SY5Y cells against Tat toxin involves regulation of extracellular glutamate and intracellular calcium. 2009;240(2):286-291.
351. Xie Q, Wu G-Z, Yang N, et al. Delavatine A, an unusual isoquinoline alkaloid exerts anti-inflammation on LPS-induced proinflammatory cytokines production by suppressing NF-κB activation in BV-2 microglia. 2018;502(2):202-208.
352. Oh W-J, Jung U, Eom H-S, et al. Inhibition of lipopolysaccharide-induced proinflammatory responses by Buddleja officinalis extract in BV-2 microglial cells via negative regulation of NF-κB and ERK1/2 signaling. 2013;18(8):9195-9206.
353. Lesniak A, Poznański P, Religa P, et al. Loss of brain-derived neurotrophic factor (BDNF) resulting from congenital-or mild traumatic brain injury-induced blood–brain barrier disruption correlates with depressive-like behaviour. 2021;458:1-10.
354. Shen Q, Hiebert JB, Hartwell J, et al. Systematic review of traumatic brain injury and the impact of antioxidant therapy on clinical outcomes. 2016;13(5):380-389.
355. Slemmer JE, Shacka JJ, Sweeney M, et al. Antioxidants and free radical scavengers for the treatment of stroke, traumatic brain injury and aging. 2008;15(4):404-414.
356. Abushouk AI, Negida A, Ahmed H, et al. Neuroprotective mechanisms of plant extracts against MPTP induced neurotoxicity: Future applications in Parkinson's disease. 2017;85:635-645.
357. Patil SP, Jain P, Ghumatkar P, Tambe R, et al. Neuroprotective effect of metformin in MPTP-induced Parkinson's disease in mice. 2014;277:747-754.

Annex 1: list of the primers used in this study

Name	Forward primer	Reverse primer
Cyclophilin	agcatacaggtcctggcatc	ttcaccttcccaaagaccac
CCL3	tgcccttgctgttcttctct	gtggaatcttccggctgtag
CCL4	gccctctctctcctcttgct	gagggtcagagcccattg
CCL5	ctcactgcagccgccctctg	ccgagccatatggtgaggcagg
TLR2	ggggcttcacttctctgctt	agcatcctctgcgatttgacg
TLR4	ggactctgatcatggcactg	ctgatccatgcattggtaggt
TNF-α	tgcctatgtctcagcctcttc	gaggccatttgggaacttct
TREM2	cgagaggctgaggtcctg	tctccagcatcttggtcatcta
GFAP	cgcgaacaggaagagcgcca	gtggcgggccatctcctcct
CD68	gacctacatcagagcccgagt	cgccatgaatgtccactg